


2022

## IDENTIFYING EPIDERMAL ENRICHED GENES REQUIRED FOR PLANARIAN REGENERATION- SP. SCHMIDTEA MEDITERRANEA

Pallob Barai

University of Kentucky, pallobkubge@gmail.com

Author ORCID Identifier:

 <https://orcid.org/0000-0002-0134-3860>

Digital Object Identifier: <https://doi.org/10.13023/etd.2022.162>

[Right click to open a feedback form in a new tab to let us know how this document benefits you.](#)

### Recommended Citation

Barai, Pallob, "IDENTIFYING EPIDERMAL ENRICHED GENES REQUIRED FOR PLANARIAN REGENERATION- SP. SCHMIDTEA MEDITERRANEA" (2022). *Theses and Dissertations--Biology*. 84.  
[https://uknowledge.uky.edu/biology\\_etds/84](https://uknowledge.uky.edu/biology_etds/84)

This Master's Thesis is brought to you for free and open access by the Biology at UKnowledge. It has been accepted for inclusion in Theses and Dissertations--Biology by an authorized administrator of UKnowledge. For more information, please contact [UKnowledge@lsv.uky.edu](mailto:UKnowledge@lsv.uky.edu).

## **STUDENT AGREEMENT:**

I represent that my thesis or dissertation and abstract are my original work. Proper attribution has been given to all outside sources. I understand that I am solely responsible for obtaining any needed copyright permissions. I have obtained needed written permission statement(s) from the owner(s) of each third-party copyrighted matter to be included in my work, allowing electronic distribution (if such use is not permitted by the fair use doctrine) which will be submitted to UKnowledge as Additional File.

I hereby grant to The University of Kentucky and its agents the irrevocable, non-exclusive, and royalty-free license to archive and make accessible my work in whole or in part in all forms of media, now or hereafter known. I agree that the document mentioned above may be made available immediately for worldwide access unless an embargo applies.

I retain all other ownership rights to the copyright of my work. I also retain the right to use in future works (such as articles or books) all or part of my work. I understand that I am free to register the copyright to my work.

## **REVIEW, APPROVAL AND ACCEPTANCE**

The document mentioned above has been reviewed and accepted by the student's advisor, on behalf of the advisory committee, and by the Director of Graduate Studies (DGS), on behalf of the program; we verify that this is the final, approved version of the student's thesis including all changes required by the advisory committee. The undersigned agree to abide by the statements above.

Pallob Barai, Student

Dr. Elizabeth Duncan, Major Professor

Dr. Jessica Santollo, Director of Graduate Studies



IDENTIFYING EPIDERMAL ENRICHED GENES REQUIRED FOR PLANARIAN  
REGENERATION- SP. SCHMIDTEA MEDITERRANEA

---

THESIS

---

A thesis submitted in partial fulfillment of the  
requirements for the degree of Master of Science in the  
College of Arts and Sciences  
at the University of Kentucky

By

Pallob Barai

Lexington, Kentucky

Director: Dr. Elizabeth Duncan, Assistant Professor of Biology

Lexington, Kentucky

2022

## ABSTRACT OF THESIS

### IDENTIFYING EPIDERMAL ENRICHED GENES REQUIRED FOR PLANARIAN REGENERATION- SP. SCHMIDTEA MEDITERRANEA

The outer epithelial layer covering an organism, commonly known as the epidermis, is crucial for maintaining homeostasis and for the wound healing processes after injury. The planarian epidermis allows flatworms to heal their wounds and virtually restore any missing tissues. Immediately after amputation, planarians contract their muscle and stretch their epidermis to heal the wound area. However, how the planarian epidermis coordinates with other tissues and mechanisms after the initial wound healing processes begins is not understood in detail. I hypothesized that epidermal cell stretching upon wound healing induces transcriptional changes that are required for effective regeneration. To test this hypothesis, I first developed a new technique for isolating the planarian epidermis from both intact and regenerating worms. Next, I optimized a custom method to deplete ribosomal RNA from total planarian RNA for preparation of RNA-seq libraries. I show that this method depletes ~99% of rRNA from planarian RNA samples. I then conducted RNA-seq experiments on isolated planarian epidermis to identify genes that change expression after tissue injury. Using these two new methods in combination, I was able to detect more epidermal enriched genes compared to similar published datasets.

Excitingly, I uncovered functional roles of several genes that were identified using our methods. For example, I showed that SHOC2 is required for eye spot maintenance and for normal blastema growth and regeneration in planarians. I also identified several wound-induced genes that are expressed in the planarian epidermis. Furthermore, at least one newly identified wound-induced gene, a novel gene WI-12 is required for planarian tail regeneration when the head fragments are amputated at a certain position. In sum, our work established tools for isolating the planarian epidermis and depleting almost all rRNA from planarian RNA samples, paving the way to detect and dissect the roles of epidermal genes in maintaining homeostasis and initiating regeneration in planarians.

KEYWORDS: Epidermis, RNase-H, Ribodepletion, SHOC2, Regeneration, Planarian

---

Pallob Barai  
(Name of Student)

---

03/28/2022  
Date

IDENTIFYING EPIDERMAL ENRICHED GENES REQUIRED FOR PLANARIAN  
REGENERATION- SP. SCHMIDTEA MEDITERRANEA

By  
Pallob Barai

Dr. Elizabeth Duncan

---

Director of Thesis

Dr. Jessica Santollo

---

Director of Graduate Studies

03/28/2022

---

Date

DEDICATION

To  
My Beloved Parents

## ACKNOWLEDGMENTS

Life is a journey and along the way I was privileged to meet countless inspiring people. Although I will not be able to mention all of them, but I want to express my inner gratitude to those who made my life more meaningful and had profound influence on my current personal and professional development. I want to start thanking my mentor and advisor Dr. Elizabeth Duncan. When I left my family and country in 2019, it could be hard for me to adapt in a different country and cultures unless I was accepted in a welcoming way in Duncan Lab. Meeting with her allowed me to discover the explorative nature of science. I am thankful to Beth, for the opportunity to join her lab and for inspiring me to overcome challenges. I will also express my gratefulness to Beth for being so polite and giving me the space to discuss my personal issues as well.

I am grateful to my parents who gave me the courage to be whatever I want to be and for their tremendous efforts to fulfil my needs. I will express my gratitude and love to the most beautiful woman in my life- my fiancé with whom I shared this journey from overseas. I will thank her for always being supportive and waiting for me so long.

I want to thank my Thesis committee members Dr. Douglas Harrison, Dr. Ashley Seifert and Dr. Jeramiah Smith for their insightful discussion and suggestions. I also want to thank Dr. Chintan Kikani for asking great questions during our joint lab meetings.

I want to express my special thanks to Shishir Biswas for helping me with bioinformatic analysis and undergraduate student Landon Howell for his help in cloning some of the many genes examined here.

I am thankful to my current and past lab members and colleagues. Thank you, Prince, as we joined in this lab together and for helping me with countless things. I am thanking John Allen, Court Waterbury, Makayla Dean, Katya Lundberg, Cameron McHargue, Saima Rahman, and Maria Kibtiya for helping me in numerous ways.

## TABLE OF CONTENTS

ACKNOWLEDGMENTS .....	iii
LIST OF TABLES .....	vi
LIST OF FIGURES .....	vii
CHAPTER 1. Introduction.....	1
1.1    Metazoan epidermis .....	1
1.2    Wound healing and regeneration across metazoans .....	3
1.2.1    Wound healing.....	4
1.2.2    Regeneration .....	7
1.3    Epidermal role in regeneration.....	12
1.4    Planarians as a model system in studying wound healing and regeneration ....	13
1.4.1    Planarian epidermis in wound healing and regeneration .....	15
1.4.1.1    Planarian wound healing.....	18
1.4.1.2    Planarian epidermis and regeneration.....	18
1.5    Stretch or morphological changes induced transcriptomic changes .....	23
CHAPTER 2. New and customized methods enhance the identification of genes in the planarian epidermis.....	25
2.1    Isolation of planarian outer epithelium.....	26
2.2    Custom RNase-H based ribosomal RNA depletion efficiently removes rRNA from planarian total RNA .....	28
2.3    SDS based epidermis isolation following RNase-H based ribodepletion enhances the ability of epidermal gene detection .....	34
2.4    GO enrichment analysis reveals the biological roles of epidermal enriched genes .....	39
2.5    Functional characterization of identified epidermal genes .....	44
CHAPTER 3. Identification of wound induced genes and their functional roles during planarian regeneration.....	53
3.1    Isolation of planarian regenerating epidermis.....	53
3.2    Detection of wound induced genes using RNase-H based library preparation methods .....	56
3.3    Validation of RNA-seq data using whole mount in situ hybridization.....	58

3.4	GO analysis unveils several biological roles of early wound induced genes in planarians .....	65
3.5	A wound induced gene encoding a putative membrane protein operates during planarian tail regeneration.....	68
CHAPTER 4. Discussion .....		72
4.1	Epidermis- a crucial player in wound healing and regeneration.....	72
4.2	Wound response program is associated with planarian regeneration .....	73
4.3	SDS based epidermis isolation is a useful method for studying planarian epidermis.....	74
4.4	Planarian epidermal genes are required for homeostatic maintenance and regeneration.....	76
4.5	Positional control genes are required for proper regeneration.....	80
CHAPTER 5. Materials and Methods.....		82
5.1	Planarian maintenance and care.....	82
5.2	Planarian epidermis isolation and RNA extraction.....	82
5.3	RNase-H ribodepletion and RNA-seq library preparation.....	83
5.4	Gene cloning .....	84
5.5	NBT/BCIP whole mount in situ hybridization .....	84
5.6	Double stranded RNA synthesis and RNAi gene knockdown experiments .....	85
5.7	Image processing and quantification .....	85
5.8	Statistical analysis and graphing .....	86
APPENDICES .....		87
REFERENCES .....		112
VITA.....		125

## LIST OF TABLES

Table 2.1 Sequencing depth and number of reads aligned to planarian genome.....	33
Table 2.2 GO terms and corresponding p-values of epidermal enriched genes .....	42



## LIST OF FIGURES

Figure 1.1 Schematic representation of the planarian epidermis .....	17
Figure 2.1 SDS based isolation of planarian epidermis .....	27
Figure 2.2 RNase-H based ribosomal RNA depletion strategy .....	30
Figure 2.3 RNase H based ribodepletion efficiently depletes rRNA in planarians .....	32
Figure 2.4 Quality analysis for RNA-seq datasets prepared from intact epidermis .....	35
Figure 2.5 RNase-H library preparation method in combination with SDS based epidermis isolation detects more epidermal genes .....	37
Figure 2.6 Optimized skin isolation and RNaseH depletion methods lead to robust detection of epidermal enriched genes .....	41
Figure 2.7 Epidermal genes required for planarian regeneration .....	46
Figure 2.8 RNAi depletion of epidermal enriched genes leads to impaired feeding behavior and locomotion in planarians .....	49
Figure 2.9 SHOC2-RNAi worms show delayed eye spot regeneration.....	52
Figure 3.1 SDS based isolation of regenerating planarian epidermis .....	55
Figure 3.2 Quality checking and DE analysis of RNA-seq data from regenerating epidermis .....	57
Figure 3.3 RNaseH based library preparation in combination with SDS based epidermis isolation sensitively detects wound induced epidermal genes.....	59
Figure 3.4 Planarian intestinal show a strong gene expression response to wound signals .....	60
Figure 3.5 In situ validation of wound induced epidermal genes .....	62
Figure 3.6 In situ validation of genes induced at later time points after wounding.....	64
Figure 3.7 GO analysis unveils the biological functions of wound induced genes .....	66
Figure 3.8 WI-12 gene functions depend on the position .....	69
Figure 3.9 WI-12-RNAi treated head fragments regenerate normally when cut at AP4..	71

## CHAPTER 1. INTRODUCTION

### 1.1 Metazoan epidermis

Epithelia are defined as sheet-like arrangements of component cells that have apical-basal polarity and are interconnected along their adjacent surfaces with belt-like junctions and attached to a underlying basal lamina (Tyler, 2003). Epithelia are believed to be the default state cells in Eumetazoa as they are the first tissues to arise from embryonic development and considered as the first indication of cellular differentiation during embryogenesis (Dickinson et al., 2011; Leys and Riesgo, 2012). Although there are structural and morphological variations in epithelia among different phyla, the underlining structure of epithelial cells (A-P polarity and organization into sheets) is conserved (Knust and Bossinger, 2002; Tyler, 2003). The structure of epithelia ranges from single cell layers of squamous, columnar, or cuboidal cells to multilayered pseudo-stratified or stratified epithelia in vertebrates (Van Lommel, 2003). Although the primary function of epithelia is to support the structure of developing embryos and internal organs, they also act as effective barriers against environmental stress and pathogens (Guillot and Lecuit, 2013). Epithelia also separate different physiological conditions and mediate the exchange of varieties of substances between body cavities and underlying tissues (Van Lommel, 2003).

Using the morphological differences of epithelia among phyla, comparative studies on different model organisms such as *Drosophila*, *C. elegans*, *Hydra*, rats, and mice have shown that some proteins underlining the cellular differentiation of epithelia are similar among these phyla (Knust and Bossinger, 2002; Kramer, 2000). In vertebrate epithelia, the apical junctions knowns as zonula occludens (ZO), proximal array zonula adherens (ZA) and desmosome together form the junctional complex. However, in invertebrates the ZA

is most apical and ZO are absent but their functions are filled by another junction called septate junction (SJ), which lies beneath the ZA (Tyler, 2003). The ZA attach to the cytoskeleton of the cells via actin microfilaments and form terminal webs, which essentially maintain the integrity of epithelia (Harrison, 1991; Tyler, 1984).

An epidermis is a specialized form of epithelium in triploblastic animals and ranges in structure from a single layer of epidermal cells, as seen in planarians, to a stratified epithelium in higher vertebrates (Lillywhite and Maderson, 1988). The invertebrate skin is embryologically and structurally diverse among the clades. The invertebrate skin is typically comprised of an ectoderm-derived monostratified epidermis which overlies a basement membrane called basal lamina. On the other hand, the adult vertebrate epidermis is multicellular, and stratified, overlying a fibrous and vascular mesoderm. Proliferative precursor cells are present in the basal layer and differentiate and proliferate to any cell types present in the outer epidermis when the epidermal cells are lost from the surface (Lillywhite and Maderson, 1988).

The epidermis has evolved to function as a protective barrier against hazardous environmental insults including microbial, physical and chemicals threats (Baroni et al., 2012). In higher order animals, the integuments or skins are typically tightened by intercellular junction and cytoskeletal proteins, which restrict the diffusion of fluids and solutes between cells by acting as physical barriers (Baroni et al., 2012; Lillywhite and Maderson, 1988). However, the composition of this primary barrier varies among phyla. In terrestrial vertebrates, a keratinized epidermis is the primary barrier whereas in Ecdysoza (Arthropoda and Nematodes) it is a cuticle covered epidermis and in Cnidarians and Lophotrochozoans a mucosal epidermis functions as the primary barrier. In Nemertea

and the Turbellaria class of Platyhelminthes, animals have a ciliated epidermis that has evolved to function for locomotion and defense mechanisms; it contains gland cells that secrete mucus to cover the adjacent substrate and allow epidermal cilia to act on this to generate a gliding motion as well as secreted mucus prevent the invading predators (Bereiter-Hahn et al., 2012).

The function of epithelia is not simply to act as a barrier, despite the importance of this role. Though the epithelial structure varies among organisms, the core functional roles are conserved. For example, despite having other functions the critical role of epithelia in responding to external injury and aiding in tissue repair is likely ancient and conserved.

## 1.2 Wound healing and regeneration across metazoans

“Homeostasis is defined as the physiological processes that maintain the constant cell numbers in renewing organs” (Blanpain and Fuchs, 2009). Because loss of cells in the epidermis would impair its barrier and morphological functions, maintenance of homeostasis in an injured epidermis is essential for organisms to survive. Wound healing is one of the key steps in maintaining homeostasis in the injured epidermis. Both the immediate response and the damage repair mechanisms are conserved among eukaryotes, although the actions and complexity of wound responses correlate with tissue and organ intricacy (Gumbrys, 2017). Generally, the wound healing process can be divided in three highly coordinated stages: inflammatory response, wound closure, and extracellular matrix (ECM) remodeling (Sherratt and Murray, 1990). The initial step in wound healing is transcription-independent and conserved among metazoans:  $\text{Ca}^{2+}$  influxes and diffusion of  $\text{H}_2\text{O}_2$  and ATP in epithelial tissues result in cell shape changes and the formation of actomyosin structures (Cordeiro and Jacinto, 2013). These responses crosstalk with each other and integrate with immune responses, which recruit immune cells to the wound area

(Tiozzo and Copley, 2015). However, considerable variation exists in this process and the time taken by each step depending on the species, size, and wound types (Sonnemann and Bement, 2011). Ideally the healed wound area should recapitulate the original tissue state after a complex wound healing process, but this not the case for all metazoans. The wound healing processes may be followed by a regenerative or reparative process, depending on an organism's immune responses and remodeling of the ECM (Arenas Gomez et al., 2020). Regardless of whether the process leads to regeneration or damage repair, wound healing is ubiquitous among metazoans.

### 1.2.1 Wound healing

Cnidaria are pre-bilaterians that diverged ~650 million years ago and animals within it consist primarily of two epithelial sheets (Dunn, 2009; Hejnal et al., 2009). Though the life cycle of Cnidarians varies from species to species, this phylum can be divided in two major groups: Anthozoa, which forms polyps, and Medusozoa, which forms medusa and polyps (Technau and Steele, 2011). Although Cnidarians are not well studied regarding their wound response, several studies have reported the cellular wound response in polyps and hydrozoans (DuBuc et al., 2014; Lin et al., 2000). In *Nematostella*, the aboral part of the animal becomes deflated immediately after body wall puncture, actin becomes enriched in the wound site, and filopodia in cells surrounding the wound site use actin to stretch and close the wound (DuBuc et al., 2014). As in other organisms (see below), mitogen activated protein kinase (MAPK) signaling pathway plays crucial roles in modulating the immune response in *Nematostella* and pharmacological perturbation of MAPK pathway leads to dramatic defects in wound healing processes (Arenas Gomez et al., 2020; Arthur and Ley, 2013; DuBuc et al., 2014).

Hydra is a well-studied Cnidarian in the field of regeneration and wound healing. Its molecular wound responses are universal regardless the site of amputation, facilitating transplantation assays in this model (Galliot, 2013). During transplantation, wound healing between grafts are initiated by filopodial interactions and gastrodermal re-adhesion; this is followed by contact between epidermal cells and reestablishment of cellular junctions on the graft site (Bibb and Campbell, 1973). Ectodermal cells also contribute to the wound healing processes in Hydra. It has been shown that immediately after decapitation the ECM is retracted at the wound site, which is followed by re-fusion of the ectoderm and endoderm layers (Shimizu et al., 2002). Days after injury, the epithelial cells reestablish the body wall, known as mesoglea and regain their initial cuboidal shape. In addition, Hydra epithelial cells can reassemble polyps from pellet of disassociated cells (Gierer et al., 1972; Petersen et al., 2015), which indicates the high degree of wound healing and tissue rearrangement potential in Hydra.

*C. elegans* is a free-living nematode and studies of their wound healing have shown that they share the conserved initial wound response program. Wounding at the syncytial epidermis (Chisholm and Hsiao, 2012) of *C. elegans* triggers a  $\text{Ca}^{2+}$  influx which is required for wound site recruitment of F-actin (Xu and Chisholm, 2011). The  $\text{Ca}^{2+}$  influx requires GTL-2, which is a transient receptor potential channel melastatin (TRPM) family channel (Xu and Chisholm, 2011). Another epidermal signaling pathway protein, EGL-30, and its upstream regulator phospholipase C (PLC) are required to induce internal  $\text{Ca}^{2+}$  release by producing IP3 (Baylis et al., 1999). Loss of function of this epidermal signal transduction pathway severely compromises the wound healing process, which ultimately leads to animal death. The epidermal wound closure requires F-actin polymerization, which

depends on Cdc42, small GTPase, and Arp2/3 (Xu and Chisholm, 2011). Functional loss of GTPase impairs wound healing by blocking the actin polymerization processes (Xu and Chisholm, 2011).

The Arthropod *Drosophila melanogaster* is a widely used model organism to study epithelial wound healing at the cellular, molecular, and genetic levels. The initial transcription-independent injury response through  $\text{Ca}^{2+}$  influx is also conserved in *Drosophila*. It has been shown that this initial injury response leads to a calcium flash in the wounded epithelium, which is followed by burst in reactive oxygen species (ROS) (Arenas Gomez et al., 2020; Razzell et al., 2013). Continuous contraction of actomyosin cables and cellular protrusions are the two main feature of epidermal cells in *Drosophila* wound closure (Wood et al., 2002). At embryonic stages, epithelial wounds are closed by the formation and contraction of actomyosin cables, which is followed by the withdrawing of some epithelial cells at the wound site. During re-epithelialization, opposite edge epidermal cells at the wound area interact with each other and the wound surface by extending filopodia, which eventually closes the wound (Millard and Martin, 2008; Wood et al., 2002).

Different from the process in embryos, post embryonic *Drosophila* initiate wound closure by rapid plug formation at the injury site; epithelial cells then extend lamellipodia and start crawling. During this process, a syncytia is formed by fusion of the lateral membranes of migrating epithelial cells, a process that is accompanied by chromosome duplication and polyploid cell formation (Losick et al., 2013; Omelchenko et al., 2003). Studies have shown the involvement of several other important signaling pathways in wound healing in *Drosophila* as well. For example, small GTPase, MAPK cascades, and

tyrosine kinase receptors (Stit and Pvr) are all required for epidermal cell migration and cytoskeleton reorganization during injury response (Galko and Krasnow, 2004; Razzell et al., 2013; Wood et al., 2002). Stit and Pvr are required for re-epithelialization in both embryonic and post embryonic wounds. Loss of function of Stit leads to failure in actomyosin ring assembly, which suggest that tyrosine kinase receptors contribute to the initial injury response (Wang et al., 2009). It has been shown that Stit dependent ERK signaling activates at embryonic wound, whereas MAPK/ERK-JNK signaling activates at larval wound epidermis (Galko and Krasnow, 2004). Knockdown of JNK *Drosophila* larvae halts the cytoskeleton re-organization processes and impairs the reepithelization, which also suggest the involvement of MAPK/ERK signaling pathways in early wound responses (Kwon et al., 2010).

### 1.2.2 Regeneration

Wound healing is reasonably conserved across the animal Kingdom. However, whether this process is followed by activation of a regenerative program, or a damage repair mechanism varies across metazoans. The capacity for regeneration is present in one or more species in almost every phylum, although some species can only regenerate some body structures while in other cases an entire organism can be regenerated from part of their body (Alvarado, 2000; Bely and Nyberg, 2010). For example, Hydra and planarians display remarkable ability to regenerate an entire animal (Alvarado, 2000; Bely and Nyberg, 2010; Duncan and Sánchez Alvarado, 2019) whereas adult urodeles, such as newt and axolotls, can regenerate their limbs, tails, jaws and ocular lenses (Dinsmore, 1991). Another extensively studied vertebrate, zebrafish, can regenerate their appendages, cardiovascular system, and central nervous system (Li et al., 2015; Poss et al., 2002). In



mammals, ability of regeneration is more restricted than any other phyla. However, rodents can regenerate the digit tips and African spiny mice (*Acomys*) can regenerate the ear pinna, and skin (Gawriluk et al., 2016; Koopmans et al., 2021; Seifert et al., 2012; Seifert and Muneoka, 2018).

Generally, the regeneration process in Metazoans involves two different mechanisms: morphallaxis and epimorphosis. In morphallaxis, redeployment of existing undifferentiated cells regenerates the missing body part or organism in the absence of active cell proliferation. In epimorphosis, cellular proliferation, and the formation of blastema tissue leads to the reconstruction of missing body parts or entire organisms (Morgan, 1901). The phenomena of regeneration can be occurred through the formation of blastema with lineage restricted cells (e.g. salamander limb regeneration); proliferation of existing cells (e.g. tadpole tail restoration); without cellular proliferation (e.g. *Hydra* regeneration through morphallaxis); or by combination of some of these mechanisms (e.g. combined morphallactic and epimorphic regeneration in planarians) (Agata et al., 2007; Bely and Nyberg, 2010; Brockes and Kumar, 2008). Morphallactic regeneration happens both in bilaterian and non-bilaterians, whereas epimorphic mode of regeneration predominates in bilaterians. In addition, several similarities between these two methods of regeneration suggests these processes are evolutionary related (Agata et al., 2007; Bely and Nyberg, 2010; Candia Carnevali and Bonasoro, 2001; Carnevali, 2006).

*Hydra* are freshwater polyps with a tubular and radially symmetric body that can completely regenerate their heads after amputation (Bridge et al., 1995; Lenhoff et al., 1986). A tiny fragment of *Hydra* can regenerate an entire organism. Moreover, it has been demonstrated that disassociated cells from *Hydra* can reaggregate and, after re-establishing

polarity, regenerate an entire organism (Gierer et al., 1972). Although Hydra are diploblastic, they have three separate lineage restricted stem cell pools that coordinate together to regenerate any missing tissue. The myoepithelium of Hydra consists of two layers of cells with characteristics of both epithelia and muscle tissue; cells in this myoepithelium are unipotent and continuously renewed (Li et al., 2015). Interstitial stem cells are dispersed in the ectodermal epithelial layer, are multipotent, and can regenerate neurons, gland cells, nematocyte and gametes (David, 2012; David and Murphy, 1977). Hydroxyurea-mediated blocking of DNA synthesis showed that head regeneration can take place without DNA synthesis or detectable cell proliferation, which suggests morphallactic regeneration is dominant in Hydra (Cummings and Bode, 1984). Later studies showed that mid-gastric bisection of Hydra activates injury-induced apoptosis of interstitial cells through the MAPK/ERK pathway, leading to the activation of Wnt3 signaling in interstitial progenitor and endodermal epithelial cells and the initiation of head regeneration (Chera et al., 2009). Activation of  $\beta$ -catenin by Wnt3 leads to the remodeling of epithelial cells, which replace the missing head. Apoptosis also induces interstitial cell proliferation, suggesting the presence of both morphallactic and epimorphic regeneration mechanisms in Hydra (Chera et al., 2009; Cummings and Bode, 1984).

Zebrafish is a well-studied model system for vertebrate regeneration phenomena. Zebrafish can remarkably regenerate their fins, cardiovascular system, nervous system, and scales (Becker et al., 1997; Bereiter-Hahn and Zylberberg, 1993; Bernhardt et al., 1996; Poss et al., 2002). The zebrafish caudal fin is comprised of 16-18 dermal bone rays that are connected by soft tissues. The epidermis covers the wound surface within several hours after amputation of caudal fins (Li et al., 2015). After that, fibroblasts and osteoblasts in

the caudal fin form a wound blastema after migrating to the wound area (Jaźwińska et al., 2007). The formation of a wound blastema involves the dedifferentiation of mesenchymal cells and recruitment of progenitor cells to the wound area (Knopf et al., 2011). Following the formation of a blastema, Hh, activin- $\beta$ A, and retinoic acid (RA) function to establish the proper pattern in the regenerating fin (Quint et al., 2002). It has also been shown that zebrafish can regenerate their hearts within 2 months after 20% ventricular amputation. Proliferation of cardiomyocytes at the epicardial edge of newly formed myocardium leads to regeneration of zebrafish heart (Poss et al., 2002). Knockdown of mitotic checkpoint kinase Msp1 leads to scar formation and regeneration failure in the zebrafish heart (Poss et al., 2002) and lineage tracing in regenerating zebrafish hearts demonstrated that both dedifferentiation and proliferation of cardiomyocytes are involved in zebrafish heart regeneration (Jopling et al., 2010; Kikuchi et al., 2010). Formation of blastema and active cellular proliferation suggest that epimorphic regeneration precedes in zebrafish.

Urodele amphibians such as aquatic salamander newts and salamander are remarkable regenerators and can regenerate limbs, tails, brains, spinal cords, and ventricle of hearts (Amamoto et al., 2016; Echeverri and Tanaka, 2002; Godwin et al., 2017; Kragl et al., 2009). Formation of an apical epidermal cap (AEC) by proliferating epithelial cells that migrated from the stump surface is the first step of salamander limb regeneration upon amputation. Proliferating stump cells beneath the AEC form a blastema at the distal end of the stump and acquire a cone shape as regeneration proceeds (Whited and Tabin, 2009). It has also been shown that adjacent multinucleate myofibers at the amputation site dedifferentiate to form mononucleated progeny and contribute to the formation of blastema (Echeverri et al., 2001; Lo et al., 1993). At the same time, there is evidence that in newt

limb skeletal muscle, Pax7<sup>+</sup> multipotent satellite cells are activated and incorporated in blastema formation (Morrison et al., 2006). Dedifferentiation of mature mesenchymal cells requires Hh signaling (Singh et al., 2012). However, proliferation and migration of dedifferentiated cells do not require Hh signaling, which suggests that in salamander limb regeneration Hh regulates the formation of blastema at early stage of regeneration (Singh et al., 2012).

Though mammals do not have a great ability to regenerate complex structures as do salamanders, they likely harbor potential to regenerate a variety of injured tissues including skeletal muscle, bone, peripheral nerve, urinary bladder, and skin (Carlson, 2005; Li et al., 2015). Progenitor cells associated with the damaged tissues are the origin of most mammalian tissue regeneration. For instance, satellite cells present in the muscle fiber are the source of myoblasts during mammalian muscle regeneration (ChargÉ and Rudnicki, 2004). The mammalian pancreas is a slowly renewing organ and believed to apply two mechanisms for regeneration: proliferation of remaining  $\beta$ -cells and differentiation from pancreatic progenitor cells (Beltrami et al., 2012). Neonatal rodent hearts also show transient potential to regenerate after partial amputation (Porrello et al., 2011). In these hearts, injury leads to the local proliferation and morphological changes of cardiac cells, but within 7 days the regenerative potential is lost due to fibrotic scar formation (Porrello et al., 2011). This last example shows that molecular pathways and mechanisms triggered by wound healing are likely those which determine a tissues regenerative potential.

### 1.3 Epidermal role in regeneration

It has been known for decades that coordination between the wound epithelium and underlying wound mesenchyme is required for proper regeneration. It has been demonstrated that salamander limb regeneration is halted if the formation of wound epithelium is prevented by the insertion of an unamputated limb stump into the body wall (Goss, 1956) or by grafting a skin flap over the amputation stump (Mescher, 1976). Wound epithelium is also important for the restoration of fingertips in children. It has been shown that if the wound edges are sutured together, children lose their ability to regenerate lost fingertips (Illingworth, 1974). The molecular mechanism underlying the contribution of wound epithelium in regeneration is described in vertebrate model systems. For example, amputation of a salamander limb leads to the formation of an AEC, which directly contacts the mesenchyme beneath the AEC, changes the shape, and polarizes the secretory machinery (Nye et al., 2003). Wound epithelia have been shown to secrete crucial regeneration signals through the interaction with underlying wound mesenchyme such as Fgfs, Shh, Bmps, and Wnts (Poss et al., 2002; Quint et al., 2002; Whited and Tabin, 2009). Secretion of Fgf10 signals are sufficient to induce regenerative response in *Xenopus* (Yokoyama et al., 2001). Exogenous induction of Fgf10 in a non-regenerative *Xenopus* limb stump is able to induce the expression of regeneration responsive genes including Shh, Msx-1, and Fgf10 (Yokoyama et al., 2001). However, formation of AEC is regulated by the wound mesenchyme. The ablation of blastema-derived signals restrict the formation and function of the AEC, which suggests that the AEC and wound mesenchyme orchestrate limb regeneration together (Beck et al., 2006).

Nerves also play crucial role in amphibian limb regeneration. It's been shown that without nerves the AEC forms but is not maintained and formation of the wound

blastema fails (Stocum, 2011). A crucial regeneration response signal nAG is induced after wounding, which is necessary for the formation of the AEC (Kumar et al., 2007). Studies in accessory limb models in axolotls also showed that a nerve dependent transcription factor Sp9 is required for the formation of wound epithelium. Expression of Sp9 is induced in basal keratinocytes of the AEC through the activation of endogenous nerve factor keratinocyte growth factor (KGF) (Satoh et al., 2008).

In summary, studies in various model systems within the animal kingdom have contributed to our current understanding of the underlying mechanisms of wound healing and regeneration. Hydra, sea urchin, *Drosophila*, zebrafish, salamander and cultured mammalian cells have provided the ground to explore the mechanisms of cellular migration, wound healing and regeneration. Comprehensive analyses of wound healing and regeneration have revealed a conserved core of molecules and signaling pathways that mediate the response to tissue damage, suggesting an ancient damage repair mechanism. However, are there any conserved wound induced mechanisms that lead a tissue to choose regeneration over reparative response is great question and still unexplored in the field of regenerative biology.

#### 1.4 Planarians as a model system in studying wound healing and regeneration

Planarians are commonly found in freshwater, are bilateral symmetric metazoans of the phylum Platyhelminthes, and have the remarkable ability to regenerate missing tissues (Reddien and Alvarado, 2004). In planarians as in other regenerative organisms, wounding elicits a series of regeneration responses that eventually restore the lost structures. Following amputation, strong musculature contraction at the injury site occurs within seconds and minimizes the wound area by mediating direct contact between the

dorsal and ventral epidermis (Baguña, 1988; Ogawa et al., 2002). A few hours after the outer epithelial cells cover the wound area, a global mitotic response is observed (Wenemoser and Reddien, 2010) and cellular proliferation near the wound site leads to the formation of an unpigmented regeneration blastema around 48 hours post amputation (Newmark and Sánchez Alvarado, 2000; Saló and Baguña, 1986; Wenemoser and Reddien, 2010). In planarians, this cellular proliferation is highly restricted to a particular undifferentiated cell with large nuclei known as neoblasts (Dubois, 1949), which are the source of new tissue in planarian regeneration. Neoblasts are distributed throughout the mesenchyme, except at the anterior tip above the photoreceptors and within the pharynx organ, which is used for both eating and excretion (Reddien and Alvarado, 2004). Moreover, it has been demonstrated that a single neoblast transplantation into a stem cell depleted host (by lethal radiation at 6000 rad) can restore the neoblast population and eventually replace all existing host cells with its descendants (Wagner et al., 2011). This experiment suggests that a specific class of neoblasts, termed as cNeoblast, can give rise to any cell type during planarian regeneration (Wagner et al., 2011).

Any injury event, even a needle poke, activates neoblast proliferation. Moreover, there are two mitotic peaks of neoblast proliferation following wounding, where the first peak is a systematic response across the animal and the second occurs at the injury site and leads to the restoration of lost tissues (Wenemoser et al., 2012). Furthermore, lineage tracing experiments with BrdU pulse of neoblasts followed by chase have shown that the regenerating blastema is mostly composed of wound induced post-mitotic descendants of neoblast cells with little or no contribution of existing cells (Eisenhoffer et al., 2008). Neoblasts are also recruited to the injury site. It has been shown that amputation anterior

to the photoreceptors, a region devoid of stem cells, accumulates neoblast cells (Wenemoser and Reddien, 2010). In short, these experiments suggest the formation of regenerating blastema requires both the cellular proliferation and migration of neoblast cells (Newmark and Sánchez Alvarado, 2000). However, the mechanisms that induce these stem cell behaviors are not fully known or understood.

#### 1.4.1 Planarian epidermis in wound healing and regeneration

The adult planarian epidermis (Figure: 1.1) is composed of a single, monostratified layer of post mitotic ciliated and non-ciliated cells (Rompolas et al., 2010). In *Schmidtea mediterranea* (S.med), a highly regenerative and well-characterized planarian species, the ventral epidermis has an overwhelming abundance of ciliated cells whereas the dorsal epidermis contains larger regions of non-ciliated cells. The ventral ciliated cells project multiple cilia that are required for planarian locomotion (Hori, 1989; Morita and Best, 1974). Comparable to other invertebrates, septate junctions tightly adhere the planarian epidermal cells to each other at their apical edge and focal adhesions attach the epidermis to the basal membrane (Hori, 1989). The planarian epidermis is also secretory and contains a large number of intracellular vesicles that are present in dorsal and ventral epidermal cells. Another signature of the planarian epidermis is a structure termed rhabdites, which are rod-shaped vesicles filled with colorless gelatinous materials that are thought to produce mucus for ciliary gliding (Caira and Littlewood, 2013).

To maintain epidermal homeostasis, planarians need to turn over the epidermal cells rapidly. However, the terminally differentiated epidermal cells have not been observed to undergo cellular division (Hori, 1989; Tu et al., 2015). The only dividing cells



in planarians are the neoblasts (Newmark and Sánchez Alvarado, 2000). Thus, the planarian epidermis is maintained by the differentiation and integration of neoblast progeny (Tu et al., 2015; Zeng et al., 2018). To do so, epidermal progenitors must traverse through the basal membrane and integrate into the epidermis where they complete the differentiation processes (Hori, 1989; Tu et al., 2015). Early single cell transcriptomic studies identified a subset of planarian neoblasts called zeta-neoblasts, which are required for epidermal cell differentiation and maintenance (van Wolfswinkel et al., 2014). The zinc finger transcription factor Zfp-1 specifies these zeta class neoblasts, which then differentiate and into prog-1 early progenitors and agat-1 late epidermal progenitors (Eisenhoffer et al., 2008; Tu et al., 2015; van Wolfswinkel et al., 2014). Another transcription factor Erg-5 is required for the final stages of maturation of epidermal progenitors and their incorporation into the epidermal layer (Tu et al., 2015). Expression patterns of epidermal progenitor markers such as Prog-1, Agat-1, Zpuf-6 and differentiated epidermal marker Vim-3 suggests that epidermal progeny cells migrate outwards and incorporate in the epidermis through their differentiation process (Tu et al., 2015).

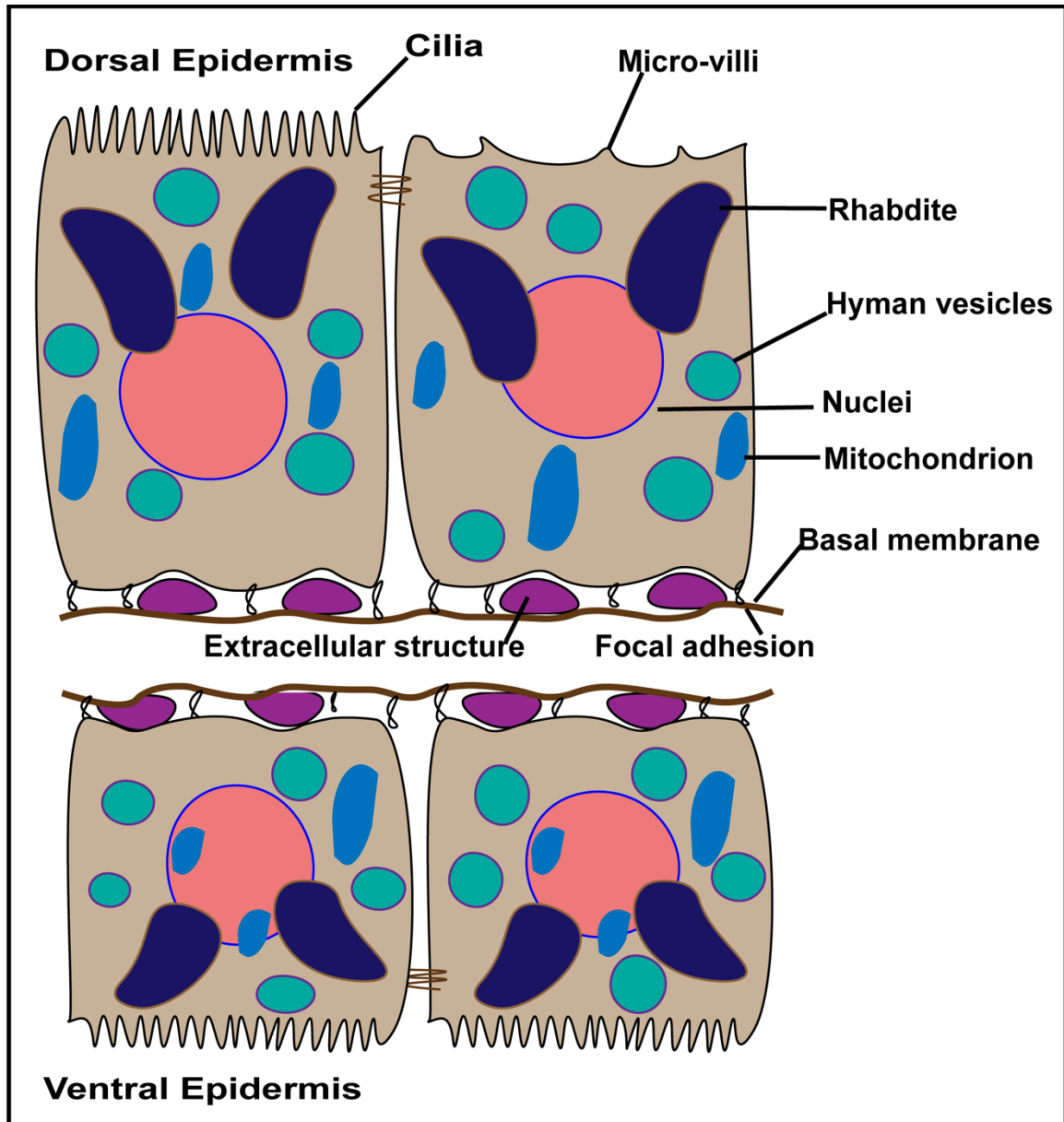


Figure 1.1 Schematic representation of the planarian epidermis  
 The planarian epidermis is a single layer sheet with both ciliated and non-ciliated cells. The ventral epidermis is composed of mainly multiciliated cuboidal cells. The epidermal cells are attached to a basal membrane by focal adhesion. Both the dorsal and ventral epidermal cells contain rhabdites and cellular vesicles.

#### 1.4.1.1 Planarian wound healing

Immediately after amputation, the planarian wound edge epidermis can begin making contacts due to the contraction of body wall musculature. At the same time, the mature epidermal cells undergo massive morphological changes by ejecting cilia, secreting rhabdites, losing apical basal polarity, and extending along the wound surface (Morita and Best, 1974). The epidermal cell extension facilitates the wound closure by stretching over the wound surface and closing the injury area. Shortly after wound closure the muscle contraction relaxes, which brings more epidermal cells to the wound area through passive migration due to the elongation of wound epidermal cells (Hori, 1989). In experiments where all neoblast cells were eliminated by a lethal dose of radiation prior to amputation, planarians can still close the wound as normal, suggesting that planarian wound closure is independent of cellular proliferation (Hori, 1979). However, polymerization of actin is critical for planarian wound closure. It has been demonstrated that perturbation of actin by cytochalasin will halt the wound healing process in planarians (Pascolini et al., 1984). Though there is some controversy regarding the assertion that muscle contraction brings the wound edge together (Chandebois, 1979), the most accepted model of planarian wound healing is the migration of epidermal cells due to stretching and extension over the wound surface.

#### 1.4.1.2 Planarian epidermis and regeneration

In planarians, wound closure is followed by a tremendous regenerating response that is achieved, in part, through stem cell proliferation and migration to the wound site (Newmark and Sánchez Alvarado, 2000). This cellular proliferation supports the formation of a regenerating blastema that eventually differentiates into cell types lost to injury. At the

second day post amputation, epidermal regeneration is observed as epidermal progenitor cells migrate from the blastema and incorporate into the wound epithelia (Hori, 1989). These epidermal progenitors are distinguished by the presence of epidermal cell specific structures, the rhabdites (Morita and Best, 1974). Integration of new cells into the wound epithelia increases the density and thickness of epidermal layers at the wound site (HORI, 1978). Following integration into the wound epithelium, these new epidermal cells reestablish cellular junctions and acquire apical-basal polarity (Morita and Best, 1974). [you need a transition sentence here; something about how although these changes have been characterized, how they impact downstream regeneration is not well understood.

In recent years, many molecular and cellular studies have been executed to understand the molecular mechanisms underpinning planarian regeneration, the large majority of them focusing on changes in the stem cell population (van Wolfswinkel et al., 2014; Zeng et al., 2018). The first published single cell analysis in planarians identified two major classes of neoblast that are functionally different (van Wolfswinkel et al., 2014). A zeta class of neoblasts ( $\zeta$ neoblasts) that give rise to the planarian epidermis and are not themselves required for regeneration, and a sigma class of neoblasts that proliferate in response to injury and give rise to all other differentiated cell lineages and the zeta class of neoblasts (van Wolfswinkel et al., 2014). This paper also showed that zeta neoblasts and their derived epidermal progenitors are distributed throughout the mesenchyme (van Wolfswinkel et al., 2014). Although the epidermal lineage class of neoblasts may not respond to injury signals, they are still important for regeneration as they give rise to the cells that maintain the regeneration blastema. For instances, knocking down of a zeta class

specific gene, zfp-1RNAi worms showed initial blastema regeneration, however after 7dpa, regenerated blastema subsequently regressed and lead to ultimate lethality (van Wolfswinkel et al., 2014; Wagner et al., 2012).

One recent RNA-seq study did examine the planarian epidermis at a molecular level, using a combination of bulk planarian epidermis isolated with ammonium thiocyanate and single cell transcriptomics (Wurtzel et al., 2017). They conclude that signaling from the mature epidermis likely regulates gene expression in the neoblasts and progenitors, driving their differentiation toward an epidermal fate during normal cell turnover (Wurtzel et al., 2017). At the same time, another group observed that a Myb-type transcription factor, Smed-myb-1, regulates temporal identity during post mitotic maturation (Zhu and Pearson, 2018) and that RNAi knockdown of Smed-myb-1 abolishes the expression of early epidermal progenitor markers (e.g., prog-1) but not late progenitor markers (e.g., agat-1). This result suggests that loss of Smed-myb-1 terminates the early progenitor state and directly shifts neoblasts to the late epidermal progenitors states (Zhu and Pearson, 2018). Based on these two different mechanisms of epidermal progenitor differentiation, it is reasonable to assume that there might be a feedback mechanism where mature epidermal cells transduce signals to the neoblast cells for progeny differentiation and neoblast cell control the differentiation mechanisms through expression of selective transcription factors.

Differentiation of zeta neoblasts into progenitor cells and ultimately maturation of epidermis is essential for both planarian regeneration and maintaining homeostasis. However, how these specific cell types respond to injury signal and whether this response triggers a subsequent regenerative response (versus a reparative response) remains a great

question in planarian regeneration. One of the few studies conducted to identify wound induced genes in differentiated planarian tissues did so by ablating neoblast cells with lethal irradiation and examining gene expression changes in irradiated, amputated animals (Wenemoser et al., 2012). From this study, two waves of wound induced genes were shown where the first wave of genes are mostly conserved immediate early genes that are reported to express in a translation independent manner due to the exposure of various stimuli (Almendral et al., 1988; Greenberg et al., 1986). In case of amputation, those immediate early genes are expressed around 30 mins of post amputation e.g., *jun-1*, *fos-1*, *egr-2*, *egr-3*, *egr-4*, and *egr11* (Wenemoser et al., 2012). Another category of genes were designated second wave genes and they express 6 to 12 hours post amputation; this wave includes *wntless*, *wnt1*, *inhibin-1*, *noggin-like1* (*nlg1*), *follistatin*, *glypican-1* (*gpc-1*), *adam-1*, *adam-2*, and *delta-1* (Wenemoser et al., 2012). Colorimetric in situ hybridization of these wound induced genes showed that most of the wound induced genes expressed near the wound and differentiated cell types including subepidermal and epidermal cells. For example, the early wound induced genes *fos-1* is induced near the wound site whereas *delta-1* and *ston* express highly in the epidermis after amputation. Another wound induced gene *hadrian* is expressed between 6-12hpa and showed increased expression in the epidermis around the entire periphery of injured fragments (Wenemoser et al., 2012; Wurtzel et al., 2015). Time course experiments in which scRNA-seq on 619 cells was performed along with bulk RNA-seq on blastema tissue has shown that a generic wound response is activated in all cell types regardless the regenerative outcome (Wurtzel et al., 2015). Bulk RNA-seq of both anterior and posterior facing wound tissues revealed 128 genes that were wound-induced at least one time point of 3h, 6h and 12h post amputation.

To identify the cell types that express these wound induced genes, sc-RNA-seq was conducted on the FACS sorted cells obtained from wound site after 4 and 12hpa and found that 10 of these genes express in all cell types and 5 genes were epidermal specific including Jun-1, TRAF-1, Ston, and Hadrian (Wurtzel et al., 2015).

Though different cell types respond to injury and induce the expression of wound induced genes, somehow these intrinsic cues must be integrated with environmental and internal signaling mechanisms to proceed with appropriate tissue regeneration. The epidermal growth factor receptor (EGFR) pathway has been shown to play multiple significant roles in planarian regeneration and may serve as one such integral pathway (Fraguas et al., 2011). Both EGFR family genes *egfr-1* and *egfr-3* are required for cellular differentiation during regeneration; RNAi of *egfr-1* showed decreased differentiation of eye pigment cells whereas, *egfr-3* knockdown showed smaller blastema formation and abnormal differentiation of *cintillo* expressing cells (Fraguas et al., 2011). Another conserved pathway is both conserved and essential role in the early stages of regeneration is the extracellular signal regulated kinase (ERK) pathway. ERK is a conserved signaling pathway that regulates a myriad of cellular functions including cell proliferation, differentiation and migration (Chang and Karin, 2001; Nishida and Gotoh, 1993). ERK activity is required for blastema cells differentiation in planarians (Tasaki et al., 2011). Both pharmacological inhibition and RNAi of *erk* showed smaller blastema growth and differentiation defects (Tasaki et al., 2011). Another study showed that activation of ERK via phosphorylation (pERK) drastically increases within 15 mins post amputation and goes back to baseline after 24h post amputation in planarians (Owlarn et al., 2017). Pharmacological inhibition of ERK by PD0325901 and U0126 resulted in robust

regeneration defects in both anterior and posterior amputation. In addition, early wound induced genes such as *wnt1*, *runt* and *notum* were repressed in drug treated worms (Owlarn et al., 2017). Moreover, the recruitment of neoblast at the wound regions was also disrupted in ERK inhibited animals, which suggest that early wound signals induce the activation of ERK in a stem cell independent manner and stem cells require ERK activation for proper regeneration (Owlarn et al., 2017).

### 1.5 Stretch or morphological changes induced transcriptomic changes

Mechanotransduction is the process by which cells respond to their physical environment or morphological changes by translating mechanical signals into biochemical stimuli (Dahl et al., 2008). These mechanical forces regulate several cellular responses and are important for development, cellular divisions, cell-cell adhesion, and cell fate regulation (Chen et al., 2004; Engler et al., 2006; Gilbert et al., 2010). Several studies have shown that mechanical forces induce transcriptomic changes in epithelial cells and cardiac cells (Kunnen et al., 2018; Ledwon et al., 2020; Rysa et al., 2018). It has been demonstrated that mechanical stretching induces the epithelial cell division through *piezo1* channel activation (Gudipaty et al., 2017). Furthermore, mechanical force triggers the cells that are in G2 phase to activate ERK1/2 and eventually activate the transcription of cyclin B that drive the cells into mitosis (Gudipaty et al., 2017). Another study has shown that mechanical forces induce the expression of several mechanoresponsive genes in a time dependent manner including *tnc*, *mmp*, *sfrp2*, *spp1*, *ccr1* *msr1* and *pla2g2f* (Ledwon et al., 2020). In addition, changes in nuclear shape also alter the expression of genes associated with nuclear envelope (Rapisarda et al., 2017). For example, loss of p63 transcription factors in developing mouse skin, epidermal progenitors undergo nuclear shape alteration



and decrease the expression of nuclear envelope components including lamin B1, lamin A/C, plectin, nesprin-3 and sun-1 (Rapisarda et al., 2017).

The aforementioned studies correlate the mechanical stretching or cell shape changes with transcriptomic changes in vertebrate system. However, how mechanical forces or cellular stretching induce the transcriptomic changes in planarian models has yet to be explored. Although it has been shown, separately, that right after amputation planarian epidermal cell stretch to cover the wound surface (Gumbrys, 2017; Hori, 1989) and that the expression of immediate early genes is induced at this time in a translation independent manner (Owlarn et al., 2017; Wenemoser et al., 2012). Yet the importance of or mechanisms underlying stretch induced transcriptomic changes in planarian epidermal cell have not been discussed yet. In this study, I will explore the genes that express right after amputation in stretched epidermal cells and, in addition, test the functional roles of epidermal genes in planarian regeneration and homeostatic maintenance.

## CHAPTER 2. NEW AND CUSTOMIZED METHODS ENHANCE THE IDENTIFICATION OF GENES IN THE PLANARIAN EPIDERMIS

The adult planarian epidermis is a single layer epithelial sheet consisting of both ciliated and non-ciliated post-mitotic cell types (Rompolas et al., 2010). As discussed above, mature epidermal cells are derived from a specific class of neoblasts called zeta neoblasts (van Wolfswinkel et al., 2014) after series of differentiation stages that are characterized by the expression of specific markers such as *prog-1*, *agat-1*, *zpuf-6* and *vim-3* (Tu et al., 2015). As they differentiate, they migrate towards the outer epithelium that eventually integrate into the mature epidermis and express mature epidermal markers such as *rootletin*, *rest*, *blimp-1* and *pax-2/5/8* (Figure 2.1 A) (Cheng et al., 2018; Tu et al., 2015). Although previous work has shown that the zeta neoblasts are not immediately required for a regenerative response to wounding and blastema formation, the planarian epidermis is absolutely required for both homeostatic maintenance and regeneration and several genes have been reported to support these functions in this tissue (van Wolfswinkel et al., 2014; Wagner et al., 2012; Wurtzel et al., 2017). Recent study has showed that regeneration competent fragments of *Schmidtea mediterranea* possess transient regeneration activated cell states (TRACS) with distinct spatiotemporal distribution in muscle, epidermis, and intestine (Benham-Pyle et al., 2021). However, relatively little is known about the activation of gene expression in the epidermis during regeneration considering its essential role in wound healing and blastema formation. In this chapter, I wanted to identify planarian epidermal enriched genes and assess their biological function in planarian regeneration.

## 2.1 Isolation of planarian outer epithelium

As I was interested in dissecting the role of epidermal cells in planarian regeneration, I first devised a method to isolate planarian epidermal cells from the intact worms. Although a previous study used ammonium thiocyanate to isolate this tissue (Wurtzel et al., 2017), we were concerned that this long incubation (20m) in high salt conditions would affect the chromatin structure and gene expression profile. Instead, I soaked the worms in 0.1% SDS (conditions commonly used in chromatin immunoprecipitation) at room temperature for only 1 min and then used syringe needle to separate the epidermal layer from the worm body (Figure 2.1 B and C).

To identify whether I had other cell types contaminating this isolated epidermis, I conducted RT- qPCR on the epidermis and rest of the worm body (worm “carcass”) using the known epidermal marker *rootletin*, the early epidermal progenitor marker *prog-1*, the late epidermal marker *agat-1* (Tu et al., 2015) and neoblast marker *piwi-1* (Zeng et al., 2018). I found that *piwi-1* and *prog-1*, markers of cells that basically reside in the worm mesenchyme (Newmark and Sánchez Alvarado, 2000; Tu et al., 2015), are significantly higher in the worm carcass compared to the epidermis (Figure 2.1: C and D) and that even the late epidermal progenitor marker *agat-1* showed little contamination in the isolated epidermis (Tu et al., 2015). Comparatively, the epidermal marker gene *rootletin*, which expresses in the outer epidermal cells (Figure 2.1 D) (Tu et al., 2015) was highly expressed in the isolated epidermis and relatively lowly detected in the worm carcass (Figure: 1C and D). In sum, here we show that 0.1% SDS can be used to isolate planarian epidermal cells with minimal contamination of other cell types.

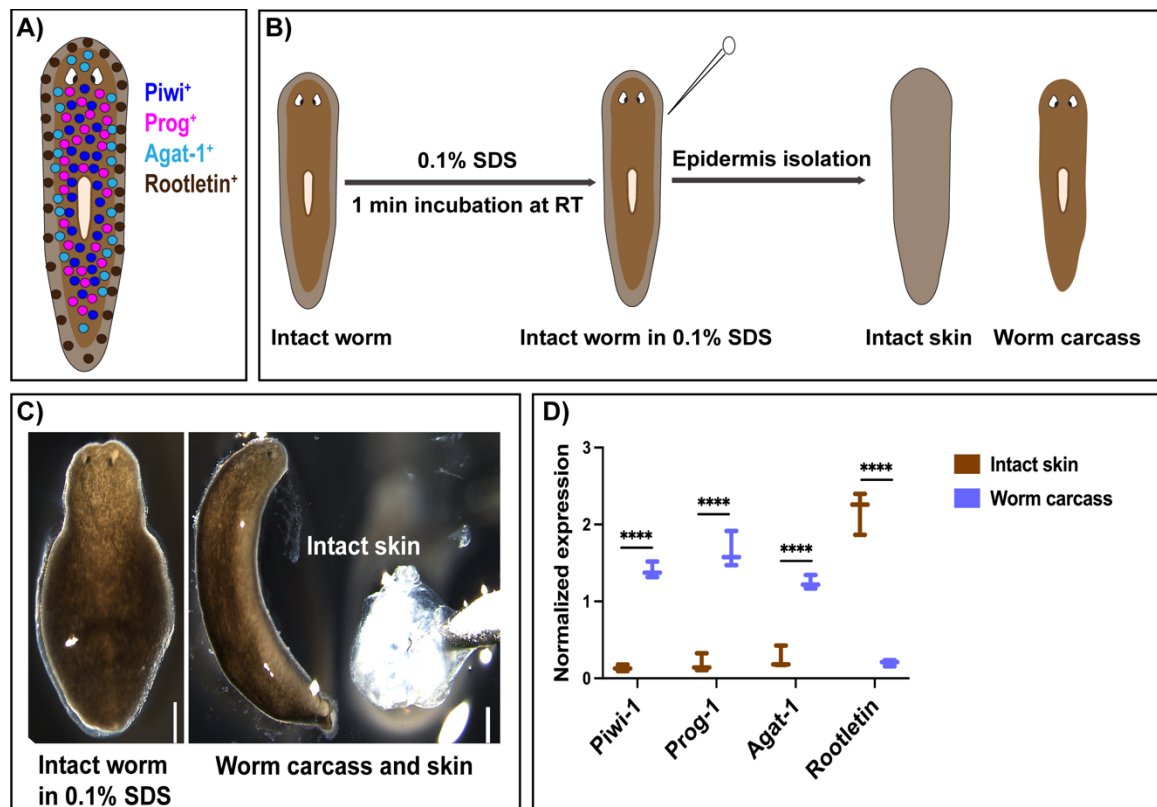


Figure 2.1 SDS based isolation of planarian epidermis

A) Cartoon is showing the expression site of different markers such as stem cells ( $piwi^+$ ), early progenitors ( $prog-1^+$ ), late progenitors ( $agat-1^+$ ), and epidermal marker ( $rootletin$ ) in intact worms. B) Schematic of planarian epidermis isolation method. C) Left panel-intact planarian soaked in 0.1% SDS, right panel- planarian after isolation of epidermis (Scale bar -500  $\mu\text{m}$ ). D) RT-qPCR analysis of isolated epidermal cells compared to worm carcass. For qPCR, neoblast ( $piwi-1$ ), early progenitor ( $prog-1$ ), late progenitor ( $agat-1$ ) and epidermal ( $rootletin$ ) markers were used. Normalized expressions were calculated using  $\beta$ -tubulin.

## 2.2 Custom RNase-H based ribosomal RNA depletion efficiently removes rRNA from planarian total RNA

Ribosomal RNA (rRNA) represents >80% of total RNA in eukaryotic cells and must be removed from RNA-sequencing samples to facilitate the reliable detection of lowly expressed but biologically important transcripts (Baldwin et al., 2021; Kim et al., 2019). The abundance of rRNA can be managed by either enrichment of mRNA using polyA tail capture or by depleting the rRNA (Kim et al., 2019). In addition, depletion of rRNA can be conducted by two different strategies: subtractive hybridization (Baldwin et al., 2021; Kim et al., 2019) or RNase-H mediated ribodepletion (Adiconis et al., 2013; Baldwin et al., 2021; Morlan et al., 2012). Though polyA selection method can have better genome coverage when sequenced at similar depth, it lacks the ability to detect important non-coding RNA, enhancers RNAs, and nuclear transcripts (Zhao et al., 2018; Zhao et al., 2014). Moreover, the planarian genome is rich in AT content, >70% (Lakshmanan et al., 2016), which contributes to the variable (10-30%) amount of rRNA in polyA selected RNA-seq libraries (Kim et al., 2019). On the other hand, it has been shown that subtractive hybridization based ribodepletion method, where biotinylated probes are used to deplete rRNA, can remove ~99% of rRNA from samples (Kim et al., 2019).

Considering the limitations of polyA selection and the high expense of biotinylated probes and magnetic beads, we decided to optimize an RNaseH-based library preparation method (Baldwin et al., 2021) for use in our planarian model, *Schmidtea mediterranea*. First, I designed ~50nt antisense DNA probes to the following planarian rRNA: 12S, 16S, 18S type I and type II, 28S, and Spacer A. I tried to minimize non-specific targeting of other transcripts by blasting the probes to the SMESG.1 genome (Grohme et al., 2018) and designed a total of 169 probes that covered most of the regions of these planarian rRNA

species. I then largely followed a previously published protocol (Baldwin et al., 2021) and optimized it for planarian RNA samples. Briefly, after extracting total RNA from either whole planarian worms or isolated epidermal tissue, the rRNA probes were hybridized to the rRNA. A thermostable RNase-H enzyme was then used to degrade DNA:RNA hybrids (Haruki et al., 2000), followed by DNase I treatment to degrade excess DNA probes and genomic DNA (Adiconis et al., 2013; Baldwin et al., 2021; Morlan et al., 2012) (Figure 2.2 A). Analyses using a bioanalyzer chip confirmed the removal of 28s and 18S rRNA peak from the samples after conducting this ribodepletion protocol (Figure 2.2 B).

As a control for non-specific degradation of RNA by RNaseH, I included “no probe” samples in my experiments. I noticed that incubation with RNase-H for 10 min (Baldwin et al., 2021) depleted the rRNA but also caused the control samples (no-probe) to have a broad shoulder, indicating possible degradation (Figure 2.2 C). To minimize this non-specific degradation, I tried optimizing the incubation time with RNaseH enzyme. I found that incubation with RNase-H for 2.5 min in my no-probe control had the lowest nonspecific degradation of total RNA (Figure 2.2 C) while still eliminating the rRNA peak in my sample with probe (Figure 2.2 B). To validate the rRNA depletion efficiency of this optimized method further, I prepared and sequenced RNA-seq libraries. To prepare the RNA-seq libraries, I isolated planarian epidermis using 0.1% SDS and extracted total RNA from both these samples and whole worms. After depletion of rRNA using RNase-H method, RNA-seq libraries were prepared according to the manuals using the KAPA RNA hyper kit (Baldwin et al., 2021).

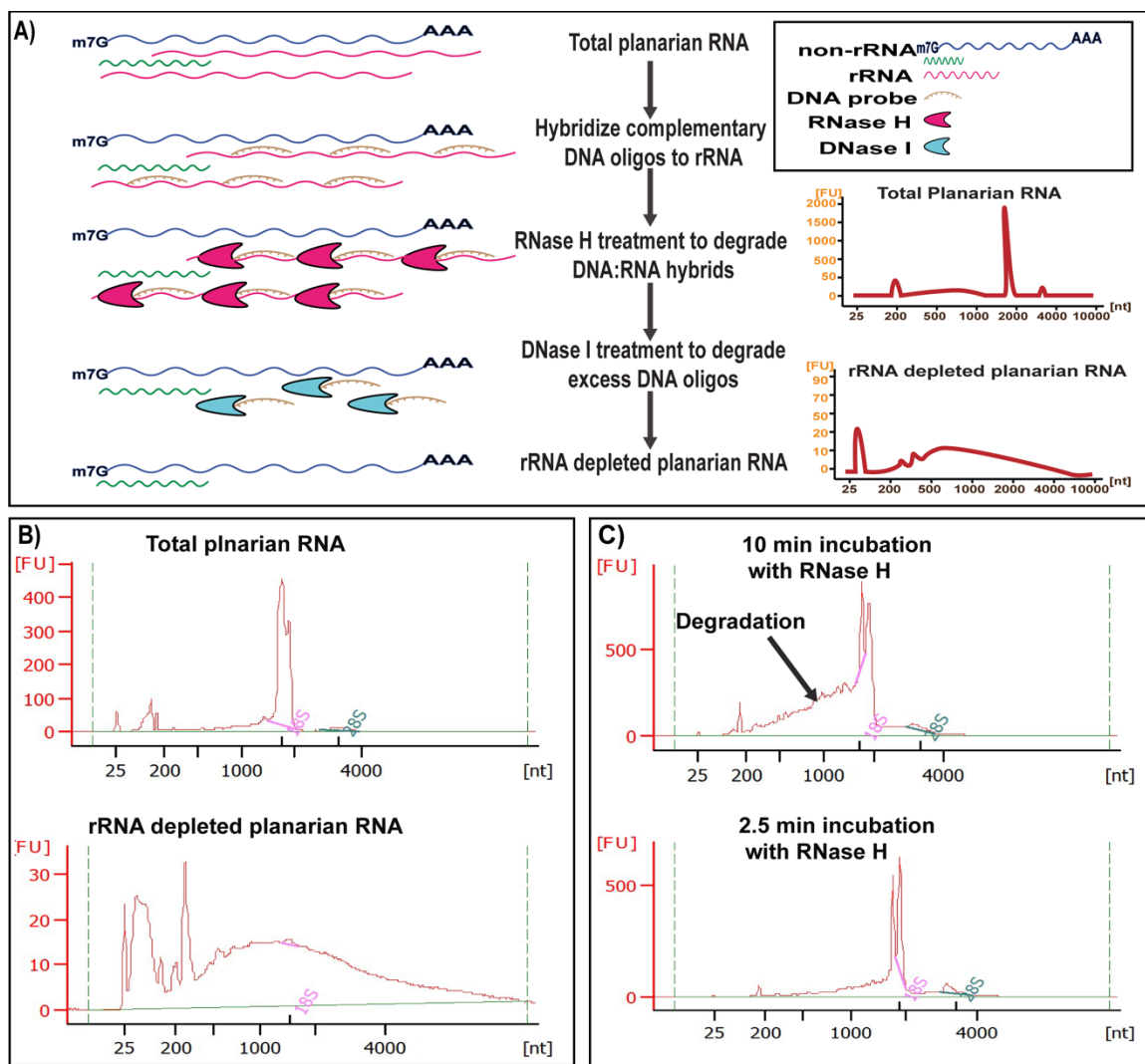


Figure 2.2 RNase-H based ribosomal RNA depletion strategy

A) Schematic representation of rRNA depletion strategy using RNase-H. Single stranded DNA probes were designed to target the complete 12S rRNA, 16S rRNA, 18S rRNA, 28S rRNA and Spacer A transcript sequences (in 50 base pair increments). B) Upper panel: bioanalyzer trace of total planarian RNA; bottom panel: bioanalyzer trace of rRNA depleted planarian RNA. C) Upper panel: bioanalyzer trace of total planarian RNA incubated with RNase-H enzyme for 10 mins but without rRNA probes. Bottom panel: bioanalyzer trace of total planarian RNA incubated with RNase-H enzyme for 2.5 mins but without rRNA probes. Ten minutes incubation showed higher non-specific degradation.

Libraries were prepared following 13 cycles of PCR amplification and sequenced in pair-end mode by the Biotechnology Center at the University of Illinois. Initially, we requested a pilot sequencing run of ~1 million reads using the MiSeq instrument to confirm that I had in fact depleted our samples of rRNA rather than simply fragmenting it. After quality checking and adapter trimming, I quantified the contaminating rRNA in the RNA-seq samples using assembled planarian rRNA as reference (Kim et al., 2019). This initial sequencing validated that I had depleted my RNA samples of rRNA, so we then requested that the core sequencing the libraries at greater depth [Table 2.1]. I then analyzed the additional sequencing in greater detail.

In addition to confirming successful ribodepletion in my samples, I also wanted to compare the rRNA levels with those in polyA selected libraries from similar planarian samples. Specifically, I downloaded an RNA-seq dataset from a published study in which the planarian epidermis was isolated after soaking in ammonium thiocyanate for 20 mins and libraries were prepared using polyA selection (Wurtzel et al., 2015). This publicly available dataset has libraries for both dorsal epidermis and ventral epidermis as well as whole worm libraries. For comparing the rRNA in the libraries, I took three available replicates from dorsal epidermis and two replicates from whole worms libraries. The polyA libraries have significantly higher amount of rRNA compared to the RNase H libraries and the amount varies between 6-24% (Figure 2.3 A). Interestingly, the most prevalent rRNA in the polyA libraries was the 16S mitochondrial rRNA, as reported previously (Kim et al., 2019). Among the ~1% of rRNA remaining in RNase-H libraries, the most prevalent rRNA was the 18S rRNA and the highest number of 18S rRNA reads among the RNase-H samples was ~48,000, a number that was significantly less than the highest number of 18S



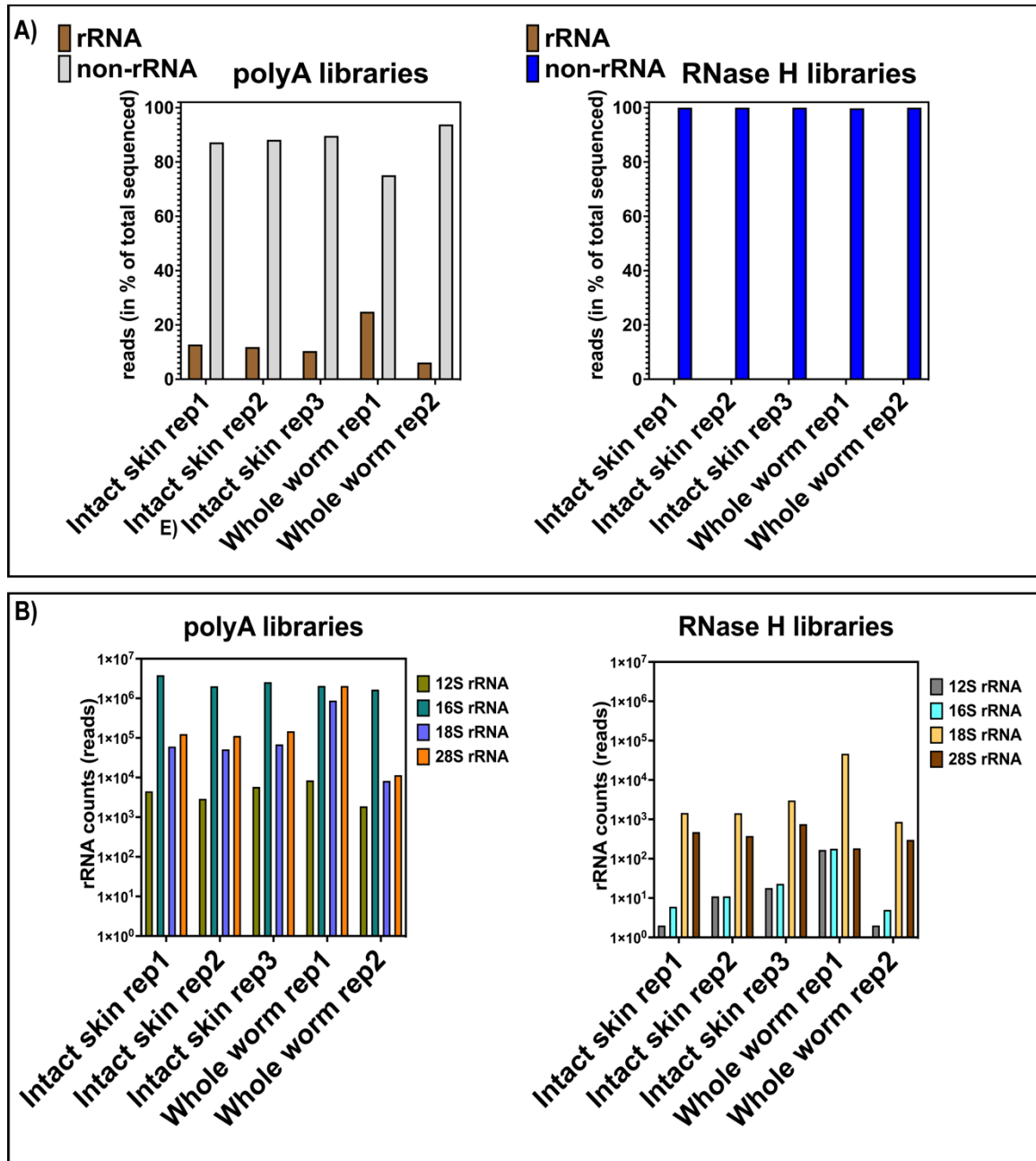


Figure 2.3 RNase H based ribodepletion efficiently depletes rRNA in planarians

A) Left panel: percent of rRNA reads in libraries generated using polyA selection (original data downloaded from Wurtzel et al., 2017 and re-analyzed). Intact skin samples for polyA datasets were isolated by incubating in ammonium thiocyanate for 20 mins. Right-panel: percent of rRNA reads in RNase-H based RNA-seq libraries generated using my optimized protocol. For RNase H libraries, intact skins were isolated using 0.1% SDS. B) Left panel: specific rRNA species in polyA selection-based libraries, Right panel: specific rRNA species in RNase-H based libraries.

Table 2.1 Sequencing depth and number of reads aligned to planarian genome

<b>Samples</b>	<b>Total reads</b>	<b>Uniquely aligned to genome</b>	<b>Uniquely aligned to genome (%)</b>	<b>rRNA Reads</b>
polyA intact skin rep1	31480903	18759291	59.60	4024048
polyA intact skin rep2	18527587	10046066	54.22	2194417
polyA intact skin rep3	26835689	17063796	63.59	2785885
polyA whole worm rep1	20075378	11492259	57.24	4989824
polyA whole worm rep2	27219985	16073766	59.1	1678836
RNaseH intact skin rep1	30232586	18038891	59.67	2556
RNaseH intact skin rep2	32754344	18164780	55.45	2427
RNaseH intact skin rep3	37079271	21112065	56.93	4975
RNase H whole worm rep1	32369168	20561020	63.52	67294
RNase H whole worm rep2	36154965	23108809	63.91	1541

rRNA reads in polyA libraries (Figure 2.3 B). Thus, we show that, RNase H based ribodepletion method can efficiently depletes rRNA in planarians.

### 2.3 SDS based epidermis isolation following RNase-H based ribodepletion enhances the ability of epidermal gene detection

Next, I wanted to identify genes that are enriched in planarian epidermis over the whole worms. I compared the intact epidermal samples with whole worms for both the RNaseH and polyA selected libraries. Before analyzing, I merged the sequencing data from the dorsal and ventral epidermal samples for the polyA libraries and considered the pooled data as intact epidermis. Then I aligned both RNaseH and polyA libraries to the planarian genome (Grohme et al., 2018). After aligning to the genome, I compared the RNaseH based intact epidermal samples with whole worms (rnase\_is\_vs\_ww) and polyA intact epidermal samples with whole worms (polyA\_is\_vs\_ww) to identify epidermal enriched genes for these two different data sets using DESeq2 (Love et al., 2014). To determine the gene expression variabilities between the samples, I did principal component analysis (PCA) and found that all four analyzed datasets appeared in separated clusters and polyA data showed more variability between replicates (Figure 2.4 A). This may be, in part, because variation in the read counts was considerably higher among the replicates for polyA selected libraries (18M-31M compared to 30-36M for our RNaseH libraries); Table 2.1). Sample distance matrix analysis showed that skin libraries and whole worm libraries clustered distinctly for both RNaseH and polyA samples (Figure 2.4 B). I then performed MA plot analysis of epidermal gene expression over whole worms and found that more genes were differentially expressed (DE) in the RNaseH sample comparison than in the polyA sample comparison (Figure 2.4 C and D). Moreover, the additional DE genes in the RNaseH samples appear to include both genes with higher and lower average normalized counts, supporting the conclusion that RNaseH libraries capture a larger dynamic range of RNAs expressed in planarian cells compared to polyA libraries.

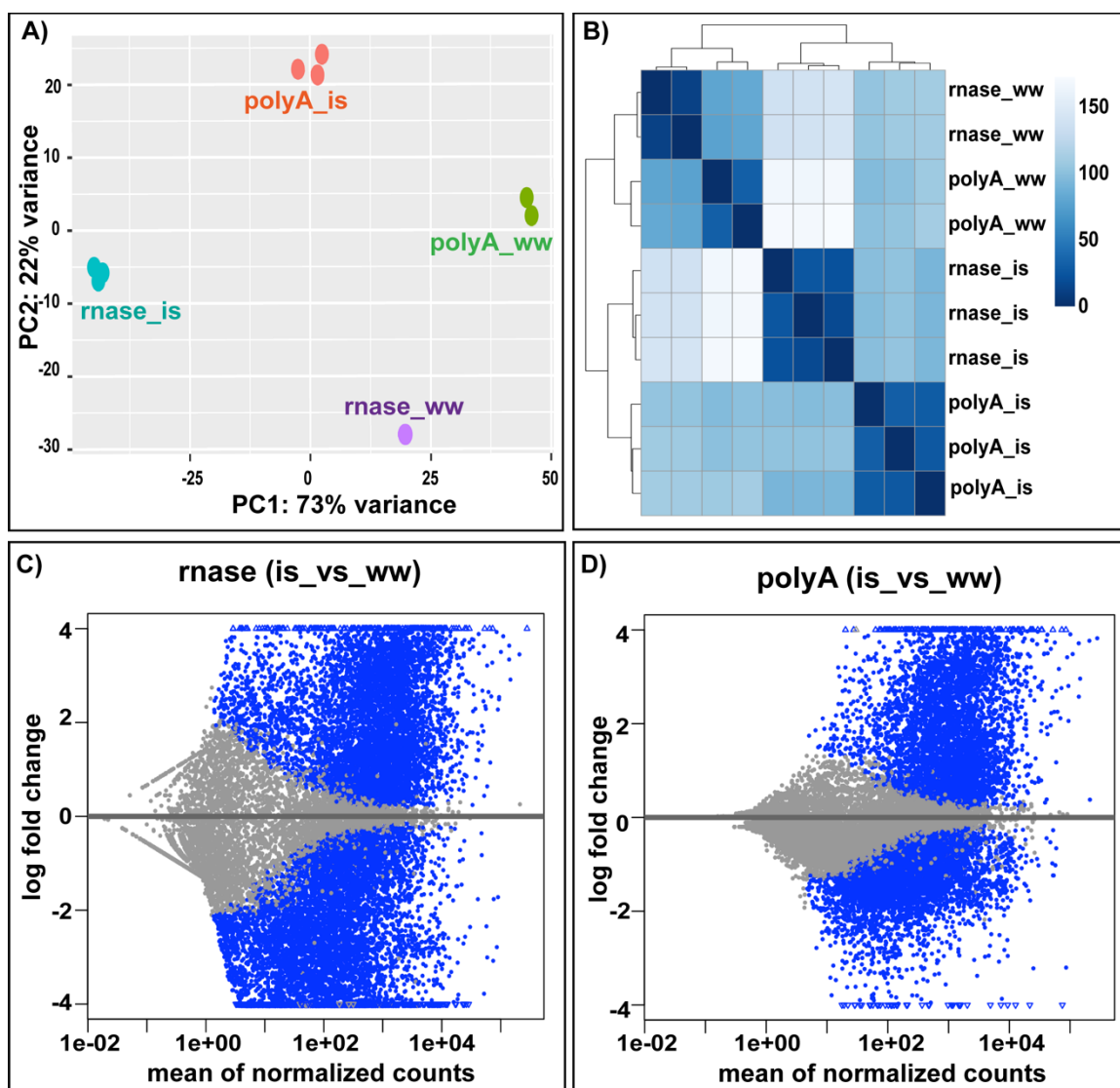


Figure 2.4 Quality analysis for RNA-seq datasets prepared from intact epidermis

A) PCA plot analysis for both RNase-H and polyA samples. Data for polyA samples was downloaded from a previously published study (Wutrzal et al); polyA intact skin samples (*polyA\_is*) were isolated using ammonium thiocyanate. RNaseH samples were generated using the optimized method described in Figure 2.2; *rnase\_is* refers to RNaseH prepared intact skin samples isolated with 0.1% SDS. “ww” = whole worm. B) Distance matrix analysis showing epidermal samples cluster distinctly compared to whole worms data sets for both RNaseH and polyA prepared samples. Scale (0 to 150) is showing the level of similarities or dissimilarities between the samples with 0 being most similar. C) MA-plot comparing the enrichment of a gene’s ( $\log_2$  fold change) to the average read counts of that gene in epidermal samples versus whole worm samples when libraries were prepared using RNaseH depletion or D) polyA enrichment. Each dot represents a gene detected. Blue dots represent genes that are significantly ( $p < 0.05$ ) differentially expressed between samples.

Upon comparing polyA epidermis libraries to those from whole worms (Wurtzel et al., 2015), I found ~3622 epidermal enriched genes (fold change  $\geq 1.5$ , p-adjusted  $< 0.05$ ) whereas I found 4929 epidermal enriched genes when I compared RNaseH epidermal libraries to those from whole worms (Figure 2.5 A). Notably, there were 3307 genes in common between polyA (is\_vs\_ww) and RNaseH (is\_vs\_ww). However, there were 1622 genes that were epidermally-enriched in RNaseH libraries only and 315 genes that were only enriched in polyA epidermal libraries (Figure 2.5 B). I then compared these lists of genes enriched in bulk epidermal RNA-seq data with recently reported single cell RNA-seq (scRNA-seq) analyses of planarian cells (Plass et al., 2018). Although there was considerable overlap between the epidermal enriched genes in the scRNA-seq with our analyses (Figure 2.5 C), the bulk RNA-seq data was able to identify many additional genes enriched in the intact epidermis. I used a list of 155 epidermal specific marker genes from this scRNA-seq data to ask if any were enriched in the RNaseH-specific or the polyA-specific epidermal genes. For doing that, I considered genes labeled as either “epidermal” or “epidermal DVb” (doral ventral boundary) clusters as epidermal genes (Plass et al., 2018). Unsurprisingly, a large majority of these epidermal marker genes (109/155) were identified as epidermal enriched in both datasets when using the indicated FC and adj p-value cutoffs (1.5 FC, adj p-value  $< 0.05$ ) (Figure 2.5 B). Additionally, 24/155 were identified as epidermal enriched exclusively in the RNaseH analysis whereas only 4/155 were unique to the polyA epidermal-enriched data (Figure 2.5 C). This suggests that our methods are more optimal for identifying high-confidence epidermal genes.

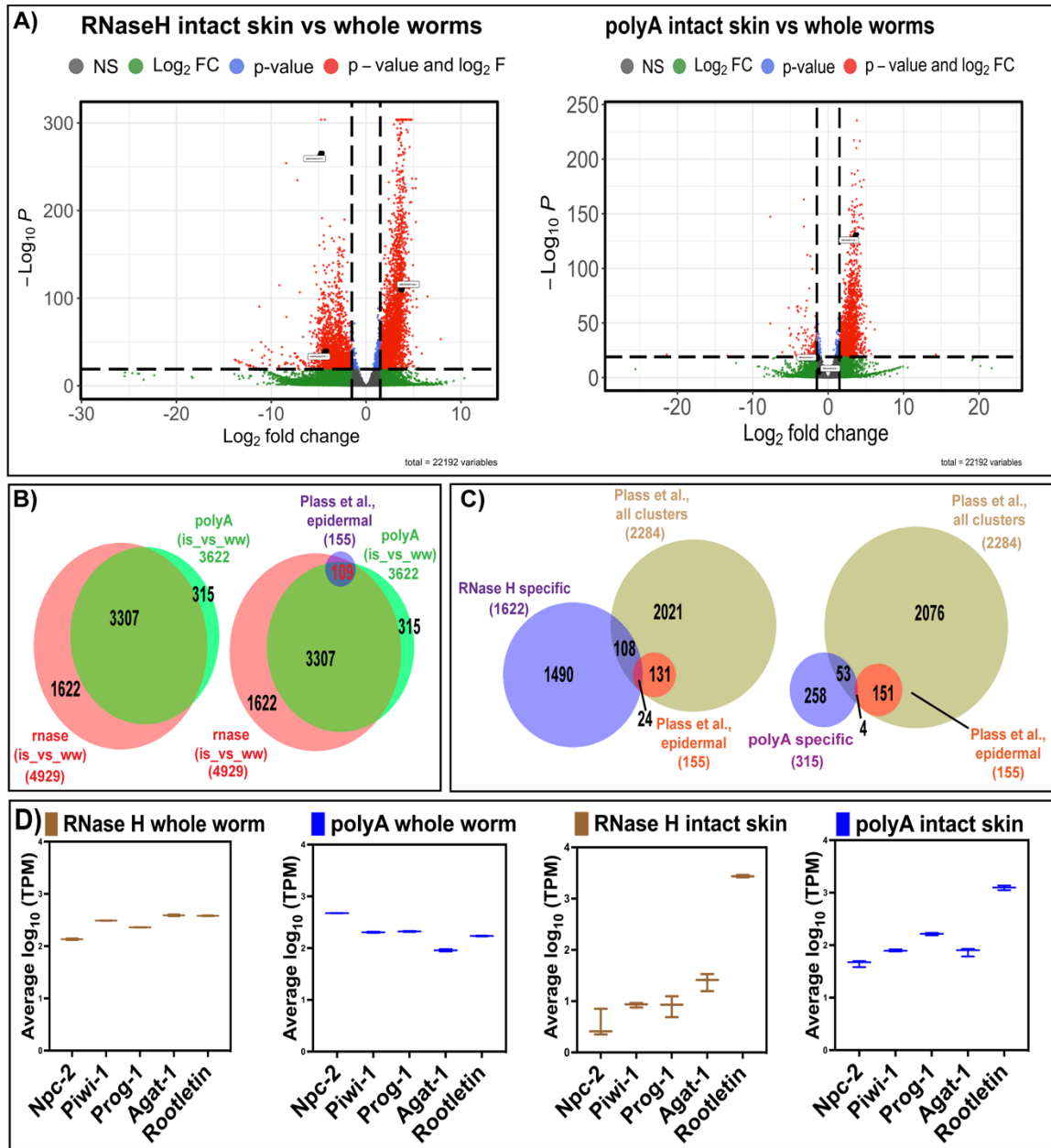


Figure 2.5 RNase-H library preparation method in combination with SDS based epidermis isolation detects more epidermal genes

A) Left panel: volcano plot of gene expression changes detected in isolated skin samples compared to whole worms using RNaseH ribodepletion for preparing libraries; Right panel: volcano plot of gene expression changes detected in isolated skin samples compared to whole worms using polyA enrichment for preparing libraries (original data generated in Wurtzel et al and re-analyzed). B) Venn diagrams comparing the genes determined to be significantly upregulated in planarian skin (versus whole worms) in RNA-seq experiments using RNaseH depletion (this study) and polyA enrichment (Wurtzel et al). Purple circle represents genes identified as “epidermal” using single cell RNA sequencing data in a previously published study (Plass et al). C) Venn diagrams comparing those genes that

were only detected as “epidermal enriched” in one dataset (RNaseH or polyA) with established single cell RNA-seq clusters. D) Average TPM of genes known to be markers for intestinal cells (*npc-2*), neoblasts (*piwi-1*), early progenitor cells (*prog-1*), late progenitor cells (*agat-1*), and ciliated epidermal cells (*rootletin*) from the datasets indicated (whole worms and epidermal libraries for both RNaseH depletion and polyA selection-based methods). polyA data was obtained from Wurtzel et al., 2017 and re-analyzed.

At the same time, only 108 genes among the 1622 RNase-H specific genes (6.7%) overlapped with a non-epidermal scRNA-seq cell marker gene (2284 total marker genes; Figure 2.5 C). In contrast, 53 genes out of 315 polyA- specific genes (16.8%) overlapped with a scRNA-seq non-epidermal marker gene (Figure 2.5 C). In sum, the polyA-specific “epidermal” gene list includes a higher relative proportion of marker genes for “other” cell types (18% versus 6.7%) and does not detect more scRNA-seq defined epidermal genes (1.5% vs 1.3%). Our methods are therefore both more robust and sensitive at identifying epidermal enriched genes without as much contamination from other cells, although I cannot pinpoint whether the isolation method or library prep method is more important.

I then wanted to characterize further the differences in gene detection in these two methods. I could not compare TPMs between these two different methods because of their considerable variation, including in sequence depth (Table 2.1). In addition, I speculated that contamination of other cell types while isolating the epidermis can result in variable detection of epidermal enriched genes. To test my hypothesis, I compared the TPMs of different cell type specific marker genes from the intact skin and whole worms datasets for both RNaseH and polyA samples (Figure 2.5D). I compared the TPMs of intestinal cell marker *npc-2* (Forsthoefel et al., 2020), stem cell marker *piwi-1* (Zeng et al., 2018), early epidermal progenitor marker *prog-1*, and mature epidermal marker *rootletin* (Tu et al., 2015) within a given dataset. Notably, the  $\log_{10}(\text{TPM})$  of *npc-2*, *piwi-1* and *prog-1* was

considerably higher in polyA epidermis samples compared to RNase-H epidermis samples even though, importantly, the  $\log_{10}(\text{TPM})$  of the epidermal gene rootletin was comparable between these two different methods (Figure 2.5 D). Thus, these results suggest there is lower contamination of other cell types when the epidermis is isolated using 0.1% SDS compared to the ammonium thiocyanate-based method. Moreover, epidermis isolation using 0.1% SDS following RNaseH based ribodepletion can detect more epidermal enriched genes. Together, these data suggest higher sensitivity DE gene detection from epidermal tissue when using these new isolation and library preparation methods compared to previously published methods in planarians.

#### 2.4 GO enrichment analysis reveals the biological roles of epidermal enriched genes

I compared the intact epidermis with whole worms to identify epidermal enriched genes for both RNaseH (my data) and polyA (Wurtzel et al., 2017) datasets. Then I clustered the epidermal enriched genes and found they showed overall similar expression patterns for both datasets (Figure 2.6 A). For example, stem cell specific marker *piwi-1* early progenitor marker *prog-1* and late progenitor marker *agat-1* are downregulated in epidermal samples for both datasets. Similarly, epidermal specific genes *prss12* and *cilia* gene *drc1* (Wurtzel et al., 2017) were upregulated in the intact skin compared to the whole worms for both the data sets (Figure 2.6 A). After confirming that my newly developed epithelial isolation and RNaseH library preparation is highly comparable to this similar polyA generated dataset that was previously published and validated (Wurtzel et al., 2017), I used my RNaseH dataset for further analysis. First, I found that upon clustering epidermal enriched genes with those enriched in whole worm samples, the epidermal enriched genes cluster distinctively (Figure 2.6 B). Then I took all the annotated genes



within the list of genes enriched in RNaseH intact epidermis (2878/4929) and ran gene ontology (GO) analysis. I found that epidermal enriched genes showed significant enrichment in many categories associated with ciliary assembly and function (Chen et al., 2013) (Figure 2.6 C and Table 2.2).

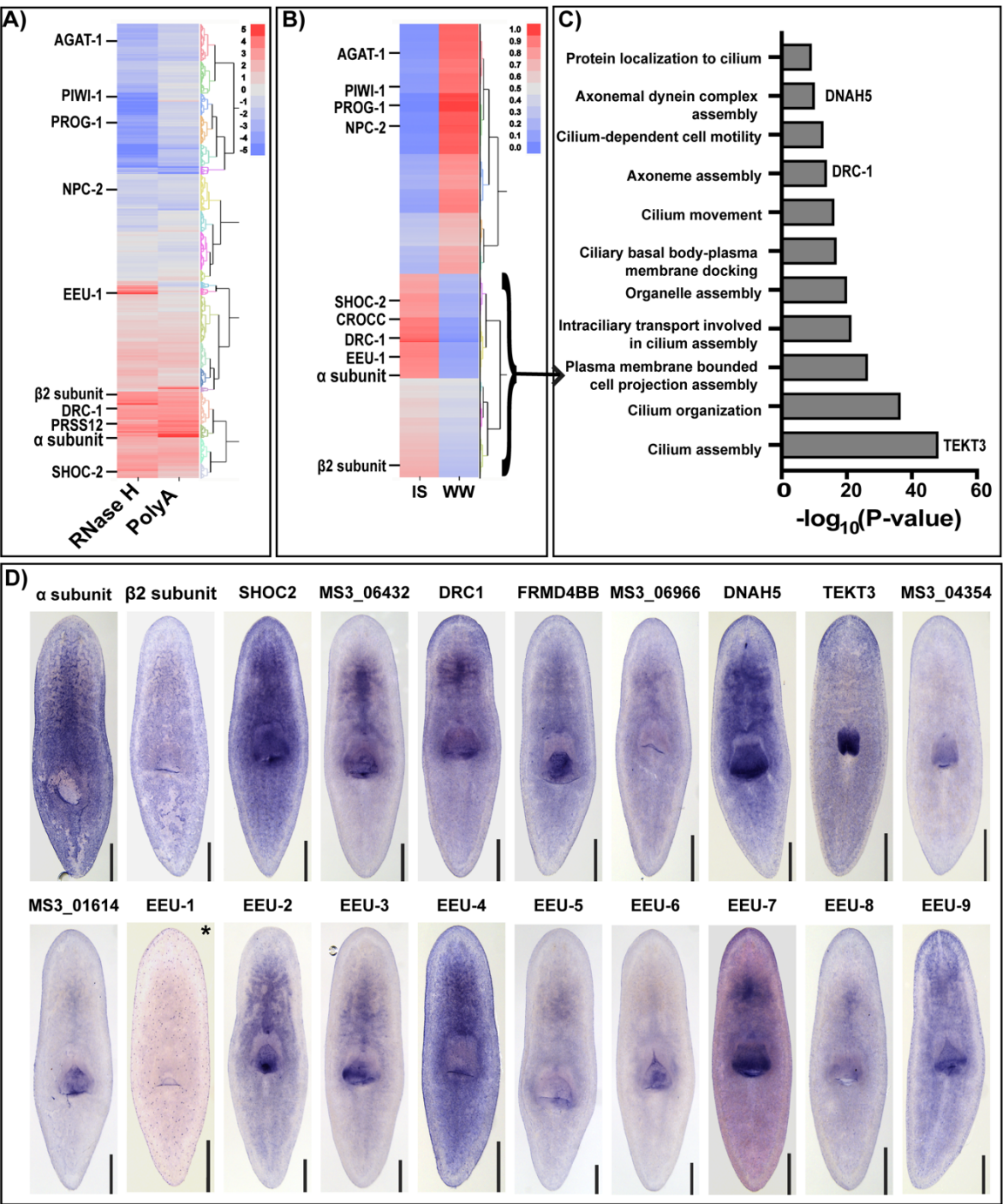


Figure 2.6 Optimized skin isolation and RNaseH depletion methods lead to robust detection of epidermal enriched genes

A) Cluster analysis of differential gene expression in intact skin (compared to whole worm samples) using RNA-seq data from both RNaseH depletion and polyA enriched libraries. Log<sub>2</sub>FC values for significantly DEG (p-adj <0.05) were used to make the clusters. B) Cluster analysis of gene expression (average TPM) in intact skin samples and whole worms, both from RNaseH depletion libraries. The following formulas were used to make this cluster: Average TPM of intact skin/ (Average TPM of intact skin+ Average TPM of whole worms) and Average TPM of whole worms/(Average TPM of intact skin+ Average TPM of whole worms). C) Gene ontology (GO) analysis on those genes determined to be epidermal enriched (compared to whole worms) using RNA-seq data from RNase-H depletion libraries. Genes with known blast hits (2697/4929 genes) were used to analyze the GO term. D) In situ validation of genes identified as epidermally enriched by analysis of RNaseH depletion data. Genes called  $\alpha$  subunit (SMESG000008146.1) and  $\beta$ 2 subunit (SMESG000064592.1) are homologs of two different subunits of the protein Na<sup>+</sup>-K<sup>+</sup>-transporter ATPase. (Scale bar = 500  $\mu$ m).

Table 2.2 GO terms and corresponding p-values of epidermal enriched genes

<b>Term</b>	<b>P-value</b>
Cilium assembly (GO:0060271)	8.58E-49
Cilium organization (GO:0044782)	4.01E-37
Plasma membrane bounded cell projection assembly (GO:0120031)	4.50E-27
Intraciliary transport involved in cilium assembly (GO:0035735)	5.34E-22
Organelle assembly (GO:0070925)	1.10E-20
Ciliary basal body-plasma membrane docking (GO:0097711)	1.76E-17
Cilium movement (GO:0003341)	9.33E-17
Axoneme assembly (GO:0035082)	1.65E-14
Cilium-dependent cell motility (GO:0060285)	2.05E-13
Axonemal dynein complex assembly (GO:0070286)	9.66E-11
Protein localization to cilium (GO:0061512)	8.03E-10
Membrane organization (GO:0061024)	2.96E-08
Microtubule bundle formation (GO:0001578)	1.55E-07
Peptidyl-glutamic acid modification (GO:0018200)	4.13E-07
Motile cilium assembly (GO:0044458)	5.30E-07
Inner dynein arm assembly (GO:0036159)	1.55E-06
Non-motile cilium assembly (GO:1905515)	1.56E-06
G2/M transition of mitotic cell cycle (GO:0000086)	2.63E-06
Cell cycle G2/M phase transition (GO:0044839)	3.17E-06
Protein polyglutamylation (GO:0018095)	3.50E-06
Regulation of cilium assembly (GO:1902017)	4.81E-06
Regulation of cell cycle G2/M phase transition (GO:1902749)	5.84E-06
Determination of left/right symmetry (GO:0007368)	7.41E-06
Cilium movement involved in cell motility (GO:0060294)	7.46E-06

Although many of the genes enriched in this RNaseH epidermal dataset are known epidermal genes, my analysis also reported many genes that do not blast to a known gene. I termed these unknown genes Epidermal Enriched Unknown (EEU) genes (Figure 2.6 D).

I then wanted to validate the genes that were epidermal enriched compared to the whole worms. From the 4929 epidermal enriched genes ( $FC \geq 1.5$ ,  $P$  adjusted  $< 0.05$ ), I chose 25 representative genes based on their fold change, adjusted  $P$  value and potential biological functions to screen by whole mount in situ hybridization (WISH). Among these 25 genes, 17 (74%) of them showed enrichment in the epidermis (Figure 2.6 D). S.med homologs for both the  $\alpha$  (DANA\GF17998I) and  $\beta 2$  (MS3\_03655) subunits of the  $Na^+/K^+$ -transporting ATPase transmembrane protein showed high epidermal enrichment (Figure 2.6 D), validating published scRNA-seq data (Plass et al., 2018). Another set of genes, the dynein regulatory complex 1 (*drc1*), tekti -3-like protein (*tekt3*), and dynein-heavy-chain-5,-axonema (*dnah5*) are known to be involved in ciliary functions and showed high epidermal enrichment by in situ hybridization as expected (Figure 2.6 C and D). *tekt3* and *dnah5* showed high expression in the pharynx as well, which agrees with published single cell transcriptomics (Plass et al., 2018).

Another transcript that showed strong epidermal enrichment was *shoc2* (Figure 2.6 D). *Shoc2* is a scaffold protein in the ERK pathway (Jang and Galperin, 2016), the activation of which is known to be essential for regeneration in both planarians and many other regenerative organisms (Tasaki et al., 2011; Wen et al., 2022). My re-analysis of the polyA libraries also detected *shoc2* as an epidermal enriched gene yet the published scRNA-seq data did not (Plass et al., 2018). Nine of the 25 genes I screened by WISH were unknown (EEUs). From those genes, EEU-1 showed very distinct expression in

subpopulation of epidermal cells (Figure 2.6 D) yet the polyA epidermal enriched dataset did not detect it and there is no single cell transcriptomic data available for this gene (Plass et al., 2018) . Other unknown genes such as EEU-4, EEU-5, EEU-8, EEU-9 also showed epidermal enrichment (Figure 2.6D). In summary, my newly developed method for isolated planarian epidermis and generating ribodepleted RNA-seq libraries robustly detects epidermally enriched genes, including many not previously identified or studied in this model.

## 2.5 Functional characterization of identified epidermal genes

I then wanted to know the functional roles of identified epidermal enriched genes in the context of regeneration. For RNAi experiments, I fed adult planarians with dsRNA complementary to each transcript for 3 times within a week; on the last day of feeding, I amputated the worms 6 hours post feeding into three similar size fragments (head, trunk, and tail; Figure: 2.7 A). I also kept feeding dsRNA to intact worms and observed the intact phenotypes along with the regeneration fragments.

Bioelectrical signals and ion transport are essential for key cellular functions. Several cellular mechanisms such as cell division, migration and differentiation can be altered through the manipulation of ion channels (Levin, 2007; Sundelacruz et al., 2009). Sodium-potassium ATPase (Na-K-ATPase) is a transmembrane protein with two core subunits ( $\alpha$  and  $\beta$ ) and other tissue-specific optional subunits belonging to the FXYD class of proteins (Li and Langhans, 2015). Na-K-ATPase is crucial for regulating sodium homeostasis in mammalian cells and in tight-junction formation in epithelial cells through Rho GTPase (Rajasekaran and Rajasekaran, 2003). When I knocked down these two subunits separately in *S.med*, I saw normal blastema growth in all blastema except the

posterior blastema of the trunk fragments for up to 8 days post amputation (8dpa). However, 41% (14/34) of trunk fragments for  $\beta 2$ (RNAi) showed indented blastema growth at 6dpa (Figure: 2.7 C). In addition, both  $\alpha$  and  $\beta 2$  RNAi worm fragments started showing motility defects after 8dpa. After 15 days post RNAi feeding, intact worms for both  $\alpha$  and  $\beta 2$  (RNAi) stopped eating, as indicated by the lack of red food paste in their gut (Figure 2.7 B). For observing the feeding behavior of the regenerating fragments, I fed normal liver paste with red food color at 14dpa and scored worms for feeding according to the red color in the gut. I observed that 88% (30/34) of the  $\beta 2$ -RNAi head fragments did not eat and 79% (27/34) of  $\alpha$ -RNAi head fragments did not eat, whereas all control (RNAi) animals did eat at 14dpa (Figure 2.8 A and B). As well, more than 80% of tail and trunk fragments for both  $\alpha$  and  $\beta 2$ -RNAi did not eat at 14dpa (Figure 2.8 A and B). Furthermore, regenerating worms after 20dpa and intact worms after 27 days post feeding (dpf) started lysing and all the regenerating animals died by 25 dpa both for  $\alpha$  and  $\beta 2$ -RNAi.

Cytoplasmic dynein is a large protein complex composed of two identical heavy chain and several intermediate light chain that mediates intracellular retrograde transport of various cargoes (Mizuno et al., 2007). In motile cilia and flagella, the nexin-dynein regulatory complex (N-DRC) stabilizes the axonemal core structure, links the neighboring microtubules, and is required for ciliary motility (Gui et al., 2019). Among the 11 reported N-DRC subunits, loss of DRC1 results in primary ciliary dyskinesia (PCD), which is characterized by dysfunctions in respiratory cilia and sperm flagella in humans (Wirschell et al., 2013). In planarians, it has been reported that knockdown of outer dynein arm docking complex (ODA-DC) causes ciliary loss and motility defects (Hjeij et al., 2014; Kyuji et al., 2020). I detected enrichment of *drc1* in the planarian epidermis using both

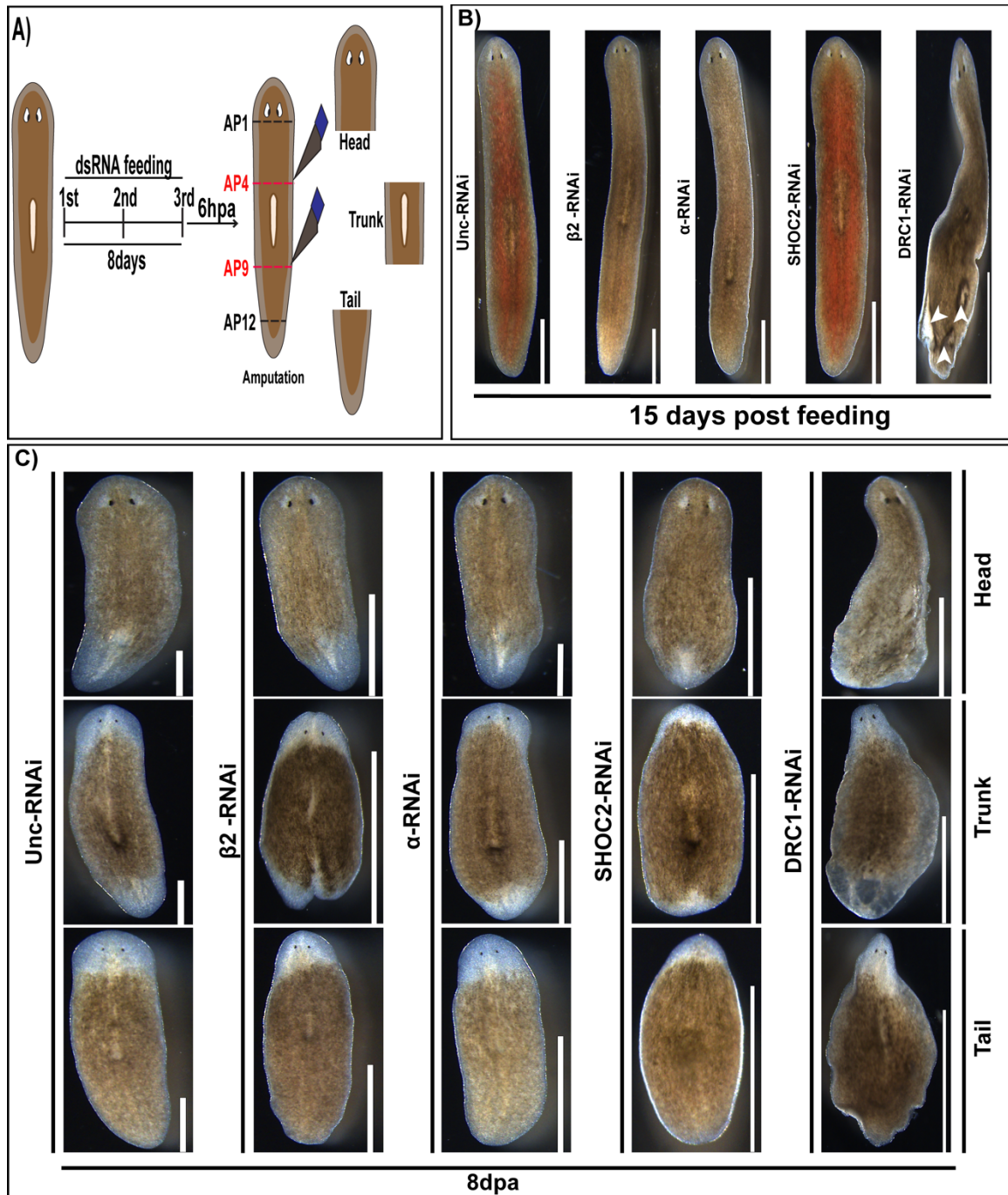


Figure 2.7 Epidermal genes required for planarian regeneration

A) Schematic representation of RNAi experiment. B) Live images of RNAi worms after a feeding with dsRNA on day 15 post-RNAi; animals were fed with dsRNA matching to a control gene (Unc-22),  $\beta 2$ ,  $\alpha$ , shoc2 and drc1 (Scale bar- 500  $\mu$ m). Alpha ( $\alpha$ ) (SMESG000008146.1) and beta-2 ( $\beta 2$ ) (SMESG000064592.1) subunits correspond to two different subunit of the protein  $\text{Na}^+ \text{-K}^+$  transporter ATPase. C) Regenerating head, tail and trunk fragments at 8 days post amputation after RNAi knockdown of the genes unc-22 (control),  $\beta 2$  subunit,  $\alpha$  subunit, shoc2 and drc1.

RNase-H and polyA datasets. After three RNAi feedings (8 dpf), the intact worms stopped eating and started showing motility defects. At 15 dpf, the intact worms showed severe motility defects and epidermal lysis (Figure 2.7 B, white arrowheads). After 18 dpf, the intact worms started lysing and all the worms died by 20 dpf.

Regenerating *drc1*(RNAi) fragments started showing motility defects and abnormal blastema formation as early as 4 dpa (Figure 2.7 B-E). At 8dpa, *drc1*(RNAi) fragments showed motility defects (100%), abnormal blastema formation (90%), blotting (84%) and bloated body (100%) out of 102 fragments (Figure 2.7 C). Moreover, after 10 dpa all the *drc1*(RNAi) fragments lysed. FoxJ1 is a transcription factor required for the expression of genes needed to assemble motile cilia across many organisms, including planarians (Vij et al., 2012). I used RNAi of foxJ1 as a positive control in my RNAi screening experiments and these worms showed similar phenotypes such as bloating and motility defects as *drc1*(RNAi) animals, which suggests normal ciliary function plays important roles for maintaining epidermal integrity and planarian survival (Vij et al., 2012).

The extracellular signal regulated kinase (ERK) or mitogen activated protein kinase (MAPK) pathway is a canonical signaling cascade that converts extracellular cues into an intracellular signals and regulates a myriad of cellular functions including proliferation, differentiation and migration (Chang and Karin, 2001; Nishida and Gotoh, 1993). Several scaffolding proteins such as KSR, MP1, IQGAP, and SHOC2 facilitate the interaction and function of core signaling molecules in the ERK/MAPK pathway (Brown and Sacks, 2009). A SHOC2 complex, comprised of SHOC2, MRAS and PP1, mutations in the *shoc2* gene are linked to Noonan syndrome in humans (Jang and Galperin, 2016). It has also been reported that SHOC2 is required for hematopoietic stem cell differentiation and normal



craniofacial development (Jang et al., 2019). However, in planarians there is no published study on SHOC2's role in regeneration and homeostasis. My RNA-seq and WISH data show that *shoc2* is enriched in planarian epidermal cells (Figure 2.6 A, B, D), though published single cell RNA-seq data suggests it may also be expressed in stem cells (Plass et al., 2018). We knocked down *shoc2* by feeding dsRNA as described above (Figure 2.7 A).

As early as 6dpa, *shoc2*(RNAi) regenerating worms showed delayed eye spot regeneration and smaller blastema growth (Figure 2.7 A, C). By 8dpa, 100% of the control (*unc-22*(RNAi)) tail and trunk fragments regenerated clear eye spot structures with white neuronal eye cups and black pigment (need to add pictures to this figure and ref here). Whereas 94% (32/34) *shoc2*(RNAi) tail fragments and 91% (31/34) *shoc2*(RNAi) trunk fragments did not to regenerate their eyes at 8dpa (Figure 2.9 A). Even at 14 dpa, only 15% *shoc2*(RNAi) tail fragments and 10% *shoc2*(RNAi) trunk fragments had faint eye spots (Figure 2.9 A). *shoc2*(RNAi) fragments showed smaller anterior blastema growth in regenerating trunk and tail fragments by 6 dpa. Both the head and tail fragments showed smaller tail blastema growth compared to control fragments as well (Figure 2.9 B and C).

To quantitate these differences, I measured the blastema tissue of the regenerating fragments and the entire body/fragment length; I then calculated a blastema to body ratio for each animal in the experiment. At 15 dpa the anterior blastema to body ratio for *shoc2*(RNAi) tail fragments was almost similar with control (Figure 2.9 D). However, the head fragments had significantly lower posterior blastema to body ratios at 4 dpa, 8 dpa and even at 15 dpa (Figure 2.9 D). I then fed normal liver paste to these animals at 14 dpa

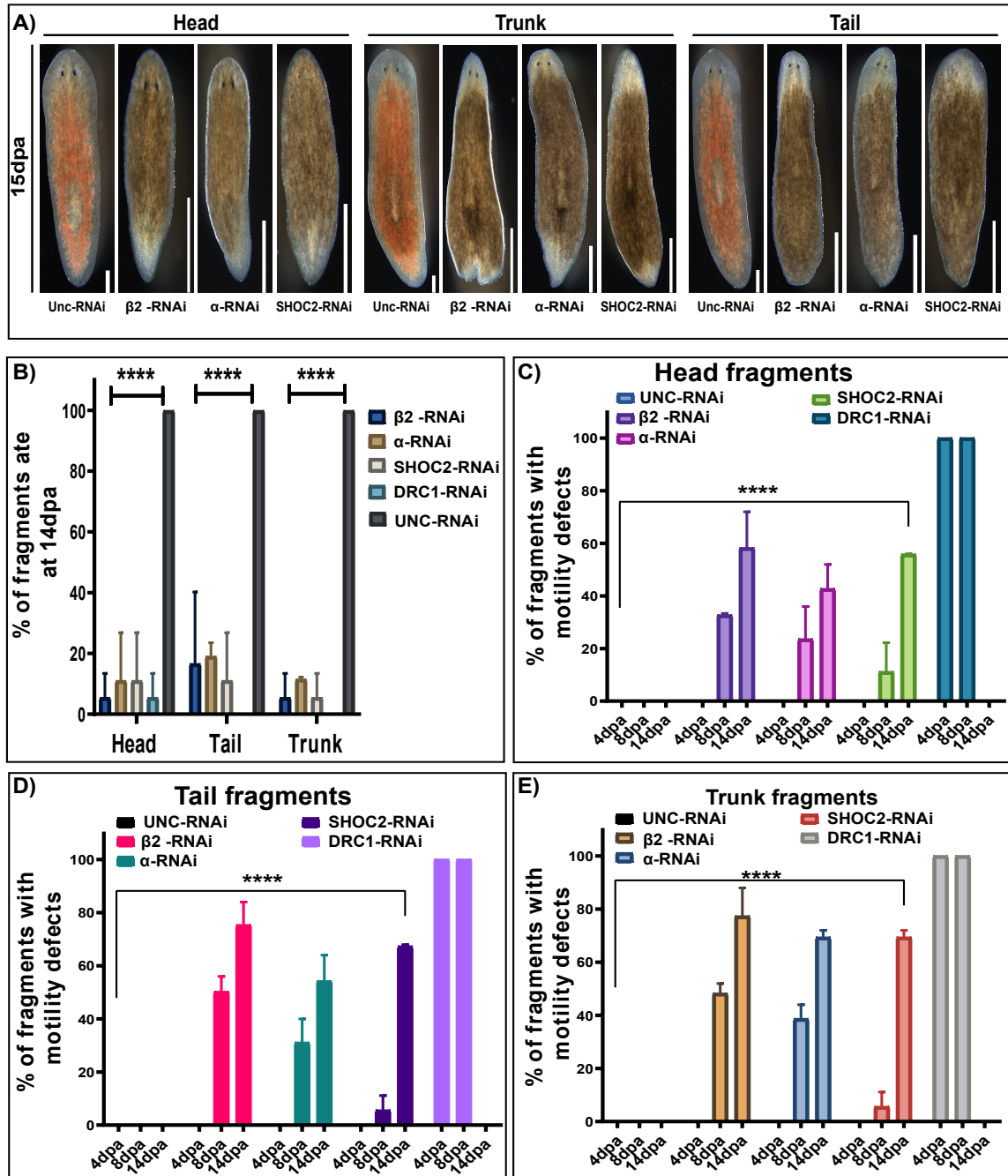


Figure 2.8 RNAi depletion of epidermal enriched genes leads to impaired feeding behavior and locomotion in planarians

A) Live images of RNAi worm fragments at 15 days post amputation (dpa). Worms were fed normal liver paste at 14dpa, scored for feeding behavior, and imaged at 15dpa. Red food color in the gut is showing that worms ate at 14 dpa. B) Percent of regenerating worm fragments that ate normal food at 14dpa. Percent of regenerating fragments with motility defects detected; head (C), tail (D) and trunk fragments (E) were scored at 4, 8 and 15dpa.

and found that only 11% head and tail fragments ate and 5% trunk fragments ate (Figure 2.8 A and B). Comparatively, for *unc-22*(RNAi) control animals, all (100%) the head, tail and trunk fragments ate at 14dpa (Figure 2.8 A and B). In addition, regenerating *shoc2*(RNAi) head fragments started losing their preexisting eye pigment at 8 dpa and 90% of the head fragments lost their eye spot structures by 15 dpa (Figure: 2.8 A). Moreover, intact *shoc2*(RNAi) worms were normal up to 5th RNAi feeding (day 15) but after that they started showing motility defects and, most relevantly, losing their eye pigment (Figure 2.9 B). Similarly, 10% of *shoc2*(RNAi) regenerating fragments showed motility defects at 8 dpa, at 15 dpa ~70% of tail and trunk fragments showed motility defects (Figure 2.8 C, D and E). Together, these data show that SHOC2 is required for both normal homeostasis and proper regeneration in *S.med* planarians, although we do not yet know if both processes use the same mechanism.

In summary, I showed that several genes I identified through my newly developed epidermal isolation and customized RNaseH ribodepletion method have strong phenotypes associated with epidermal function. Loss of *drc1* had drastic cilia defects whereas, knockdown of *MS3\_03655*RNAi and *DANA\GF17998* showed abnormal motility and defects in feeding behavior. *shoc2*-RNAi showed the most striking regenerating phenotypes, such as delayed regeneration, smaller blastema growth, motility defects and loss of eye pigments. Given the conserved and essential role of ERK/MAPK signaling in animals regeneration and the implication of SHOC2 in human disorders, this finding is significant and will be important to characterize further in future studies.

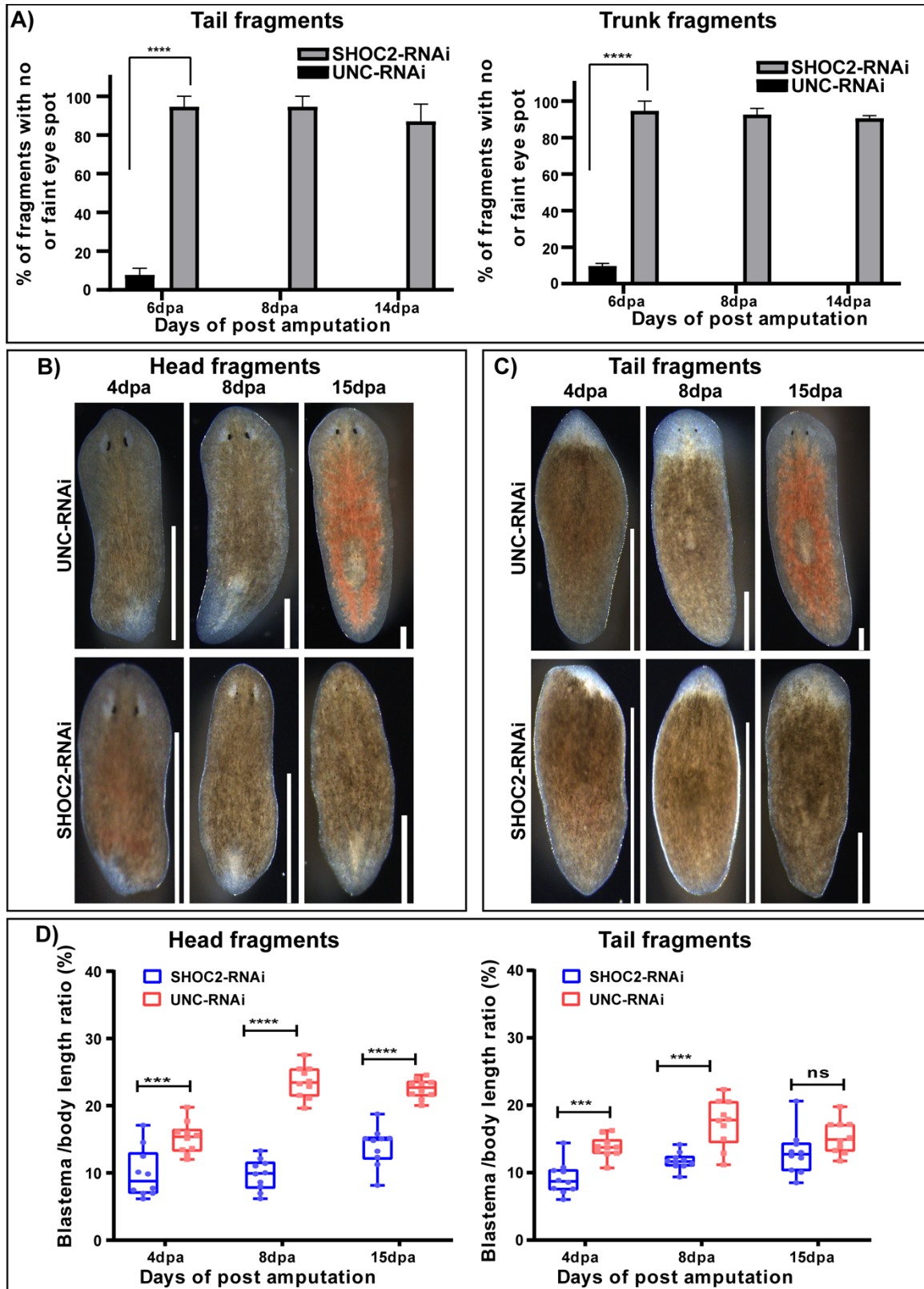


Figure 2.9 SHOC2-RNAi worms show delayed eye spot regeneration

A) Plots showing percent of worm fragments that were scored as having faint eye spots or none at all separated by trunk (left) and tail (right) fragments. Scoring was done on 6dpa, 8dpa and 14dpa. B) Live images of head fragments and tail fragments (C) at 4dpa, 8dpa and 15dpa. Shoc2-RNAi fragments possess smaller blastemas. D) Blastema to body length ratio of Shoc2-RNAi treated head and tail fragments at 4dpa, 8dpa and 15dpa. Length of the worms and blastema were measured using tools in Fiji imaging software. For statistical analysis, ten images from two independent experiments were quantified for each group.

### CHAPTER 3. IDENTIFICATION OF WOUND INDUCED GENES AND THEIR FUNCTIONAL ROLES DURING PLANARIAN REGENERATION

Upon wounding, adult planarian epidermal cells undergo extreme morphological transformation; as the body wall muscle contracts, the dorsal and ventral epidermis come together and closes the wound surface, a process which is considered the first step of planarian regeneration (Gumbrys, 2017; Hori, 1989). This happens right after amputation and lasts for approximately 90 minutes (Gumbrys, 2017). Several wound induced genes have been reported to be expressed in the epidermis immediately after amputation in planarians. For instance, *fos-1* expresses within 30 minutes after wounding and knockdown of *fos-1* results in cyclopic blastema formation (Wenemoser et al., 2012). Several other wound induced genes have been reported to be expressed in epidermal cells as well, including *jun-1*, *ston*, and *hadrian*, which are all induced within 3 hours of amputation (Wurtzel et al., 2015). However, there is paucity of research that describes functionally important, wound-induced genes in the planarian epidermis at early time points after amputation. I hypothesized that epidermal stretching triggers gene expression changes in planarian epidermal cells after injury and that some of these genes may be essential for regeneration to proceed. I therefore aimed to identify epidermal genes that express in the planarian epidermis after amputation.

#### 3.1 Isolation of planarian regenerating epidermis

After confirming that I can isolate intact planarian epidermis using 0.1% SDS with minimal contamination, I wanted to know how well this method would work for injured epidermis. I amputated worms and the epidermis was isolated using 0.1% SDS after 3 hours post amputation (Figure 3.1 A). I then conducted qPCR on isolated regenerating skin at 3

hpa, intact skin, worm carcass at 3 hpa and intact worm carcass. For qPCR, I used rootletin as epidermal marker (Tu et al., 2015) and hadrian as a positive control for gene induction in the epidermis at 3hpa (Figure 3.1 B) (Wurtzel et al., 2015). After conducting the qPCR, I found minimal contamination of stem cell marker piwi-1 in both intact skin and regenerating skin samples (Figure 3.1 C). I also found that expression of the epidermal marker rootletin was significantly high in the epidermis compared to the worm carcass as expected (Figure 2.1 D and 3.1 C). The expression of hadrian was significantly higher in both intact and regenerating skin compared to both wild type and 3hpa worm carcasses (Wurtzel et al., 2015) (Figure 3.1 C). Although normalized hadrian expression was not significantly higher in regeneration epidermis at 3hpa compared to intact epidermis, it did trend toward upregulation.

In addition, we used hadrian as a wound induced epidermal gene based on the RNA-seq data where hadrian was showed to be induced in epidermis at 3hpa (Wurtzel et al., 2015). However, another study showed by in situ hybridization that hadrian expression is not increased in regenerating epidermis until 6hpa (Wenemoser et al., 2012). These differences might help explain why my qPCR data was suggestive but not statistically significant. I also used tubulin to normalize between qPCR samples, which may not work well as a house-keeping gene in this context. In summary, my 0.1% SDS method can isolate the planarian epidermis after injury, still appears to contain low amount of contaminating cells, and is sufficient for detecting wound induced genes in the injured epidermis.

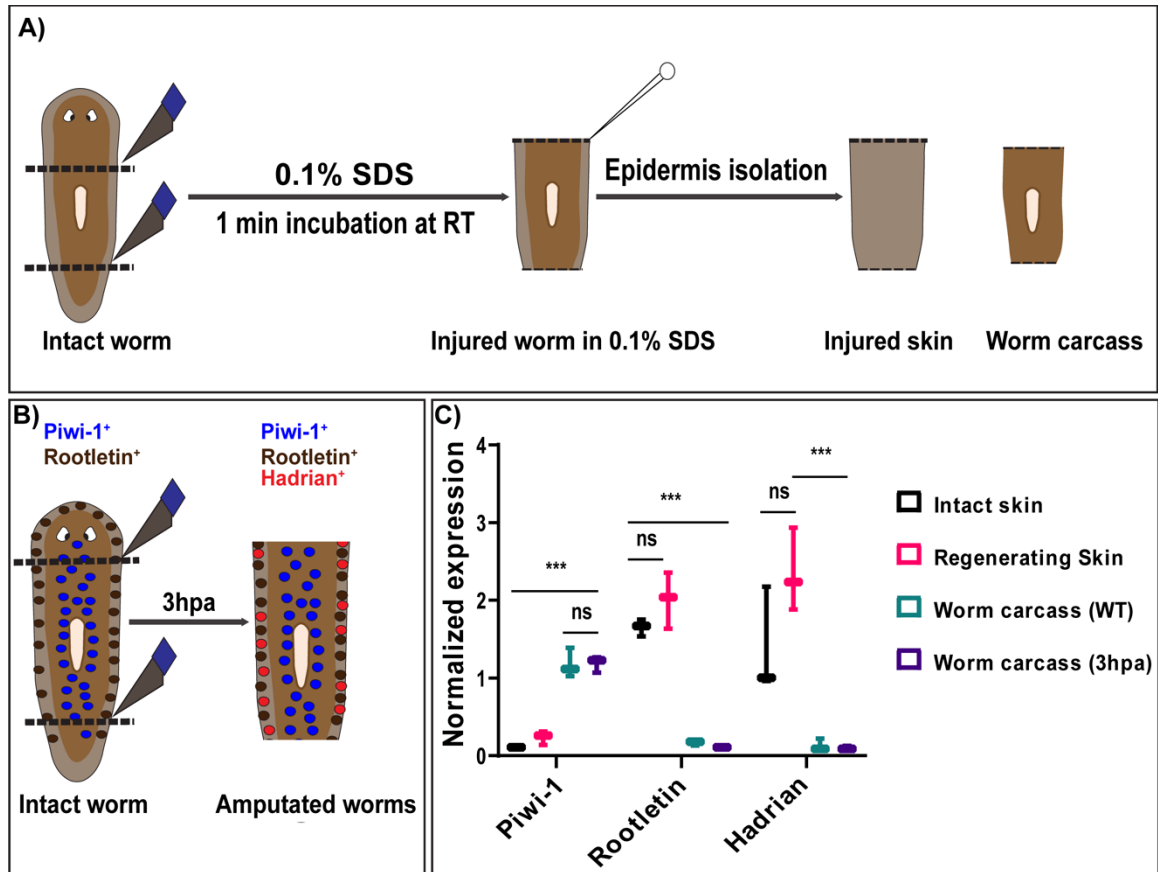


Figure 3.1 SDS based isolation of regenerating planarian epidermis

A) Schematic of how the epidermis of regenerating planarians was isolated. B) Cartoon illustrating the location of cells in the planarian body expressing different marker genes. Hadrian expression is induced after amputation (Wenemoser et al., 2012). C) RT-qPCR analysis of gene expression in regenerating skin compared to intact skin and the remaining worms tissue (“carcasses”) after skin isolation; the epidermis was isolated from injured worms at 3hpa. For qPCR, primers specific to neoblast (piwi-1), epidermis (rootletin) and wound epidermis (hadrian) marker genes were used.



### 3.2 Detection of wound induced genes using RNase-H based library preparation methods

I showed that regenerating planarian epidermis can be isolated by 0.1% SDS with minimal contamination of other cell types. I then wanted to identify a comprehensive list of genes that are wound induced in the epidermis after amputation. Right after amputation, planarian epidermal cells near the wound site stretch to cover the wound area (Hori, 1989; Morita and Best, 1974) and this process last about 90 minutes (Gumbrys, 2017). I therefore decided to isolate RNA from epidermal samples collected at different times points during and after this “stretching window” yet before the regeneration blastema forms. I amputated planarian head and tails and took the trunk fragments for further experiments. I isolated the epidermis from these trunk fragments at 10 min, 1hr, 3hr and 24hrs post amputation. After extracting RNA from these isolated epidermal samples, I used our home-brewed RNaseH method (discussed above) to prepare RNA-seq libraries and then sequenced the libraries in single end (SE) mode.

I first checked my RNA-seq libraries for rRNA and found they all contain very low amount of rRNA reads. I also conducted sample distance matrix analysis to check the quality of my RNA-seq samples and found that almost all the samples from different time points clustered distinctly (Figure 3.2 A). I then performed pair-wise differential gene expression (DEG) analysis using DEseq2 (Love et al., 2014), comparing epidermal samples from each early time point with those from 24hpa (Figure 3.2 A,B and C) . Given that previously identified wound induced genes (e.g., jun-1, fos-1, and tyr-kinase-1) express within 30 minutes of amputation and decline within 6-12 hours (Wenemoser et al., 2012) and, at the same time, that the wound sites should not have changed significantly its

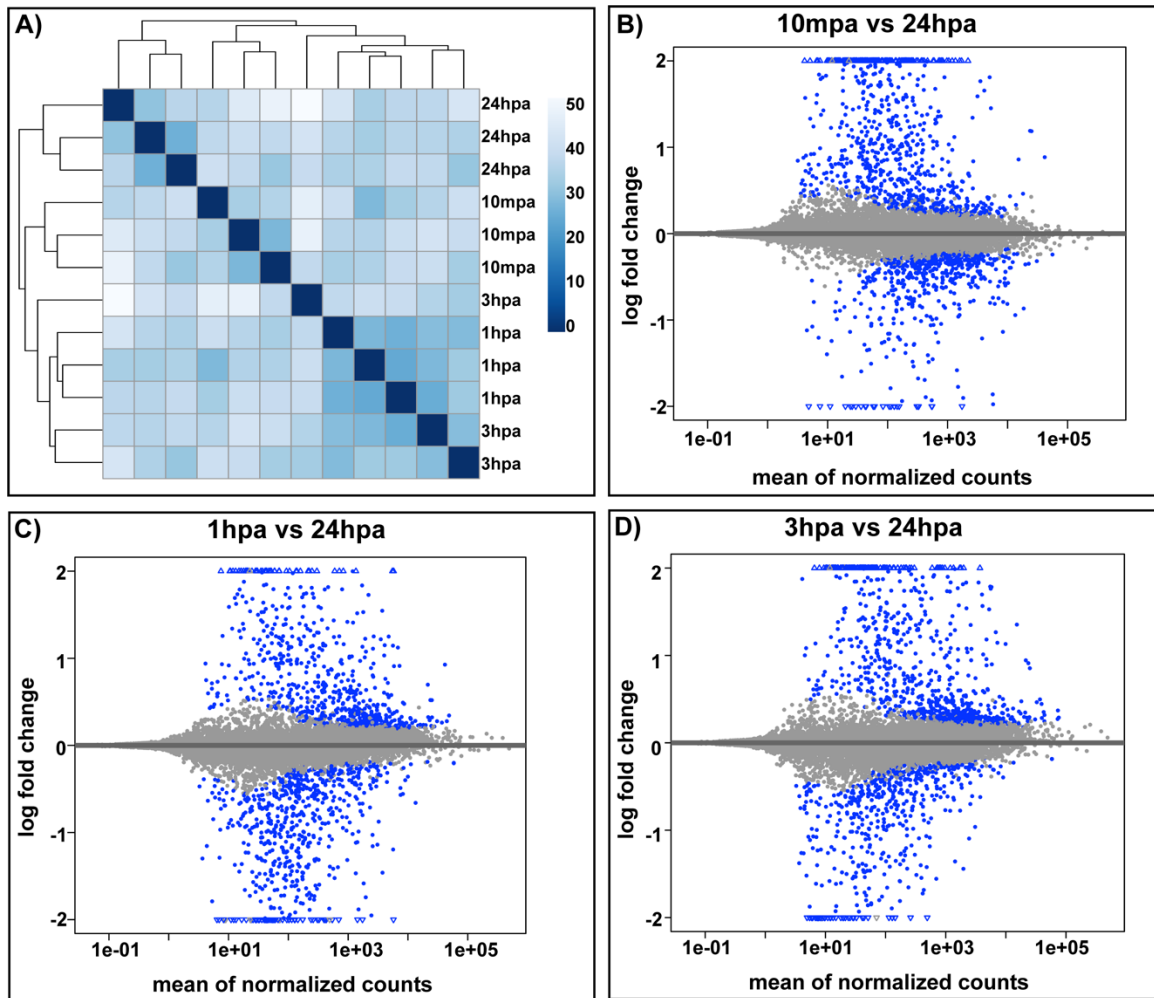


Figure 3.2 Quality checking and DE analysis of RNA-seq data from regenerating epidermis  
A) Distance matrix analysis of RNA-seq data from different timepoints showing that samples from different timepoints clustered distinctly. Scale (0 to 50) is showing the level of similarities or dissimilarities between the samples, with 0 being the most similar. MA-plots representing the Log2FC and average counts for significantly DEG at 10mpa (B), 1hpa (C), and 3hpa (D) compared to 24hpa. Each dot is representing one gene detected during analysis. Blue dots represent the genes that are significantly ( $p\text{-adj} < 0.05$ ) differentially expressed between samples. Differential analysis was conducted using Deseq2.

their cell composition at 24 hours, I hypothesized that this strategy would best identify genes that are induced after injury versus changes in cell composition during regeneration.

After analyzing the RNA-seq data, I found approximately 980 differentially expressed genes (DEG;  $p$  adjusted  $<0.05$ ) at each time point compared to 24hpa. Among these DEG, 586 were upregulated at 10mpa, 515 at 1hpa, and 624 at 3hpa (Figure 3.3 A). I then clustered the  $\log_2$  fold change ( $\log_2FC$ ) values for those genes that are significantly differentially expressed ( $P$  adjusted  $<0.05$ ) at least one time point compared to 24hpa (Figure 3.3 B and C). Genes that were upregulated mostly in all the time points were clustered in cluster 1, 4, 5, and 6, whereas downregulated genes were mostly clustered in cluster 2 and 3 (Figure 3.3 C).

### 3.3 Validation of RNA-seq data using whole mount in situ hybridization

To validate my RNA-seq data, I selected candidate genes based on the  $\log_2FC$  and  $p$ -adjusted values from different clusters and performed whole mount in situ hybridization (WISH). I selected 70 candidate genes in total and screened them by WISH in both intact worms as well as after amputation at different time points (10mpa, 1hpa, 3hpa and 24hpa).

Within my selected candidates, many of them had no BLAST hits so I termed them wound induced (WI) genes if they were upregulated at 10mpa, 1hpa or 3hpa. For those genes identified as downregulated (which could mean reduced transcription at 10m, 1hr, or 3hr, or upregulation at 24hpa), I termed them wound induced late (WIL) genes. Genes that were dramatically upregulated after amputation and stayed upregulated clustered in cluster 1 and 6 (Figure 3.3 C). Several genes from cluster 1 and 6 were previously reported to be expressed in intestine. For example, *rpz3*, *klk13*, *npc2*, and *cyp2j2* express in the intestinal goblet cells (Forsthoefel et al., 2020; Plass et al., 2018). After performing WISH,

I observed that many of the screened genes from these two clusters (1 & 6) were indeed upregulated in the intestine (Figure 3.4 A and B), which may be due to their high expression and proximity of the gut to the thin wound epithelium. In most of the examples from Cluster 1 and 6, gene expression is induced in multiple tissues, including the epidermis and/or wound site, although the intestinal expression is dominant.

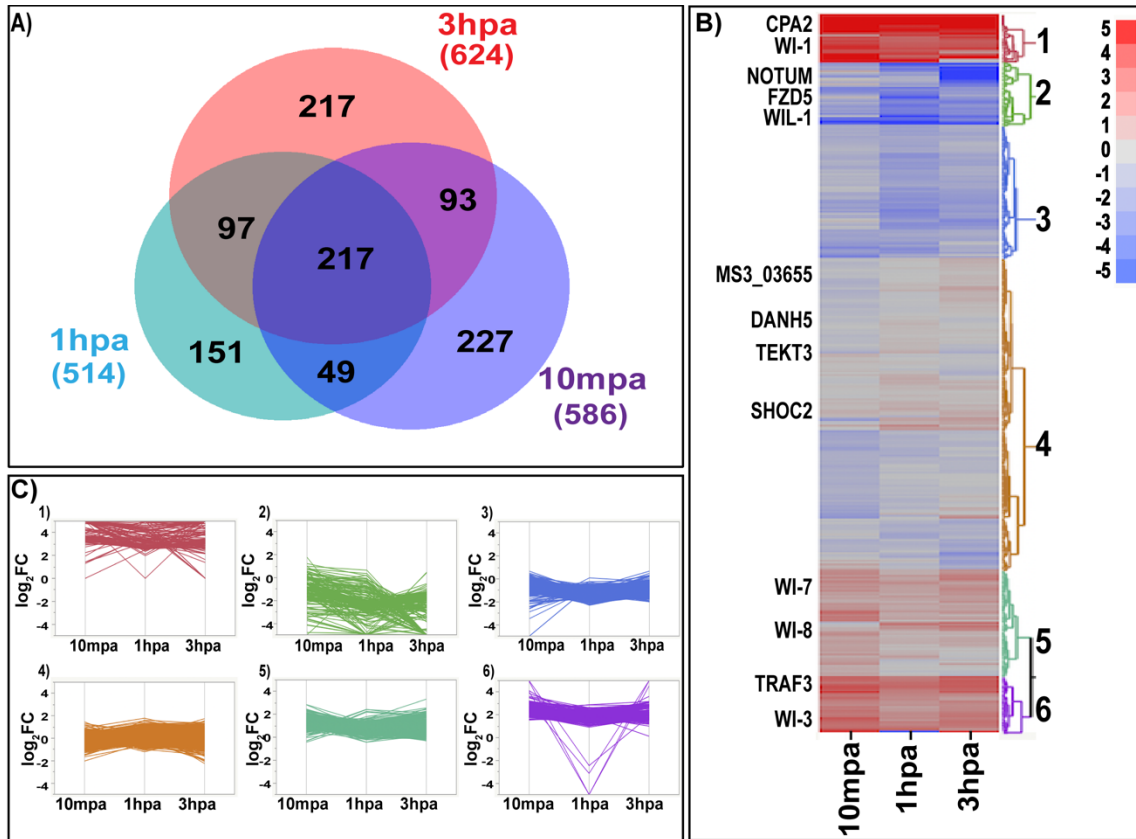


Figure 3.3 RNaseH based library preparation in combination with SDS based epidermis isolation sensitively detects wound induced epidermal genes

A) Venn diagram showing the number of significantly wound induced genes at 10mpa, 1hpa and 3hpa (each compared to 24hpa).  $p\text{-adj} < 0.05$  was used to filter significantly wound induced genes. B) Heatmap showing the log<sub>2</sub>FC for DEG at different timepoints. C) Cluster analysis of DEG genes across all 3 timepoints. Cluster numbers refer to numbers on heatmap.

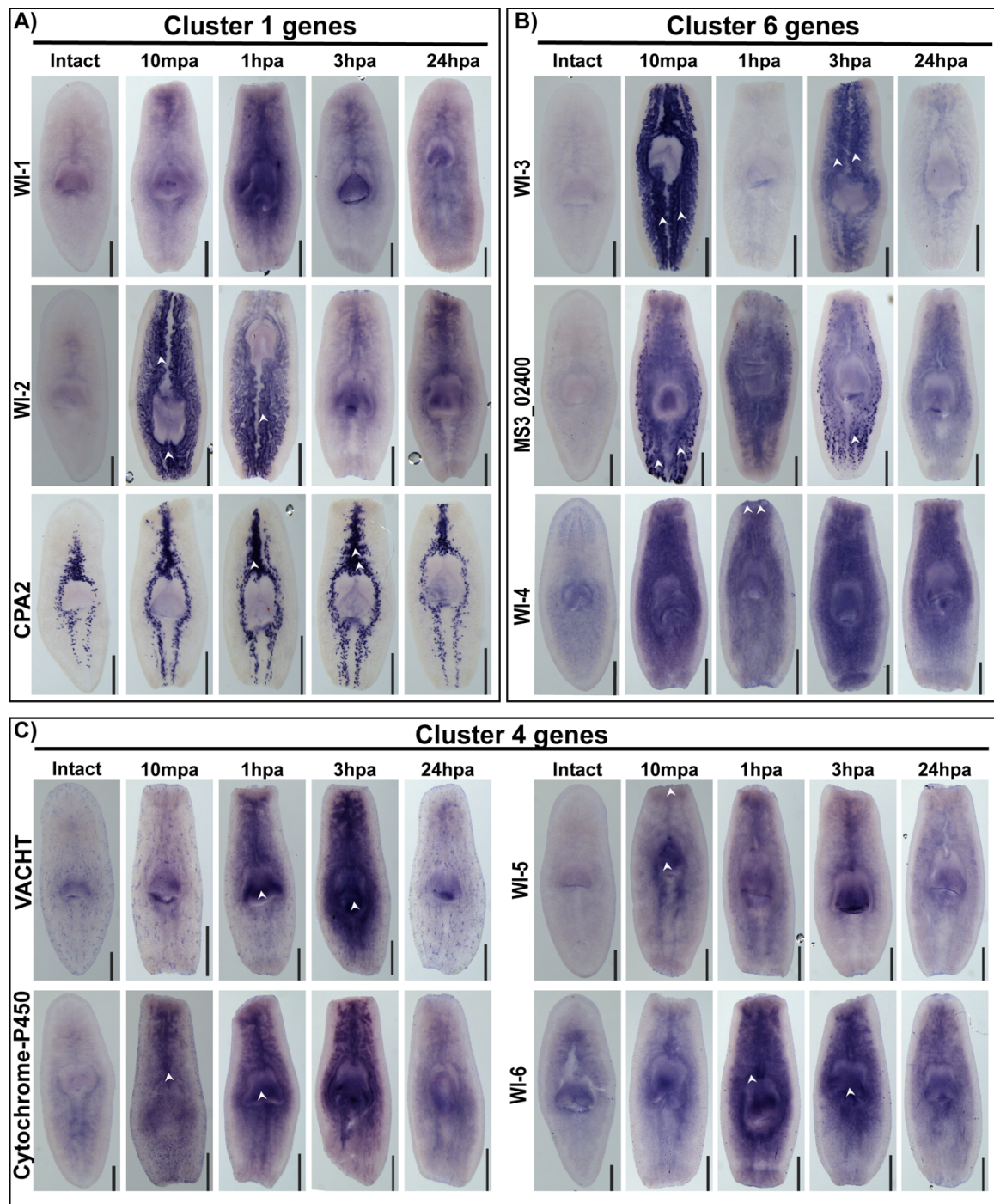


Figure 3.4 Planarian intestinal show a strong gene expression response to wound signals. Whole mount in situ hybridization of candidate genes from cluster 1 (A), 6 (B) and 4 (C). Genes from cluster 1 and 6 showed dramatic increase in expression in intestinal cells at early timepoints. Cluster 4 genes showed variable tissue expression. White arrowheads are showing the induction of expression at particular regions. Scale bar -500  $\mu$ m.

Cluster 4 genes are largely upregulated at 1hpa, continued to be expressed at 3hpa, then decline at 24hpa (Figure 3.4 C). For example, vesicular acetylcholine transporter (vacht) showed low parenchymal expression in wild type worms, but at 3hpa the expression was dramatically increased (Figure 3.4 C). cytochrome-450 and WI-6 genes were highly upregulated at 1hpa and 3hpa but ceased expression at 24hpa (Figure 3.4 C). Most of the candidate genes tested in cluster 5 were unknown proteins, showed high expression at 10mpa, and continued to express at 3hpa (Figure 3.5 A). Among the known genes in this cluster, dimethylglycine dehydrogenase (dmgdh) is reported to be expressed in pigment cells in intact worms (Plass et al., 2018) but showed induced wound site expression at 3hpa (Figure 3.5 A).

Importantly, a significant number (50%) of screened genes from cluster 5 showed wound induced expression in epidermal cells (Figure 3.5 A). For example, wi-7, wi-8, wi-9, wi-10, wi-11 had very low or no expression in intact animals but showed clear upregulation after injury (Figure 3.5 A). Other genes in cluster 5 showed more variable expression patterns (Figure 3.5 B). For example, wi-12 is lowly expressed in intact animals, but after injury it showed increased expression in the pharynx. The planarian single cell transcriptomic ATLAS showed that wi-12 is expressed in the planarian glial cells (Plass et al., 2018) however, after injury it showed wound site expression at 1hpa and 3hpa (Figure: 3.5 B).



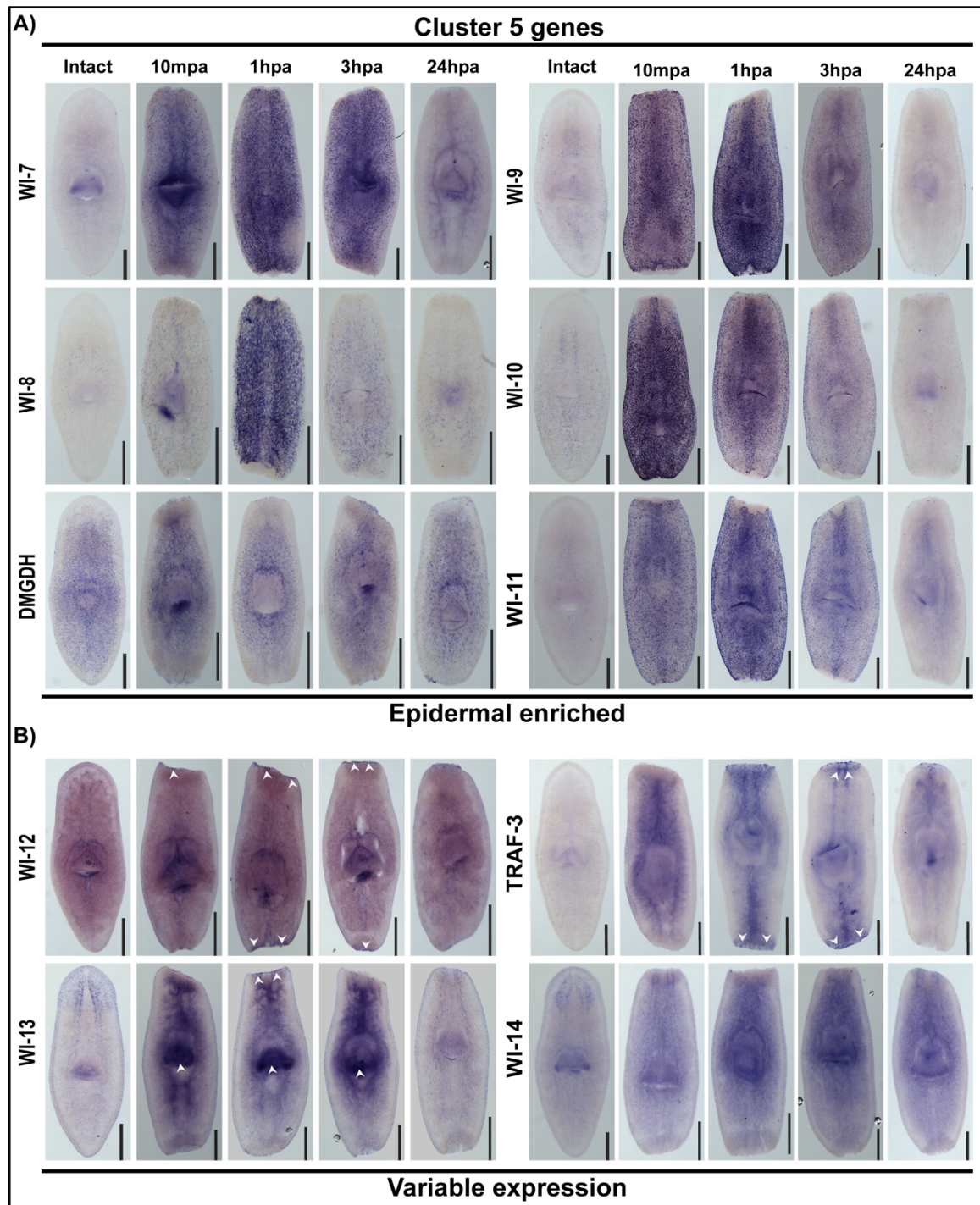


Figure 3.5 In situ validation of wound induced epidermal genes

A) Whole mount in situ hybridization of cluster 5 genes, which showed activation of expression in the epidermis. B) Variably expressed (in multiple tissues) early wound induced genes from cluster 5. White arrowheads are showing upregulated expression at specific sites. All scale bars are 500  $\mu$ m.

Cluster 2 includes genes that appeared downregulated at early time points compared to 24hpa (Figure 3.6 A) but may in fact be upregulated at 24 hpa. By performing WISH on some candidates from Cluster 2, I found that indeed several genes in this cluster are induced to express at later time points (18-24hpa). For example, the wound induced gene *notum* expresses highly at 18hpa in anterior facing wounds (Petersen and Reddien, 2011) and my data identified *notum* as significantly downregulated at early timepoints compared to 24 hpa (Figure 3.3 B). Wound induced late (WIL) gene *wil-1* had very low baseline expression in wild type worms, but at 24hpa it showed distinct wound site expression that was not observed at 10mpa, 1hpa or 3hpa (Figure 3.6 A). Although cluster 2 gene *wil-2* is expressed moderately in the epidermis before injury, it showed significant upregulation at the wound site at 24hpa in amputated worms (Figure 3.6 A and B). Another gene, CG6763, is expressed in the intestinal cells of intact worms but showed upregulation at 24hpa compared to early timepoints (10mpa, 1hpa, 3hpa). Finally, frizzled family genes are known to be activated in planarians after injury and we found that *frizzled-5* is induced at 24hpa, particularly at the wound site (Figure 3.6 A, B) (Petersen and Reddien, 2011).

So far, I showed that my RNA-seq data from epidermal tissue isolated after amputation successfully detected wound-induced genes. Many of these genes had not been previously identified as wound induced and several are genes with no homology to other proteins. After performing WISH, I was able to corroborate my DEG analyses, suggesting that this RNA-seq dataset can inform the many important changes occurring in the epidermis in the early stages of wound healing and regeneration.



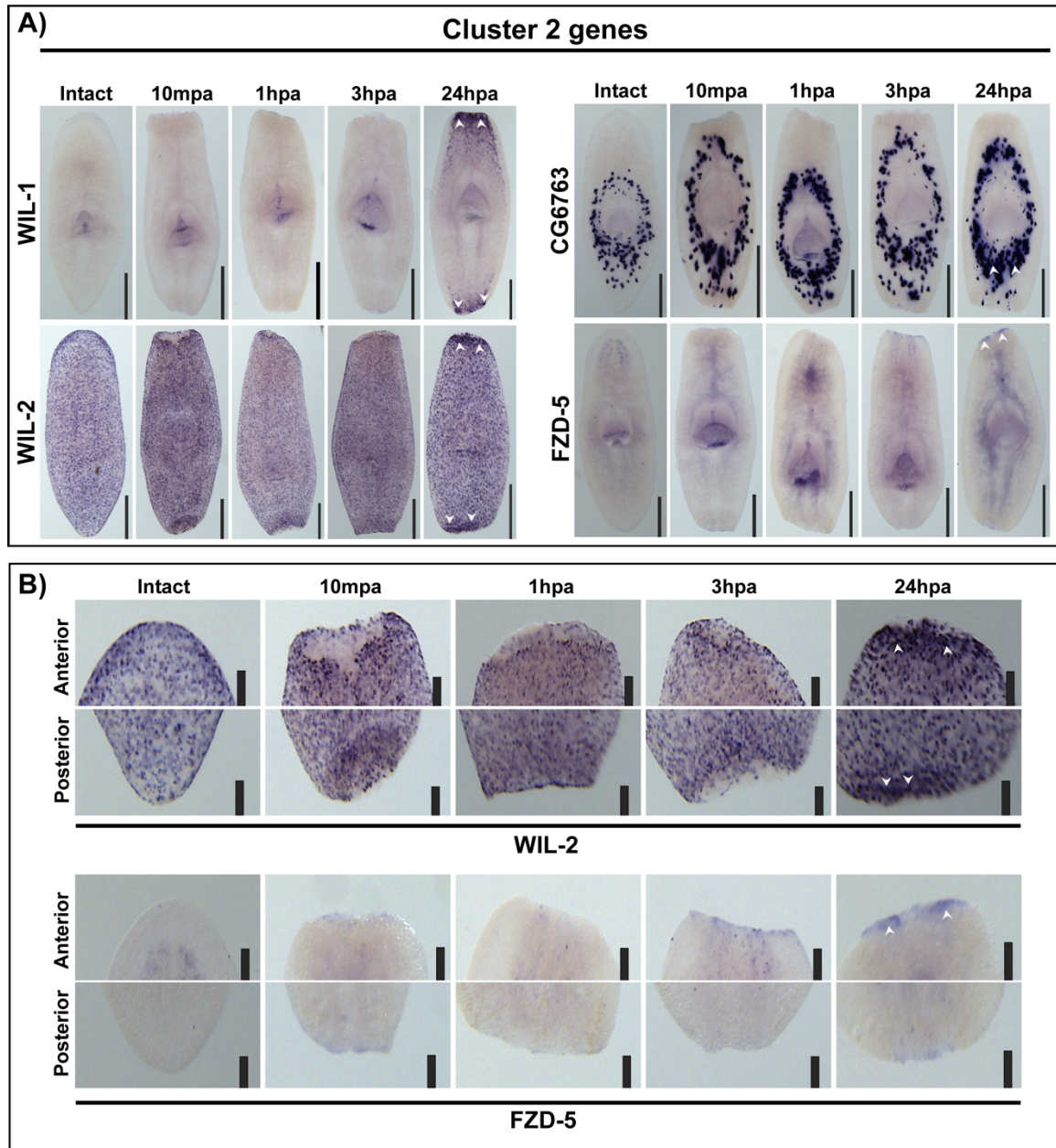


Figure 3.6 In situ validation of genes induced at later time points after wounding  
A) Whole mount in situ hybridization of cluster 2 genes at different regenerating time points. Cluster 2 contains genes that are downregulated at early time points, which often means they are upregulated at 24hpa. White arrowheads are showing the site of gene induction. B) Images focusing on the anterior and posterior wound sites after wil-2 and fzd-5 WISH show that they are upregulated at 24hpa at the wound site. All scale bars are 500  $\mu$ m.

### 3.4 GO analysis unveils several biological roles of early wound induced genes in planarians

Comparing the 10mpa and 1hpa and 3hpa RNA-seq data with data from 24hpa revealed hundreds of differentially expressed genes at each time point. To better understand the larger trends of gene activation in this early response to injury, I ran GO analysis on the DEG with known BLAST hits. 367/586 genes upregulated at 10mpa had known blast hits; GO analysis indicated that they are broadly involved in immunity, such as lytic vacuole organizations, neutrophil mediated immunity and early stress response signaling pathways (Figure 3.7 A). Further, gut enriched cells goblet cells and phagocytes are known to be involved in planarian immunity (Peiris et al., 2014) and expression patterns of several early wound induced genes were enriched in the planarian intestine (Figure: 3.4 A and B). In addition, I detected the activation of several goblet cell genes early after amputation, such as *klk13*, *npc2*, *rpz3* (Forsthoefel et al., 2020), which are known to be involved in several protein catabolism and antimicrobial activities (Prassas et al., 2015). Another wound-induced epidermal gene, *traf3*, has also been reported to regulate immune response and inflammation (Lalani et al., 2015).

There were 514 genes upregulated at 1hpa compared to 24hpa and GO analysis revealed that they are mostly involved in transporter functions (Figure 3.7 B). ATP binding cassette (ABC) transporters are reported to function in regeneration and tissue defense (Huls et al., 2009). Detection of the ABC family gene *abcc1* upregulated at 1hpa (Figure 3.3 B) supports our findings that early wound induced genes are linked to transporter function, which are needed for tissue regeneration. Platelet derived growth factor also plays an important role in wound healing and tissue regeneration (Pierce et al., 1991). The GO

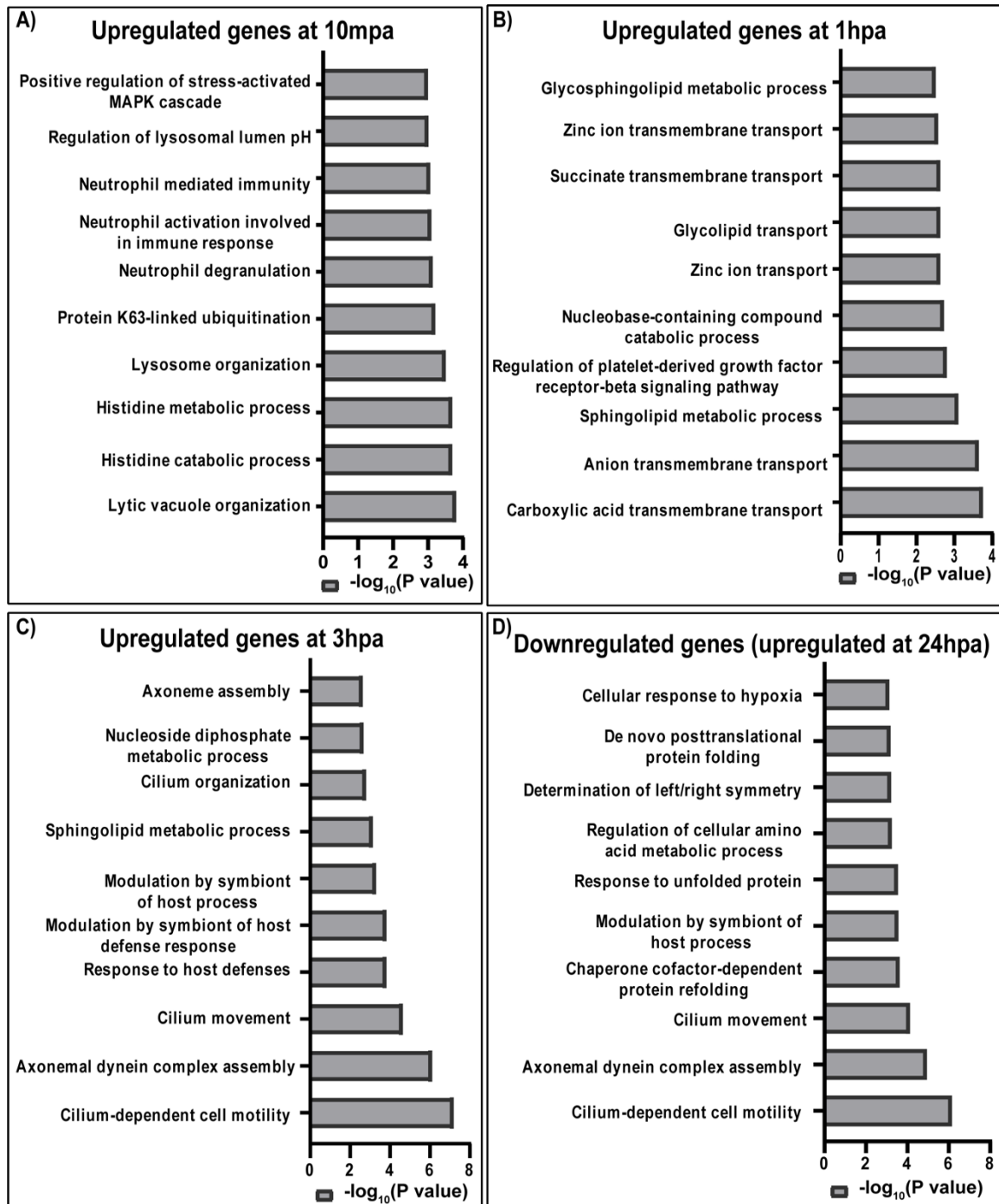


Figure 3.7 GO analysis unveils the biological functions of wound induced genes  
GO analysis of genes upregulated at 10mpa (A; n= 367 genes), 1hpa (B; n= 291 genes) and 3hpa (C; n=381 genes). Genes with no GO annotations were excluded from the study. D) GO analysis of all the downregulated genes from three time points (10mpa, 1hpa and 3hpa) (n=798 genes).

analysis also showed that several genes upregulated at 1hpa are involved in platelet derived growth factor regulating signaling pathways (Figure 3.7 B). These analyses reveal that immunity related biological functions initiate immediately, with host defense mechanisms and modulation of defense mechanisms following soon after (Figure 3.7 C). However, at 3hpa the most significant biological functions identified by GO analysis were cilium dependent cell motility, cilium movement and dynein complex assembly (Figure 3.7 C). Several cilia related dynein family genes were upregulated at 3hpa, such as *drc1*, *dnah3*, *dnah17* (Rompolas et al., 2010), suggesting that cilia are needed for cellular functions that occur at or soon after this time point.

I also performed GO analysis on the genes that were downregulated at different time points. I pulled all the downregulated genes from each time point and ran GO analysis. Notably, cilia related functions were found to be enriched at 3hpa but were also identified as enriched among those genes induced at 24hpa as well (Figure 3.7 D). Furthermore, several heat shock protein related genes that are involved in protein refolding and degradation such as *hspa8*, *hspa4l*, *hspa5* were upregulated at 24hpa (Miller and Fort, 2018) (Figure 3.7 D). Upregulation of heat shock protein family genes might explain genes that were expressed at earlier timepoints and remained unfolded during translation.

In short, GO analysis suggests there are several important biological pathways that are activated at very early stage of regeneration. Among them, immunity related functions and cilia assembly and function are the most obvious categories that are activated in the epidermis after planarian amputation.

### 3.5 A wound induced gene encoding a putative membrane protein operates during planarian tail regeneration

To identify the biological functions of the candidate genes that were selected for RNA-seq data validation, I performed RNAi screening of those genes. Among the candidate genes, we found one gene *wi-12*, which encodes a putative homolog of a CD-20 family membrane protein. Upon performing RNAi of this candidate gene, I found that two small head fragments did not regenerate their tails at 10dpa. Noticing that those fragments were smaller and suspecting they may have been amputated closer to the eye spots (versus closer to the pharynx), I repeated the RNAi screening of *wi-12* and amputated the worms at AP1 and AP9 planes (Figure 3.8 A).

To quantitate any regeneration defects, I measured body length and blastema lengths at multiple time points post amputation and then calculated a blastema length to body length ratio of head fragments. Even though the AP1 head fragments of *wi-12* -RNAi worms were comparable to controls at 2dpa, by 15dpa the total body length of control (RNAi) AP1 fragments was higher than *wi-12* -RNAi fragments (Figure 3.8 B). Moreover, we found that the tail blastema to body length ratio of *wi-12* -RNAi animals were significantly smaller than that of control animals in AP1 head fragments. *wi-12* -RNAi animals did not regenerate normal tails even at 15dpa (Figure: 3.8 C and E). I also performed a feeding assay at 14dpa and found that only 17% of *wi-12* -RNAi AP1 head fragments ate at 14dpa where 84% of control animals ate at 14dpa (Figure: 3.8 D). However, all the other head and tail fragments for both for *wi-12* -RNAi and control animals ate at 14dpa, which was confirmed by red food color in the worms gut (Figure: 3.8 D).

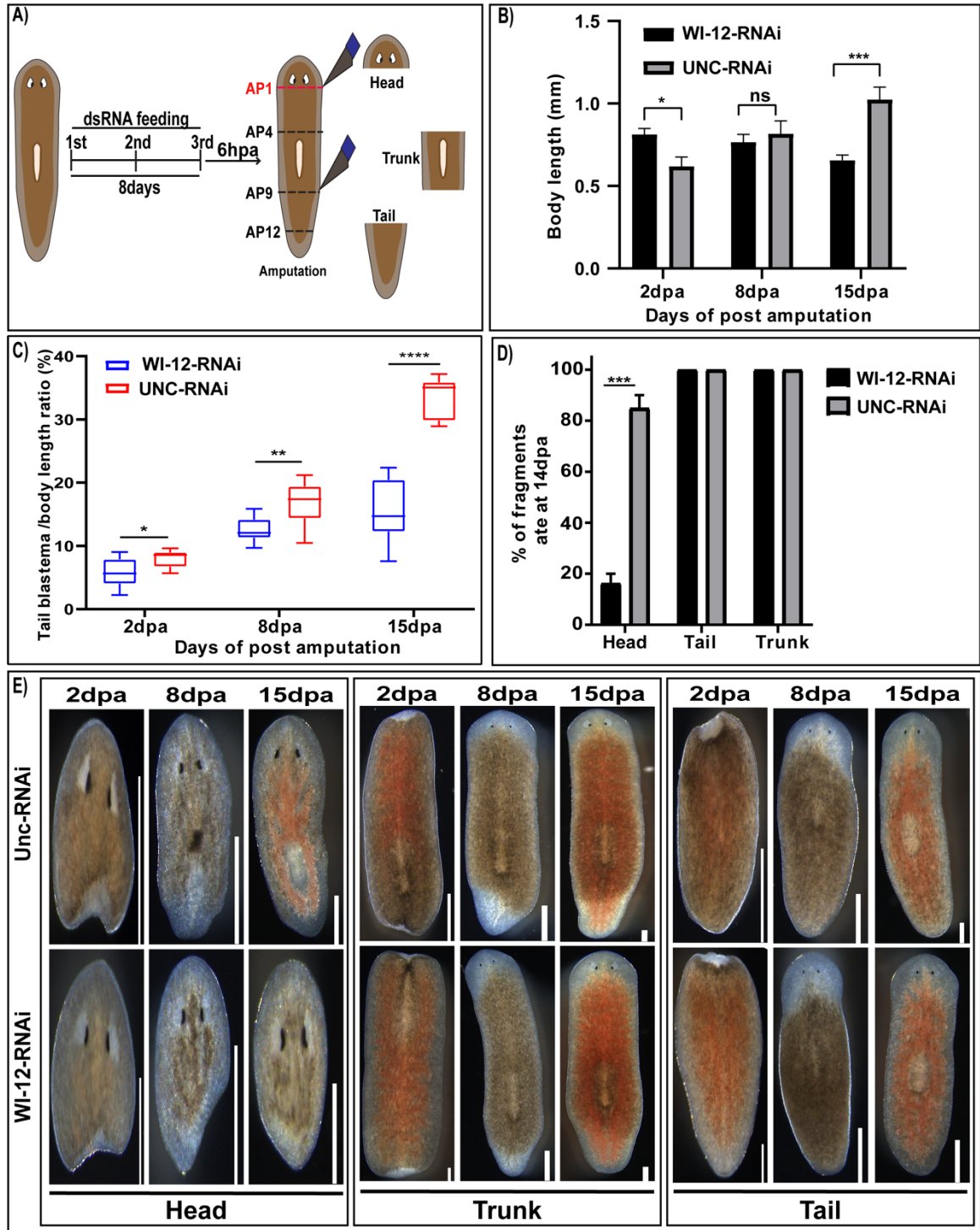


Figure 3.8 WI-12 gene functions depend on the position

A) Schematic representation of RNAi experiment. Red line shows the position of amputation. B) Total body length measurement of *wi-12* and *unc*-RNAi treated head fragments at different days post amputation. The *wi-12* gene corresponds to the gene ID (SMESG000046786.1). Length of the worms were measured using tools in Fiji. For

statistical analysis, ten images from two independent experiment were quantified for each group. C) Tail blastema to body length ratio of wi-12 and unc-RNAi treated head fragments at different days of post amputation. D) Plot summarizing a feeding experiment showing the percent of different regenerating fragments that ate at 14dpa. E) Live images of regenerating worms fragments at different days of post amputation. (Scale bars-500µm)

I also fed wi-12 dsRNA to planarians and amputated the animals at the AP4 and AP9 positions (Figure 3.9 A); I found that all these head fragments were able to regenerate normal tails by 15dpa (Figure 3.8 C). Moreover, all (100%) AP4 head fragments fed with wi-12 -RNAi ate at 14dpa, just as control animals. Furthermore, I fed dsRNA to the intact worms as well and they did not show any sign of abnormalities even at 28 days post feeding (Figure 3.9 B). Thus, I conclude that wi-12 -RNAi only affects tail regeneration in head fragments that were amputated at AP1 position.

Here I have shown that using an SDS-based epidermal isolation and RNaseH ribodepletion, I identified hundreds of DEG in the regenerating planarian epidermis. Genes expressed early after amputation involve in immune function, external signaling cascade, and transporter functions. I also identified several unknown genes that are expressed in the planarian epidermis after amputation. Among the candidate genes we have screened for function, I found that a putative membrane protein is required for planarian tail regeneration when the head fragment is amputated at a specific position.



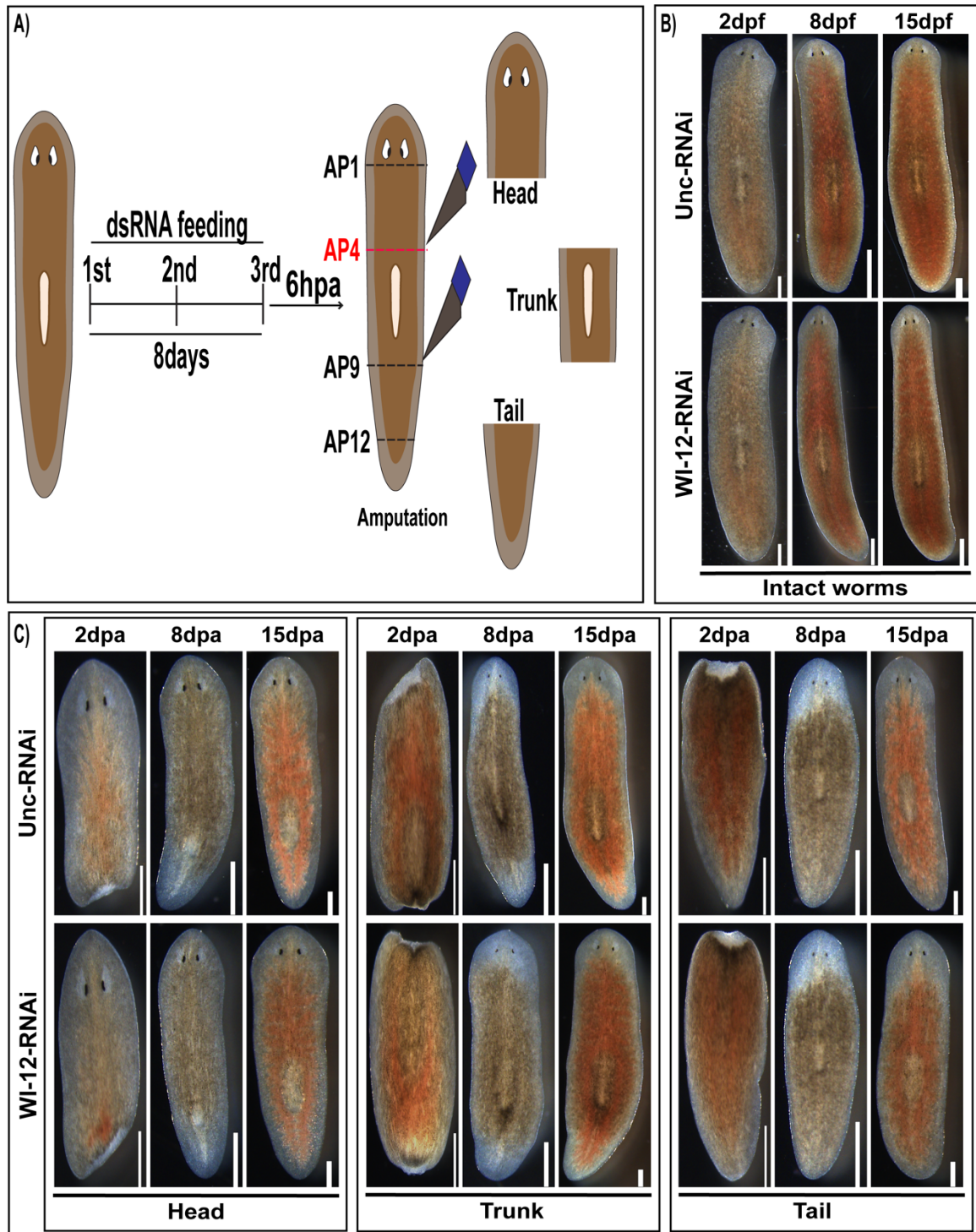


Figure 3.9 WI-12-RNAi treated head fragments regenerate normally when cut at AP4  
A) Schematic representation of RNAi experiments. Red line shows the position of amputation. B) wi-12 and unc-RNAi treated intact worms at different days of post RNAi feeding (Scale bars-500µm). C) Live images of wi-12 and unc-RNAi treated worm fragments (head, trunk and tail) at different days of post amputation (Scale bars-500µm).



## CHAPTER 4. DISCUSSION

### 4.1 Epidermis- a crucial player in wound healing and regeneration

While all animals can heal their wounds, specific wound closure mechanisms vary across species, tissues and developmental stages. Despite this variability, among Ecdysozoans the cellular and molecular mechanisms of wound healing have been restricted to a small number of model organisms (Galko and Krasnow, 2004). Moreover, Lophotrochozoa, a large metazoan group, has remained largely unexplored regarding the study of molecular wound healing mechanisms. Furthermore, the widely studied Ecdysozoan model *Drosophila* and *C. elegans* have specialized epidermis and both are covered by cuticles whereas Lophotrochozoa such as planarian flatworms have ciliated epidermises that are more similar to mammalian respiratory epithelia (Rompolas et al., 2013). Thus, it is highly likely that studying the Lophotrochozoa epidermis may inform the molecular wound response in other organisms.

Although among metazoan the phenomenon of regeneration is widely spread, it is not fully understood why such remarkable capacity has been lost/reduced in numerous organisms, tissues, or developmental stages. Numerous studies have suggested that the epidermal wound response is crucial to the process of regeneration (Erickson and Echeverri, 2018). Furthermore, it has been shown that if formation of wound epithelia is perturbed, regeneration processes is halted in salamander and mice (Goss, 1956; Mescher, 1976). However, many of the cellular and molecular mechanisms underpinning tissue regeneration are yet to be determined. Studying wound healing and injury response across metazoan species that vary in regeneration capacity will help to unveil factors associated with and underpinning mechanisms of tissue regeneration.

#### 4.2 Wound response program is associated with planarian regeneration

Studies on planarians offer extensive opportunities to explore mechanisms of wound healing and tissue regeneration for several important reasons. For examples, planarians can regenerate virtually any missing tissues and can survive with extensive tissue damages. Planarian epidermis can heal the wound area within hours without dividing the epidermal cells (Hori, 1989). Moreover, studies show that application of protein synthesis inhibitors such as cycloheximide during the planarian wound healing process are unable to perturb wound healing, which suggest that proteins already present in the planarian epidermis facilitate the healing processes (Wenemoser et al., 2012). In planarians, the wound healing processes is followed by a robust regenerative process when significant tissue is missing (Wenemoser et al., 2012; Wenemoser and Reddien, 2010; Wurtzel et al., 2015). The planarian model therefore allows us to study both the wound response program and mechanisms associated with proper regeneration, which can then be compared with low or non-regenerative organisms. Such studies will provide opportunities to explain the injury response and wound healing processes as well as the reason behind reduced regenerative capacities.

Identification of wound and stretch induced genes that are induced immediately after amputation will provide the opportunity to study their roles in the context of injury response and tissue regeneration. Although the next generation sequencing technology allowing single cell RNA-seq has arrived at a remarkable stage, several factors make the process of identifying new wound induced genes challenging using this method. For example, epithelial sheets that make up the epidermis are more resistant to dissociation than other cell types, increasing the odds that they will be excluded from collection. Furthermore, the available RNA-seq library preparation method is not sufficient to identify

important classes of RNAs such as non-coding RNAs, which play significant roles in regulating gene expression (Kim et al., 2019). Single cell RNA-seq is also often not sensitive enough to capture lowly expressed genes due to its bias of transcript coverage and high technical noise (Chen et al., 2013). Thus, tissue specific bulk RNA-seq can be useful in detecting transient tissue-specific early wound response genes during planarian regeneration (Forsthoefel et al., 2020; Wurtzel et al., 2017).

As planarian epidermis initiates the wound healing processes, identifying genes that express immediately after amputation in the planarian epidermis can help to identify downstream signals that are required for proper planarian regeneration. However, the only reported way of isolating the planarian epidermis is by soaking worms for 20 minutes in ammonium thiosulfate (Wurtzel et al., 2017). As I showed here, this treatment likely increases the contamination of other cell types in epidermal samples, increasing the noise within the dataset and making it more difficult to detect real changes.

#### 4.3 SDS based epidermis isolation is a useful method for studying planarian epidermis

My work shows that using 0.1% SDS to isolate the planarian epidermis allows us to do so within minutes and with little contamination from other cells. When combined with RNaseH ribodepletion and RNA-seq library preparation, I was able to deplete almost ~99% of ribosomal RNA which comprises >80% of total planarian RNA (Baldwin et al., 2021; Kim et al., 2019) and create a comprehensive list of epidermal enriched transcript. RNaseH based ribodepletion is also useful in detecting nuclear transcripts, which may facilitate the study of alternate splicing during mRNA maturation (Potemkin et al., 2022). We have shown that RNaseH based library preparation in planarian epidermal cells and whole worms efficiently depletes ribosomal RNA. Thus, SDS based epidermis isolation

followed by RNaseH based library preparation method provides more complete coverage of all epidermal transcripts than single cell RNA-seq. Furthermore, comparison with ammonium thiosulphate-based epidermis isolation followed by polyA based library preparation method showed that my methods detected more significantly differentially expressed genes in planarian intact epidermis. I then used both the epidermis isolation and library preparation methods to detect wound induced genes during planarian regeneration.

Cell type specific wound response and transduction of these signals to the neoblast cells is essential for proper regeneration. For example, it has been shown that muscle cell specific expression of myoD is responsible for forming the longitudinal muscle fiber is required for planarian regeneration (Scimone et al., 2017). Multiple epidermal cell specific wound induced genes have been reported to have functional roles in planarian regeneration as well, including fos-1 (Wenemoser et al., 2012) and jun-1 (Van Huizen, 2021). Several other genes have been reported as to have functional role in planarian epidermal cells maintenance during homeostasis and regeneration, such as transcription factor egr-5 (Tu et al., 2015) and transcription factor myb-1 (Zhu and Pearson, 2018). Yet while the role of the epidermis and its wound healing are essential, many details about the genes, pathways, and downstream events activated by this tissue remain unknown.

I have showed that 0.1% SDS can also be used for isolation of regenerating epidermis ever rightly after amputation with minimal contamination of other cells. Isolation of epidermal cells from different regenerating time points allowed me to identify genes that are activated in the epidermis during regeneration, including many that have not been reported. In addition, by increasing the number and robustness of genes detected, I can perform functional analyses on these gene lists that would be much less meaningful

with less complete lists. For example, the immune system plays an indispensable role in maintaining homeostasis and tissue regeneration (Abnave and Ghigo, 2019). I have shown by GO term analysis that early wound induced genes activated immediately after amputation are involved in host immune response. Additionally, mitogen activated protein kinase family member ERK signal is activated upon injury and required for pro-regenerative cellular events such as cell survival, cellular differentiation, cell fate turnover and migration (Wen et al., 2022). I also showed that, genes that are involved in this extracellular signaling pathway are enriched in planarian epidermis during regeneration e.g., *shoc2*, a scaffold protein that regulates the ERK signal.

#### 4.4 Planarian epidermal genes are required for homeostatic maintenance and regeneration

I have reported several genes that are required for planarian epidermal homeostasis and regeneration. The RNAi phenotypes for some genes shown here have not been reported before. For example, I showed two sodium potassium ATPase genes that are required for homeostatic maintenance. These two genes *ms3\_03665* and *dana\gf17998* encode the two different subunit Na-K-ATPase  $\alpha$  and  $\beta 2$  respectively (Li and Langhans, 2015). Na-K-ATPase is known for maintaining sodium homeostasis in mammalian cells and required for tight-junctions formation in epithelial cells through Rho GTPase (Rajasekaran and Rajasekaran, 2003). Enrichment of *ms3\_03665* and *dana\gf17998* in planarian epidermis and their functional roles during homeostatic maintenance and regeneration agrees with the earlier findings. Perturbation of these two genes showed homeostatic and regeneration phenotypes where the worms had motility defects and impaired feeding behavior both in intact worms and regenerating worm fragments. Reports

show that biophysical signals and membrane gated voltage channel is required for proper planarian regeneration. For example,  $H^+,K^+$ -ATPase mediates membrane depolarization and is required for planarian anterior specific gene expression and head regeneration (Beane et al., 2011). Perturbation of  $H^+,K^+$ -ATPase membrane depolarization activity using SCH-28080 also showed impaired head regeneration. Interestingly,  $H^+,K^+$ -ATPase independent manipulation of membrane depolarization using ivermectin showed head regeneration in posterior facing wound and which suggest the importance of membrane channel protein functions during planarian regeneration (Beane et al., 2011). Thus, identifying genes that encode Na-K-ATpase subunits and revealing their functions in homeostatic maintenance and regeneration further agrees with the findings that membrane gated channels are required for planarian regeneration.

Cilia are basically cellular projections with a ring of nine doublet microtubules growing from the basal body (Glazer et al., 2010). Ciliary dysfunctions in humans result in several chronic disorders including chronic bronchitis, immotile sperm, kidney cysts, situs invertis and polydactyly (Badano et al., 2006). It has been reported that mutation in cilia genes such as *dnai1*, *dnah11*, and *dnah5* are responsible for primary ciliary dyskinesia (Eley et al., 2005). The planarian ventral epidermis is composed of a monostratified epithelial layer containing multiciliated cells that are required for planarian locomotion (Rompolas et al., 2010). Planarian motile cilia share the similar structure of typical respiratory cilia, which is composed of dynein powered 9+2 microtubule doublet axonemes (Rompolas et al., 2013). The nexin-dynein regulatory complex (N-DRC) in motile cilia and flagella stabilizes axonemal core and regulate the ciliary motion (Gui et al., 2019). In planarians it has been demonstrated that the outer dynein arm docking

complex (ODA-DC) is required for primary ciliary functions in planarians and loss of oda-dc showed ciliary loss and motility defects (Hjeij et al., 2014; Kyuji et al., 2020). Though the function of drc1, a subunit of N-DRC, has not been reported in planarians yet, in humans the loss of DRC1 shows primary ciliary dyskinesia (PCD) (Wirschell et al., 2013). As many planarians epidermal cells are multiciliated, identification of DRC1 in planarian epidermal enriched samples supports our data. Furthermore, the phenotypes I have shown here after knockdown of drc1 resemble the typical cilia dysfunctions such as motility defects, bloating and lysis (Vij et al., 2012).

As we discussed earlier, planarians use several canonical signaling pathways to regulate cellular differentiation, cell fate determination and finally regeneration (Jaenen et al., 2021). For examples, Hedgehog and Wnt/ $\beta$ -catenin signaling pathways are required for anterior-posterior axis determination (Gurley et al., 2008; Rink et al., 2009), BMP signaling determines the dorsoventral axis formation (Reddien et al., 2007) and the EGFR pathway is required for stem cell differentiation (Barberan and Cebria, 2019). However, although these signaling pathways play pivotal roles in proper regeneration, little is known about the upstream cues that initiate and coordinate these signaling pathways. Recently, it has been reported that ERK signaling activates in a stem cells independent manner within minutes after decapitation and required for proper regeneration (Owlarn et al., 2017). Furthermore, by blocking the protein synthesis using cycloheximide, they showed that ERK signal activates due to the wound signals irrespective of newly synthesized proteins (Owlarn et al., 2017). However, how the process is started upon wounding and in what cell type(s) the signaling occurs is not known. I have identified shoc2, a scaffold protein in the

ERK pathway known to positively regulate ERK signaling, as upregulated in the epidermis after injury. There have been several studies that pointed out the biological significance of SHOC2, including that embryonic knock out of SHOC2 is lethal in mice (Jang and Galperin, 2016) and that SHOC2 is required for cellular proliferation (Moon et al., 2011). I have shown that, knockdown of shoc2 results in smaller blastema formation and delayed regeneration, which may agree with earlier findings where shoc2 is described as a potent modulator of cellular proliferation (Moon et al., 2011). As shoc2 coordinates the ERK activity, it will be interesting to ask how loss of shoc2 affects ERK activation and its downstream effects.

Our findings on shoc2 as an epidermal enriched gene and its functional roles in planarian blastema size and eye spot regeneration raise several questions. Does SHOC2 coordinate ERK activation in planarians? Does it coordinate specific downstream pathways of ERK activation? Is the upregulation of shoc2 dependent on ERK activation? As it has been reported earlier, epidermal stretching induces transcriptomic changes in vertebrate skin cells (Ledwon et al., 2020). This raises this question, does epidermal stretching following amputation induce the expression of shoc2 in planarians? This question might be answered by introducing stretch inhibitors and observing the shoc2 expression in presence of this stretch inhibitor after amputation. In addition, transcriptomic and proteomic analysis in shoc2-RNAi background will inform us about downstream signaling events that might be regulated by co-activation of shoc2 and ERK during planarian regeneration.



#### 4.5 Positional control genes are required for proper regeneration

$\beta$ -Catenin functions simultaneously as a regulator of several cellular processes including organizer formation (Schneider et al., 1996), cell fate specification (Hindley et al., 2011; Logan et al., 1999), proliferation and differentiation (Gurley et al., 2008). Furthermore, it has been demonstrated that in planarians  $\beta$ -Catenin regulates head versus tail polarity and loss of  $\beta$ -catenin leads to the formation of posterior facing heads instead of forming a tail (Gurley et al., 2008). On the other hand, the wound induced gene *notum* specifies head formation at anterior facing wounds and knockdown of *notum* causes the formation of anterior facing tails instead of heads (Petersen and Reddien, 2011). These phenomena demonstrate that anterior-posterior axis polarity is regulated by Wnt signaling during planarian regeneration. Another Wnt pathway gene, *follistatin*, is also required for planarian head regeneration but only if worms are amputated at certain positions along the AP axis, which suggests the importance of positional sensing mechanisms during planarian regeneration (Tewari et al., 2018). My findings on gene *wi-12* showed that if I amputate worms at position AP1 the head fragments cannot regenerate tails but they can if I amputate at position AP4; this is the opposite of the *follistatin*-RNAi phenotype, as *follistatin*-RNAi trunk fragments cannot regenerate heads if the worms are amputated at the AP4 position but can when amputated at AP1. Thus, it suggests, as a putative gene, *wi-12* might sense the Wnt/ $\beta$ -Catenin gradients and act accordingly during planarian regeneration. Then again, as  $\beta$ -Catenin specifies the formation of tails, the *wi-12* gene might be required for establishing a  $\beta$ -Catenin gradient in the smaller AP1 head fragments. Studying *wnt*/ $\beta$ -catenin pathway genes and *notum* activation in AP1 head fragments in the *wi-12*-RNAi worms will help us to identify the mechanistic roles of *wi-12* in planarian tail regeneration.

In summary, in this study I have shown that, 0.1% SDS can be used to successfully isolate planarian epidermal cells with minimal contamination of other cell types. I have demonstrated that an RNaseH based rRNA depletion method can efficiently deplete ribosomal RNA from planarian total RNA. Furthermore, libraries prepared by RNaseH depletion detected more epidermal enriched genes compared to polyA selection-based method. In addition, I have shown that using these methods I can detect wound induced genes that are required for planarian homeostatic maintenance and regeneration. Although, I have reported 75 genes in this study, but more genes can be screened and someone else is working on that. Additional analysis and screening would allow us to identify non-coding genes that might be required during planarian regeneration. Finally, I have created a rich source of datasets that could be used for additional studies.

## CHAPTER 5. MATERIALS AND METHODS

### 5.1 Planarian maintenance and care

Asexual strain of *Schmidtea mediterranea* (clonal line CIW4, RRID: NCBI Taxon: 79327) (Sanchez Alvarado et al., 2002) were maintained in 1X Montjuic water (1.0 mmol/l calcium chloride, 1.6mmol/l sodium chloride, 1.0mmol/l magnesium sulfate, 0.1mmol/l magnesium chloride, 0.1 mmol/l potassium chloride and 1.2 mmol/l sodium bi carbonate in Milli-Q water, pH-6.9-8.1) (Cebria and Newmark, 2005). Animals were fed beef liver paste and worms were kept starved for a week before conducting any experiments.

### 5.2 Planarian epidermis isolation and RNA extraction

Before isolating the epidermis 6-8mm worms were kept starved for a week. Intact and amputated worms (10mpa, 1hpa, 3hpa and 24 hpa) were used for isolation of epidermis separately. Either uninjured or injured (trunk fragments) worms were soaked in 0.1% SDS for 1 minute on a glass plate. After that, the epidermis of the worms was scraped off the worms using the 21G syringe needle under stereo microscope. Then the skin was transferred in 0.5ml of TRIzol reagent kept in ice. For each skin samples 10 worms were used to isolate the skin. After isolating the skin samples from all the worms, the samples were stored at -80C and in parallel whole worms were put in TRIzol. RNA extraction for samples in TRIzol were performed using Zymo Research RNA clean and concentrator-5 kit according to manufactures protocols with minor variation. For extracting the RNA, we did size selection for further RNA-seq library preparation (Kim et al., 2019).

### 5.3 RNase-H ribodepletion and RNA-seq library preparation

RNase H mediated rRNA depletion protocol was partially adapted from the rRNA depletion method developed for bacteria (Culviner et al., 2020) and human cells (Baldwin et al., 2021). For this method, ~500 ng of RNA from isolated intact skin, injured skin, or whole worms was taken for each replicate. Then 1000ng of probe pool (169 probes) and probe hybridization buffer (0.75uL 1M Tris HCl (pH- 7.5) + 0.3uL 5M NaCl+ 0.3uL 1M EDTA) were mixed with RNA to a final volume of 15uL. Probe-RNA mixtures were heated in a heat block at 95C for 2 mins and then slowly cooled (-0.1°C/sec) at 65C. The mixtures were then heated for additional 5 minutes at 65C. After the hybridization reaction, 5µl preheated Hybridase RNase H reaction (3µL Lucigen Hybridase™ Thermostable RNase H enzyme (Catalogue #H39500) (+ 0.5µL 1M Tris-HCl (pH 7.5) + 0.2µL 5M NaCl + 0.4µL 1M MgCl<sub>2</sub> + 0.9µL nuclease-free water) was added to the sample mix and incubated at 65C for 2.5 minutes. After that in-column DNase I treatment was performed to degrade excess probes and genomic DNA. For in-column DNase I treatment 30 uL of prepared DNase I reaction mix (3µL TURBO™ DNase [ThermoFisher AM2239] + 5µL 10X TURBO™ DNase Buffer + 22µL nuclease-free water) was added to the samples immediately and incubated at 37C for 30min. Then the ribodepleted RNA was cleaned using Zymo Research RNA clean and concentrator-5 kit and RNA-seq libraries were prepared using KAPA RNA hyper kit (Catalogue # 08098107702) along with KAPA unique dual index adapters (Catalogue #8861919702) according to manufactures protocol.

#### 5.4 Gene cloning

For cloning the candidate genes, gene specific primers with overhanging nucleotides (forward- and reverse-) homologous to pPR-T4P vector was used. After extracting RNA from whole worms and worms epidermis iScripts reverse transcriptase supermix (Biorad Cat #1708840) was used to prepare cDNA libraries. pPR-T4P vector was linearized by treating with SmaI (NEB Cat # R0141L). After treating both the PCR product and linearized vector with T4 polymerase (Novagen Cat #70099) mixed and incubated at room temperature for 60 minutes. Constructs were transferred to E. coli DH5 $\alpha$  and minipreps were prepared using ZymoPURE Plasmid Miniprep Kit (Zymo Research Cat #D4211). Minipreps for each gene was selected by doing PCR and further verified by sequencing. Primers used in this study are listed in appendix 2.

#### 5.5 NBT/BCIP whole mount in situ hybridization

Nitroblue tetrazolium/5-bromo-4-chloro-3-indolyl phosphate (NBT/BCIP) colorimetric whole mount in situ hybridizations were adapted from previously described (Guerrero-Hernández et al., 2021) with minor modification. Briefly, 3-5 mm worms were starved 7-10 days prior starting the in situ. Animals were killed in 0.5% HNO<sub>3</sub> and fixed with 5% formic acid for 45 minutes. Following the bleaching with 1% formamide and 5% H<sub>2</sub>O<sub>2</sub> solutions for 2 hours, worms were treated with proteinase K (2ug/ml). Animals were hybridized overnight with riboprobes and then samples were washed 2X with wash buffer, 1:1 wash buffer-2X SSC, 3X with 2X SSC, 0.2X SSC and 1X MABT buffer. Subsequently, 0.5% Western Blocking Reagent (Roche Cat # 11921673001) with 5% inactivated horse serum in 1X MABT was used as blocking solutions. Anti-DIG antibody in blocking solutions (1:2500) was used as antibody solutions and samples were incubated

in antibody solutions for overnight at 4C. Post antibody washes and colorimetric development was performed as described (King and Newmark, 2013).

#### 5.6 Double stranded RNA synthesis and RNAi gene knockdown experiments

In vitro double stranded RNA (dsRNA) synthesis was conducted as previously described protocol (Rouhana et al., 2013). Gene knockdown was performed by feeding corresponding dsRNA to the target gene with liver paste. For RNAi scheme, animals were starved 7 days prior to start the dsRNA feeding. Animals were kept in dark for at least 1 hour before each feeding. For each experiment, dsRNA was mixed with homogenized beef liver (1:3) and fed for 3 times in 8 days period. On last day of feeding, animals were cut into head, tail and trunk fragment after 6 hours post feeding and each fragment was allowed to regenerate for 15 days. In this period worm fragments were monitored for every two days for regeneration defects. On 14dpa, animals were fed normal liver paste to see their feeding behavior. Animals were scored based on the liver paste in animals guts.

#### 5.7 Image processing and quantification

All the live images of live animals and in situ hybridizations reported in this study were taken using Leica stereoscope model M205 FA. Images were captured using Leica image processing software LAS X version 3.7.4. We quantified the whole planarian body and blastema size in FIJI by tracing the structures (Schindelin et al., 2015).

## 5.8 Statistical analysis and graphing

All the statistical analysis and data visualized was conducted using GraphPad Prism version 8.0. Unpaired student T-test with Bonferroni correction was employed for all the statistical analysis.

## APPENDICES

### APPENDIX 1. Planarian rRNA probe set used for RNase-H based ribodepletion

Ribosomal RNA transcript sequences were obtained from Kim et al., 2019 paper. The designed probe sets for each specific transcript almost covers the entire transcript and each probe is ~50nt in size.

Probes	Targets	Sequences
Probe-1	12S rRNA	GTAAACAACCACCAATAAACTATAGCGTTTAACAG CATGCCAGTTTAAAAAGCCAAGACAAAACCTATAT
Probe-2	12S rRNA	CTCAAGCAATCAATTTACATTAAATTTTAAAATATA CACGCCTAATAAAACCATTAAACAAAATTAATA
Probe-3	12S rRNA	CTAACATAGTAATACAAAGTGTAACCGCAGAAGCT GGCACTCATTTGATCTCCTAATAGCATATACCGA
Probe-4	12S rRNA	GTATTAAAATCTACCACTAGTCATACATAAAGTCTC TTATTGAAACTTAACCAATTTAAACCAAATAATAAA
Probe-5	12S rRNA	TGAGGAAATAAAATAAACAACCCTTATAAATAAAG CCAGATTCATGTCTAAAAAGGAAGTAAACTAATA AAA
Probe-6	12S rRNA	CGGATACTCTTTTCTAAACCCACACTCCCCAAATAA TTAGAACAACCTGCCAAGTCTTTTCATTTTGA
Probe-7	12S rRNA	AGCATAACTATAAGGCCATTACATATGTACAACC GTACACTAACCATAATCTTAGCGAGATATTGAG
Probe-8	12S rRNA	CAAAAGGTATCTAACCAATGTAGTGAAAGCATAAT CTAAGATAAGCAGCACAATGATTTGCATTAAAGAA



Probe-9	12S rRNA	CTAAGTCCTAGAAAAGATTCAAAAAAGCCAATTCA TCTAAATTTACTATTTAGTCCTGATCAACACCAATT ATTT
Probe-10	12S rRNA	GTACAATTTCTATTATACTTACCATGTTACGACTTA ACTCCTCTTAAAGAACGGAGATTGACGGGCGGTGT GTA
Probe-11	16S rRNA	GAATAAAACATAAAATACCTACAAACCGTAATA CAAAAAGGAAAATATCACAACTAAACAGTGCAATA C
Probe-12	16S rRNA	ATGTAATTCTAATGTTAACCAAAGAAAATAAAACA AAACACACAAAAGATATATCATATTCCATTTCGAGA
Probe-13	16S rRNA	CAAAAGCTTATCCTAAAGACAATTAAAACTAGAT AAAGAAATCCGAAAACATATCACTACTATCAATTA
Probe-14	16S rRNA	CAAATCTTAAACAATCTAAAGAAATACTATTAAGA ATAACTAAACAAATAAGAAAAAAAAACAAGTAAA A
Probe-15	16S rRNA	GCATAATTCATATTAATTACGTAATTGCTAAAAAGA ATTACTAAAACCATATAAGCAAACAAACGACTAA
Probe-16	16S rRNA	GCAGGGACTACATTTTACAAAAAATGAAATGTTTTT AAAAAACAGTTGTAGACGCATTGAGTTATAAATA
Probe-17	16S rRNA	GAATTAGTAGACAAGTAATTATGCTACCTTCGTACA GTCAAAGTACTGCAGCTATTAACTTATCAGTGA

Probe-18	16S rRNA	GTATAAATTAAAAACAAGGCTAAATAAAAACTTG CTATCTATCAATAAACCCATTCAAACAATTCTA
Probe-19	16S rRNA	GAAACACCACTAAGTTAAAACTCTCTAGGGTCTTT TCGTCCTTGAAATAACAAACTGTATCTTTACAGAAA
Probe-20	16S rRNA	AGGAAGTTCATAATGTAATAAATAAGTATTCAAAA TAAATACCGTTACCCCAACAAATAACTAAAGTAA
Probe-21	16S rRNA	ATTCAACATCGAGGTAGAAAACAAAATCTTCGATA TGTCTCCAAGATTCTATATCCCTGTTATCCCTA
Probe-22	16S rRNA	CTCAAATCACGAATAATATTATTAGTCGAACAGACT AAAAGTAAAGGCCTCTACACCTATCTTTAACTACA
Probe-23	16S rRNA	CAATCCAATTCCTTTCGTACAATGGACAGAAATTCA GGATAAAAACCAACCTGATTCACATCGGTCTAAA
Probe-24	18S rRNA	ATAGCCAGAATCAATAGCTTTTTTATATACACTATC AACTCATTTGACTCTCAATATATACCAGTAGC
Probe-25	18S rRNA	CGAACAGCATCTCCACTATTGCAGTCTATATACACC CCATATCCATAAAGGTATATGAGATTACATTGA
Probe-26	18S rRNA	CTATATGTTACCAGATACATTTGTGGTACGTAGCAG TCGAAAAGGTCCACGGCTTTGGACAACCCAATAC
Probe-27	18S rRNA	ACTGAATCTGACATAATACCAATCCTGGGCCAATA AAATGTAAATTGCAAACACTCCTAGGCGTAAG
Probe-28	18S rRNA	ACCGCTCATTAAGCTAGAAGCATTGCCTCTAACAAG CAGTAATCAATCGCATTTGAAGCCTCAATAGCA

Probe- 29	18S rRNA	CTTGGTCAATAAATAACCAATTTACAGGACCGTTAT AGCTATGATAAATATCATAACATTTATTCGTTTA
Probe- 30	18S rRNA	CATTAAATATGCATAAATTAGCCACGACGTATTTTT CGACAATAAACATACGAATTTTTTATTCAATCG
Probe- 31	18S rRNA	ACGGTAATTGAATATAAATAAATCCAATATACACA AGCAATACCATCGGCAATGTCTACTCAATGCATC
Probe- 32	18S rRNA	CTTTAATACACATGATATCCCACTAAAGTAGATTAT CATCCTTTCAACAATGTCGAGTTTTTTGTATTACT
Probe- 33	18S rRNA	GATCAACCAGATATTTATTACGTATTCTACTTATGA TAAAAGTAGTTATTATCGAAATACATCAGGCA
Probe- 34	18S rRNA	AGAGTACTAGTCTGTGTACTAAGACATGCATGGCTT AATCTTTGAGATAAGCATATGACTACTGGCAG
Probe- 35	18S rRNA	CAGTTATCTTGTGGCAAAATGATAAAATCTCTCAAA TCATAGCTGTTATAATGAGCCATCCGCGGTTTC
Probe- 36	18S rRNA	TTGATCTAATAAATCCGCCGCTTCGTGAGTCACGGC ATTCTTAAAAATATTAGCTCTAGAATTACCA
Probe- 37	18S rRNA	ACACAAAGGTCGTACGATCAGTAAAATTATCCAGA GTCATCAAAATACCGCCTTTCAGCGGGTTGATT
Probe- 38	18S rRNA	CAACCATGGTAAGCGTTTATCTTACCATCGAAAGTT GATAGGTCAGCCACTTCAAGAGATATGTCGTCA
Probe- 39	18S rRNA	CGTGGATGTGGTAGCCGTTTCTCAGGCTCCCTCTCC GGAATCGAACACTGATTCCCCGTTACCCGTTA

Probe-40	18S rRNA	GCCCATATTGTTATTTTTGTCACTACCTCACCGAAC CGGTATTGGGTAATTTACGCGCCTGCTGCCTTC
Probe-41	18S rRNA	ACTTGCCCTCCAATTGATACTTGATAAAGTATTTAA AATGTTCTCATTGCAATTATGAAACCACTAGG
Probe-42	18S rRNA	AGCTTTTAACTGCAACAACTTTAATATACGCTATT GGAGCTGGAATTACCGCGGCTGCTGGCACCAG
Probe-43	18S rRNA	CGACTTCGAAGGACAAGATAGCTCTCAATCATAGA TTTCAAACCATCTTTTTCCTCAATTCAACTACG
Probe-44	18S rRNA	ACTCTAATTTTTTCAAAGTAACTTGTCGGTCATCC TCAACACCCATTAAAGAGCATCAAAGATATACA
Probe-45	18S rRNA	CAAAATAAAACCGAAGTCCTATTTTATTATTCCATG CAACAATATACAAGCGTAAGCCTGCTTTAAGC
Probe-46	18S rRNA	ACCTCTAGCACCAGCATACATATGCCCCCGGCAGTC TCTTTTAATCATTACTTCAGTTTCGAAAACCAA
Probe-47	18S rRNA	TGATTAATGAAAACATTCTTGGCAAATGCTTTCGCA GTAGACTGTCTGCTGATGATCTAAGAATTTC
Probe-48	18S rRNA	AGTTGGCATAGTTTATGGTCAGAACTAGGACGGTAT CTGATCGTCTTCGATCCTCTGACTTTCGTTCT
Probe-49	18S rRNA	CGGAACCCATAGACTTAGGTTTCCCGGTGACTTCTC GCAAGGAGATTTGAATTACCTTCGCGAACTGTC
Probe-50	18S rRNA	CGCAGGCTCCACTCCTGGTGGTGCCCTTCGGTCAAT TCCTTTAAGTTTCAGCTTTGCAACCATACTTCC

Probe- 51	18S rRNA	AGCTATCAATCTGTCAATCCTCACAGTGTCCGGACC GGGTGAGATTTCCCGTGTTGGGTCAAATTAAGC
Probe- 52	18S rRNA	ACGGAATTAACCAGACAAATCGCTCCACCAACTAA GAACGGCCATGCACCACCACCCACCGAATCAAG
Probe- 53	18S rRNA	CTCTAAGAAGTCAGCATTTGCGTTAGAACACAAAT GTACTATTTAGCAGGTTAGAGTCTCGTTCGTTA
Probe- 54	18S rRNA	GCCCCGGACATCTAAGGGCATCACAGACCTGTTATT GCTCAATTTCAATTTAGCTAAACGCTATTTATTC
Probe- 55	18S rRNA	TAGCAGGTTACCCGGCCATTTCTAGCTAGGAATAAA ACTCGCTGTTACTGCCATTGTAGCGCGCGTGCG
Probe- 56	18S rRNA	TGCGCTTACTAGGAATTCCTCGTTCAAGTGGAATAA TTTCAATCCACTATTCCTGACACGACAGTGATT
Probe- 57	18S rRNA	TCAATCGGTAGTAGCGACGGGCGGTGTGTACAAAG GGCAGGGACGTAATCAGCGCAAGCTAGTGACT
Probe- 58	18S rRNA	TGTCTTCTCCCAATTATAGAAATGTTGCCATTCCTTA AATCAGAATCCAACGATCTCACTAAACCAT
Probe- 59	18S rRNA	ATCCTTCCGCAGGTTACCTACGGAAACCTTGTTAC GACTTTTACTTCCTCTAAATGATCAAGTTTGAT
Probe- 60	18S rRNA	AGCACGATTATAGCATATCAGCCATAATTTTGAATC GAATTACATTTCAATCGTTTAGAACTAATAATG
Probe- 61	18S rRNA	AGTAATTTACTTAATATATTGGTACAGATCTTCTGT TCTTTTAATTATTGGCCAGCCAGACTCGAACCA

Probe-62	18S rRNA	TCAATAACTCATGTGCATACCGATAATATACACACT TGAAATAAATAGTTATTCCCAGTGAACAATACT
Probe-63	18S rRNA	GTAAAAGTGTAATTAACAGAAAGACCACCAATACA TATATTACTCGTAATACGGGTCTGAATTGATTGT
Probe-64	18S rRNA	CAACAATAACAATGACATATTATTAGCTTGTGTAAC AATGTATAAAATCATCCAAACCATAGGCACCTC
Probe-65	18S rRNA	AATGTTATCGTCTTAATATAAATGTTATATCAATCA GTCACCAAAAAAAGTAACTACATATCTATAAC
Probe-66	18S rRNA	AGATTCATATGAGTACTAGGTTTGAAAATATATAAA TGCTTATCAAACAAACAAAATGTCATTATGATA
Probe-67	18S rRNA	TATTTCAAACAATTCAAAAAGAAATACCACACTCC AAAATAATAACTGTCATATGAAACAGCATTTTA
Probe-68	18S rRNA	ACAATATCCTGATAACGCTTTGATATTGTAAAATTT TATCAGTGCCAGCTTACCATGTTTGTCGCATTG
Probe-69	18S rRNA	ACTGCAACATAAATTTGTTATTACGTGTACGAATAA CATATCATTCTACTAGACTTTTTTAAACCTTGC
Probe-70	18S rRNA	AGATTATAGCAACTAAATCGGTATTAGGTCTACAA AGCAGTATAGACCAGTTGACAATAATC
Probe-71	18S rRNA	TAAACGTTTTTATTACGAGGCAGCGTTTCGAATGATA TTTGAACAAATTTTTTGGCCAATTGCAGATT
Probe-72	18S rRNA	CTCAAATACTAAAAGTAAACGAGGATCGCTAGCAT AGATTGTCACCAACCAATGCCGTAAATTGAATATG

Probe- 73	18S rRNA	GAGTGATCCATCGCTTAAAGTGATACAGAATACAG ATGCATATAGCGATCCGTATTTTAATTTGGATCT
Probe- 74	18S rRNA	ATGATCAGAGCGTTGTGCAGTTCACATTAGTTCACA TATTTTGCTACGTTCTTCATCGACGTGCGAGCC
Probe- 75	18S rRNA	TACTATGCCGACCCTCAGACAGATGTGGCTATAGGT TGACCCATAGCCGCCATTTGCGTTCAAAGTGTC
Probe- 76	18S rRNA	AAGGGCACTCTCGATAGAAATACCAAAAGTGAACC CTTCAAAACATTACTATAGAACGTAATGAT
Probe- 77	18S rRNA	CACATATACATATATATAGTGTAATACTCTATGTTT CCATAGAGGTGTATTTTCATACACTATCACCTTA
Probe- 78	18S rRNA	TTCAAAAATTGATTTCTACACTTGCAAACATAGAAT GAAAAACCATACTATTGTACACATACACATATA
Probe- 79	18S rRNA	TATGTCAGTACATAGCATATATAAGATTCTCCAAAA CTATATCGACAAATGTCATATTAAATGAAATC
Probe- 80	18S rRNA	TAAATCCAGGATTTCCGTCCTATTTGAGACCAACAC ACAGACACACACACACACACATGAAT
Probe- 81	18S rRNA	ACCAATGCACAACTCATTAAGCTGTGGCACTGGCCT ACTGAAAGATCAGAAAACGAATTTTCA
Probe- 82	18S rRNA	TTAAATATAAATGAAATCCCTTATGATAAATGATTA ATAAAAACATCATAATCCGACAGA
Probe- 83	18S rRNA	ATCGGGTAATCTCATCTGATCTGAGGTCGGGTAATA ACGCATGTTTCAGAGACAAATAGGATT

Probe- 84	28S rRNA	GAAATCCTTGTTAGTTTCTTTTCCTCCGCTTAATGAT ATGCTTAAGTTCAGCGGGTAATCTCATCTGATC
Probe- 85	28S rRNA	ACCACAACCTCCTAGTATCAAAGATACAGGATTCAG TGCTGGGCTAATTCCCGGTCGTTTCGCCACTACTAGG
Probe- 86	28S rRNA	ACCCTCTATGGACAACATCACAATCAAGTGAATTTG GAGTATACTCAACCATTAAAAACACAACCTGTAC
Probe- 87	28S rRNA	CTGCATTCTCAAACAATCCGACTCATAGGAAGTGTC AATAACAGCCTTGTATACTCCAACGGGTCTAAC
Probe- 88	28S rRNA	CACGGTACTTGTTTACTATCGGACTCGCACAAGTAT TTAGCCTTAGATGGAGTTTACCACCCAATTTGGA
Probe- 89	28S rRNA	CACTCGTTTACCTCTAAGCGATTTCACGTACTATTT AACTCTCTCTTCAAAGTTCTTTTCAACTTTCCCT
Probe- 90	28S rRNA	CTTGAGAGATTTCAATAAAGACAAGATAACACACA ATCAACTGAATCCCATACATCAGCTTCGGCTC
Probe- 91	28S rRNA	CTATTGGTCGCAGTTTTGATGCATAGAAAGTGCATT GATCGCATATTACGAGCTCATCTCTAGAGAATC
Probe- 92	28S rRNA	ACCGTGCATTGAACTATAAAACCGATTCCGAAGAA CTGGTCACCTTTATCAACACGACAGAAAAACAGCT
Probe- 93	28S rRNA	TAACCATCAAACAATCAGCATTGACAATCACTAAA ATTAGCAAATCGCAATCACCAATACACTATGTTTA
Probe- 94	28S rRNA	CTGCAGACTATAGATTTACCCTTTAGCAATCATCTA CACCAACCATTCAACAGCTATCTCGTTTCGAGC



Probe- 95	28S rRNA	ACTCGCGATCATATAAAACTCCTTGGTCCGTGTTAC AAGACGGGACGAGCAGGTAACCTACATATACA
Probe- 96	28S rRNA	GTCACATCACAGCTTACCGAAGCAAGCCTTTACATT AATTCGCCATGGGGTTTCGTAAAGCCCTTTG
Probe- 97	28S rRNA	ATCGCTCAAACCTCCGCCCAGATGCGAACATCTTTAG ACGGGTCGATGTTGCACTCTGTGTTTCCACGAG
Probe- 98	28S rRNA	GTCCTCCATCAGAGTTTCCTCTGACTTCAACCTGCA CAAGCATAGTTCACCATCTTTCGGGTCTCTACATG
Probe- 99	28S rRNA	GATGGTTCGATTAGTCTTTCGCCCCTATACTCATGT CCGACGATCGATTTGCACGTCAGAACCGCGGCG
Probe- 100	28S rRNA	TACCAGGTAAAACTACAATCACAAATGCCAGCTAT CCTGAGGGGAACTTCGGAGGGAACCAGCTACTA
Probe- 101	28S rRNA	CTTCGAACCCATTATAAGTTTGAGAATAAGTTGAGA ACATTTCGTCCCCAATACTTCTAATCATTCGCTT
Probe- 102	28S rRNA	GTTCTGCTTACCAAAAATGGCCCACTAGGCATTCGT ATTCGATGTACATCTCCAATAAAGAGAGACATA
Probe- 103	28S rRNA	CTTTTGTGGTTTCTCATGAGCGTGATGTTAGGCACC TTAACCAGATGTTTGGTTCATCCACATCGCCA
Probe- 104	28S rRNA	GTTGTTACACACTCCTTAGCGGATGACGACTTCCAT GTCCACCGTCCTGCTGTCTTTATCAACCAACAC
Probe- 105	28S rRNA	ACATCGATCCGGTATAGGTCCCACGCTACAGCGCC ATCCATTTTCAGGGCTGGTTGATTCGGCAGGTGA

Probe-106	28S rRNA	GCTTCTTAGCAACCACGGCACCCCTCCTACACGATAT CGCATACTCGTTCGGTGTA AACACCAACTTACG
Probe-107	28S rRNA	TCACTTGAATAATTGCTACTACTACCAAGATCTGTA CCCGTGACCGCTCCACTCTGACTCACGCCAGTA
Probe-108	28S rRNA	TAGGACCGACTAACCCATGTTCAAATACTGTTTACA TGGAACCCTTCTCCACTTCAGTCTTCAAGGATC
Probe-109	28S rRNA	ATAACTAGACAAACTATCAATTAATAGACGTCTATC ACCTCCATCTGATAACTGAGTTACCAGATCGCT
Probe-110	28S rRNA	ACCAAATTTCCGTATTCAAGTTCAGGAATGTAAACC TGATTCCCTTTCGCTTCAGGAGGCTATTGAATCA
Probe-111	28S rRNA	GAACTCTTCCCGAAACACTTGATGACGTCTCTGAGA TCGCTTGTGTTACCACCTTGTGTTGCCGAAACA
Probe-112	28S rRNA	TTGACATTTACATCCCTTTCTCCAGATAACCTGATT CTAGGGACATGTTTATGTATACAAAGAAAAGA
Probe-113	28S rRNA	TATAACTGCTCCCTCAGATTTTCAAGGGCCATCAGG GGCGCTTCGGACACCACAAGAACCGCGGTGCTT
Probe-114	28S rRNA	TGTTCTAAGACTATAGGCTGCTCACCTTGGAGACCT GCTGCGGATATCGGTACGGCTTGAAACGAAATT
Probe-115	28S rRNA	ACCCGGTCCCTAGAGCCAATCCTTTTACCGAAGGTA CGGATCTAATTTGCCGACTTCCCTTACCTACAT
Probe-116	28S rRNA	AGGGTTTCCCCAAAACAGAATCAAAACAGCCCAAT TCCAATTCAATCGACTTCTTGATTAAGCCCATCAT

Probe-117	28S rRNA	CGAAAACCTCACAAATCATAGCCTAACCCGCCCATC AATCAAGTCGAAAAAGTTCCACTTCAACTCCATCT
Probe-118	28S rRNA	ACAGTCGGATTCCCTCTAGTCCATGCCAGTTCTAGGT TGACCGTTAATTGCACAATGACGACCATGAATC
Probe-119	28S rRNA	TGGCACTGGGCAGAAATCACATTGCGTCAAAGCCA TTTACTAGCCATCGCAATGCTTTGTTTTAATTAG
Probe-120	28S rRNA	ACCTGAAGAGAGTCATAGTTACTCCCGCCGTTAACC AGCGCTTGTTTGAATTTCTTCACATTGACATTCA
Probe-121	28S rRNA	GATAGGGACAGTAGGAATCTCGTTAATCCATTCATG CACGTCACCTAATTAGATGACGAGGCATTTGGCT
Probe-122	28S rRNA	CAACAGGGTCTTCTTTCCCGCTATATTTTCCAAGC CCGTTCCCTTGGCTGTAGTTTCGCTAGATAGTA
Probe-123	28S rRNA	GTCGACGTGAGTCTCCCACTTATACTACACCTCTAA TGTCTCCCTACAAAGTCGGACTAGAGTCAAGCT
Probe-124	28S rRNA	ATAAATTGACCTGAATCAACTGCACTGCATTACTGA GTAAGTAAAGAAACGATCAGAGTAGTGGTATTTCA CT
Probe-125	28S rRNA	AACTCCCCACCTGACACTGTCCTCAGAACAGCTCGA AAGCATCCGAAGATCGCTTTCTTTTCTCCACA
Probe-126	28S rRNA	GTTTCTGTCCTGGTTGAGCTCACCTTGGGACACCTG CGTTACCATTTGACAGATGTACCGCCCCAGTCA
Probe-127	28S rRNA	GCTTTCACGGTCTGTATTCGTAAGTAAATCAAAT CAAGTGAGCTTTTCCCCTTTTGGTCGACACCAG

Probe-128	28S rRNA	TATCCCTGTGGTAACTTTTCTGACACCTCTTGCTTCA AACTCTGAAGACATCAAAAGGATCGATAGGCCGC
Probe-129	28S rRNA	GAAGAGCCGACATCGAAGGATCAAAAAGCGACGTC GCTATGAACGCTTGGCCGCCACAAGCCAGTTA
Probe-130	28S rRNA	AGCTCACGTTCCCTATTAGTGGGTGAACAATCCAAC GCTTTGTGAATTCTGCTTCACAATGATAG
Probe-131	28S rRNA	GAATTACCATTGTAATGACACTTTATATAGTAGGGT AAAATAACCTGTCTCACGACGGTCTAAACCC
Probe-132	28S rRNA	GCCAATGACCTTTCGATCAAGCACATTTACCAGTGA TCCGAATCTGCGGTTCTCTCGTACTGAGCA
Probe-133	28S rRNA	ATCATTACTTCTGGGCGAGATTCAGACTTAGAGGCG TTCAGTCTTAATCTCTCGGATGGTAGCTTCGT
Probe-134	28S rRNA	AGCCACATCCGATGGACGAACCACCAGATAATACA TTTGCCTCTTTACGAGGTAGGCACTGAATT
Probe-135	28S rRNA	AATCATAAAATATGATTCAAACATCCAACCTATTTT CATAGATTGGTTCGAGTTTAAATATATGGCTA
Probe-136	28S rRNA	CTCGAAATCTTACGCTTCCCCGACCGTAAGGTAAGT CGTATGCAAACGATTTAATGCCAACACGTA
Probe-137	28S rRNA	CCAACACGTAAATCCAAATCATCGCGTCAGATGGG GTTGAAGTTCAGATTCTCGCAGTTTAAACCG
Probe-138	28S Partial rRNA	AAATATCACATTATAATTAGAGCTTGACCGATTGCA TTATTCTTCGATTGTCCCGATTGTAATTCCAAT

Probe- 139	28S Partial rRNA	ATGAGCAACTCATT TTTATGTTATTTAAATTAATAGA TTTGACAATCTATCACAGTAGAGACGAAATTCA
Probe- 140	28S Partial rRNA	CTTTATGGTCATAACCAATAAAGGCCGTTGTTACAA TTTTTACTAGGAGTGCAAACATTTTTGACACTG
Probe- 141	28S Partial rRNA	TATGCAAATTTCCATTTAAGAATTAGAGTATTGCGC GCCGAGAATGCAATCTACGGACTTTCAGAATTA
Probe- 142	28S Partial rRNA	TATTTAAAAATCCCTAACATCAGGAATTTTTTTCAA GACATGGGGAATAGAATAATGTGAGCAAATGT
Probe- 143	28S Partial rRNA	TAATCTCCTATGTTCTTCAAATTTCCCTTTTAACCTT TCAATTCAAAATATCGTGTCTTAAACTTGAAGT
Probe- 144	28S Partial rRNA	TAGTAAACTTTATTATGAATTCTAGTACAAGTAGTT AAA ACTAAATTTTATATGAAATCTAAGATTCGT
Probe- 145	28S Partial rRNA	ATAACTCAATGAACCGACATATAAACTATTAAAAC AAAAGGTACATTTTGATACAAACCACTGAAGCTT
Probe- 146	28S Partial rRNA	ATATCAAGTATTCGAATATTCAAATTGTGATGTCTG ATTACGCTTATTTTCCTTTAATGATTTGGTAAAG
Probe- 147	28S Partial rRNA	ACCATACAAAAAGAAATACTTTACTCTAACATGAA AACTGTCATATGAAAAAATATTTAATATATTTGA
Probe- 148	28S Partial rRNA	CTGATAATACTTTGATATTATTCAATTTTAACAGTG CCAGCTTACCATGTGTGTCGCATTGTATTTCAA
Probe- 149	28S Partial rRNA	ATATGGATTTGTTATTACGTCTATATATAACATATC ATTCTACTAGACTTATTAAATCTTGCACAATATC

Probe- 150	28S Partial rRNA	AGATTATAGCAACTTAATCGGTATTAAGTCTACAAA GCTTCAATAGACCAGTTGATAATAATCACTGCA
Probe- 151	28S Partial rRNA	GAAATAAACGTTTTATTACGAGGCAGCGTTTCGAAT GATATTTGAACAAATTTTTTGGCCAATTGCAGATT
Probe- 152	28S Partial rRNA	TCAAATACTAAAAGTAAACGAGGATCGCTAGCATA GATTGTCACCAACCAATGCCGTTAAATTGAATAT
Probe- 153	28S Partial rRNA	TGATCCATCGCTTAAAGTGATACAGAATACAGATG CATATAGCGATCCGTATTTTAATTTGGATCTAC
Probe- 154	28S Partial rRNA	AGCGTTGTGCAGTTCACATTAGTTCACATATTTTGC TACGTTCTTCATCGACGTGCGAGCCGAG
Probe- 155	28S Partial rRNA	ACCCTCAGACAGATGTGGCTATAGGTTGACCCATA GCCGCCATTTGCGTTCAAAGTGTCATGATCAG
Probe- 156	28S Partial rRNA	TCGATAGAAATACCAAAAGTGAACCCTTCAAAACA TTACTATAGAACGTAATGATAAATACTATGCCG
Probe- 157	28S Partial rRNA	TATATAGTGTAATACTCTATGTTTCCATAGAGGTGT ATTTTCATACACTATCACCTTAAAAGGGCACTC
Probe- 158	28S Partial rRNA	TCTACACTTGCAAACATAGAATGAAAAACCATACT ATTGTACACATACACATATACACATATACATA
Probe- 159	28S Partial rRNA	TAAGATTCTCCAAAACCTATATCGACAAATGTCATAT TAAATGAAATCAAAAACAATTCAAAAATTGATT
Probe- 160	28S Partial rRNA	CGTCCTATTTGAGACCAACACACAGACACACACAC ACACACATGAATATATGTCAGTACATAGCATATA

Probe- 161	28S Partial rRNA	CAACTCATTAAGCTGTGGCACTGGCCTACTGAAAG ATCAGAAAACGAATTTTCATAAATCCAGGATTTC
Probe- 162	28S Partial rRNA	GATTTTAAATATAAATGAAATCCCTTATGATAAATG ATTAATAAAAACTCATAATCCGACAGAACCAATGC A
Probe- 163	28S Partial rRNA	GCTTAAGTTCAGCGGGTAATCTCATCTGATCTGAGG TCGGGTAATAACGCATGTTTCAGAGACAAATAG
Probe- 164	Spacer A	ACATTTACCAGTGATCCGAATCTGCGGTTCTCTCG TACTGAGCAGAATTACTATTATCATGACAAATTAT
Probe- 165	Spacer A	TCAGACTTAGAGGCGTTCAGTCTTAATCTCTCGGAT GGTAGCTTCGTGCCACTGACCTTTCGATCAAGC
Probe- 166	Spacer A	ACTTGCGTTAATGAATAATAATATTGCCTCATTACG AGGATGGCACAAAATATCATGATTTTTAGGCGAGA T
Probe- 167	Spacer A	ATGATTCAAACATCCAAACTATTTTCATAGCCTGGT TAGAGTTTAAATATATGGCTAAGCCACATCCATTA
Probe- 168	Spacer A	CTCGAATTCTTACGCTTCCCCGACCGTAAAGTAAGT CGTCTACAAACGATTTAATGCCAACACGTAAATCAT TA
Probe- 169	Spacer A	ACGAATGAATCATAAAGATCCAAATCATCGCGTCA GATGGGGATGAAGTTCAAAACCTCGCAGTATAAAC TG

APPENDIX 2. Primers used for cloning candidate genes

<b>Gene_ID</b>	<b>Gene Name</b>	<b>Forward Primer</b>	<b>Reverse Primers</b>
SMESG0000 18025.1		TCGATCAAATCCGTC ATGGTCA	ACACTTATATCGCCA CCCCATC
SMESG0000 26815.1		ATGAGGAGTCCGATT CGTGAAG	TGCGCATTCAATAGC AACTGTT
SMESG0000 11684.1	WI-14	CTCTGGTTAAGTCCC TGTGACC	TAGCATAGGGTTGCC ATACGTC
SMESG0000 14352.1	WI-1	CCGGACTCGCATTAT TTATAGTGG	TATCGGAATGTCGCT TTTCCCA
SMESG0000 35330.1	WI-3	ACGCAAACATATGGT GCATCAG	AGGGTTTGAAGCGTC G TTCATA
SMESG0000 43423.1	WI-7	GAAACCCGACAGAGC CTTATCA	TTTGGGCCACATCTT GATCTGA
SMESG0000 74187.1	MS3_02400	GACGTGTGGCTAGGA AACAGTA	TTTGTCCAAGTTCAC CAATCGC
SMESG0000 81234.1	WI-5	AGTGACCTCTTCAAA TTTGCCA	AAAATTACTGGCCCA AGGTTGC
SMESG0000 52762.1	WI-6	TGCTGCGGGTAAAAC AACAATT	CTGAATGTGCCACTT GTGAGTC



SMESG0000 39178.1	WI-4	AGTAACCTTAAATGG CGACGGT	CGACGCATGGATATT CTGCTTT
SMESG0000 35328.1		ATGGTTTCTTGCATCC GTTTGG	GTTTGTGAAGCTCGT CCGAATG
SMESG0000 35333.1	WI-2	ATGGTTTCTTGCATCC GTTTGG	TGTGGAAATCCTTCG GCAATTG
SMESG0000 46026.1	SULT1C2	CAACCTGCCATGTCA TCTGTTG	TTGACGTTTCCTCGC TGTAAGAA
SMESG0000 50244.1	MS3_02162	GTAATCATAACGCAA CCTGGCC	CACATAGTCCATGTC GCGTTTC
SMESG0000 52741.1		AATTTGGGATGTCGG AGGTCAA	TGCTGATAATTTCCC TGCCGAT
SMESG0000 04912.1	RPZ3	AGAAGCGATTGGAAG TTTTGCC	TTCCATTGCAAGCCT TTAGTGC
SMESG0000 42264.1	DMGDH	GGTTCACTGCTGTAG AACGAGA	TCTCCCACTAAGTCG ACAGCTA
SMESG0000 46786.1	WI-12	ACATCCGTTCTTCAC AGGTACC	TTGCCGTTTACAGCA TACCTCT
SMESG0000 56175.1	WI-13	TTGCAAGTGTCGCTT TTGGATT	TCATTATCGGGCTGT GACAACA

SMESG0000 20958.1		AGCAGCTGACTTCGA TGAAGAA	TGAAGGGGAAGACG AGACATTG
SMESG0000 43826.1		GCATTTAGCGGCCAA TTCAAGA	ACGCCTCTTACGACT TTTCCAT
SMESG0000 43821.1		GCATTTAGCGGCCAA TTCAAGA	ACGCCTCTTACGACT TTTCCAT
SMESG0000 57282.1		ATGCCATTATGACTG GTGGGTT	TGGAATCATCGTGCT CAAGGAA
SMESG0000 43391.1	WI-9	AATTTACTGTGCCGA GGAGGAG	ACCATGAGTCATACA CCCACAC
SMESG0000 43388.1	WI-10	AATTTACTGTGCCGA GGAGGAG	CGAAGCACGGCTAGT TCTTTAA
SMESG0000 16291.1	DGRI\GH17 028	TGCTGTTCCGTTGGC AATTTAG	AACTGTGGAGTTGTC GGCTTAT
SMESG0000 43422.1	WI-8	AAGCCGTTACCAGTT ACCAGAG	AGCGAGGTTTACATA TCCGTCC
SMESG0000 41535.1	VACHT	AATAGCAGCGCAATG TTTTGGT	AAACGCCCAAACATA ATCCTTGC
SMESG0000 72726.1		TCGACGAAATCAAAC AGTTGGC	CGTGGACAGTACTTC ATTGGGA

SMESG0000 18404.1	TRAF3	GTACCACTAGGGCAA CGGTAAA	TGAAACTTTCTGTCG AAACGGC
SMESG0000 40596.1	WI-11	GTTGGTTCGATTTACT GTGCCG	TTTGCAGAGTCTTCG ACTTCGA
SMESG0000 66311.1	CPA2	ACACAGCAGAGAATG GTTAGCA	TGGTCTGAGTTCCAA CGTGTAG
SMESG0000 03701.1		GGTGTTCAAACGCAT TTCTCCA	GTTCTGTTGAATGAA GCGCCTT
SMESG0000 14240.1		GGCTTGTTTATTCGTC GACCAG	GGTAACAAGCTATCA GACCACCA
SMESG0000 00730.1	GM2A	ACCCCAATAACTTGA AAATGGGC	ACACGTCATAAGTAC CACTGGA
SMESG0000 35313.1		CGAACATCTTGGACC TCTGTCA	ATGGGCCAAGATGTT GAAGGAT
SMESG0000 42389.1	KLK13	GCACATTGCGTTTGG GATATGA	ACAGTCGGTTTATTT GCTTGGC
SMESG0000 67191.1		CTCTCTAGCACGTCC AACCATA	CTTAGACCCGGAGAG TCAAAGC
SMESG0000 42349.1	KLK13	GGACTAGAGCGATAA TGCACGA	CAAGCTGAAGTTGAC AGACTGC

SMESG0000 35312.1		TATCCTCCACTCCTCT TGAGCA	ATTCGCCGTTCTTCG ACTGATA
SMESG0000 56319.1		ACATTGCCTACTGAA CGGGATT	AGCAGCTCAATTCAA CTCGAGA
SMESG0000 60313.1	WIL-1	GCCAATCATCAACGA GGATGTG	CTCAGATGCTGCAAC TTCTTCG
SMESG0000 72804.1	CG6763	GATTTGTTTATGGGA CTCGGCG	AAACCGAGAGCGTG GATAAACT
SMESG0000 75831.1	MS3_04019	TGCTCAGCACTCTAA AGTCTGG	TGGAAATGAAATTCA CCACGGC
SMESG0000 70784.1		TCGCTTGTTTAGGCTT TGTTTCG	GATAACGACAGGTCC AGTGGTT
SMESG0000 43452.1	WIL-2	CAACGTTTCACTGAG TCTTCGT	TCCCTTGTCAAACGA CCAGAAA
SMESG0000 11613.1		AAGCGTTTTGATTTC ATGCCGA	ACCCAATCAGGCACC CAATTAT
SMESG0000 12544.1		CCTGCTTGGA CT CAG TTGAGAT	TTCGGACAAAAGGC AAGCAAAA
SMESG0000 31852.1	FZD5	TATGCATCAGCGCTA GAGAAGG	AAAAACCCTGTGCCA ACCAAAA

SMESG0000 18684.1	DWIL\GK2 5726	TGCGCTCTGTAAAGT TTGTTGA	GGCATCCATTAAACT GGGCTTG
SMESG0000 29171.1	SLC38A11	AGGAATGCCTTACGC TTTGAGA	TGTTGGCACATAAAG GCGAAAG
SMESG0000 29446.1	MS3_08312	TGCTCAGCACTCTAA AGTCTGG	TGGAAATGAAATTCA CCACGGC
SMESG0000 28264.1	CPIPJ_CPIJ 006813	CTATGATGAAGCTAC CCGCCAA	CCCGGATAGTTTGGT TCTCCTC
SMESG0000 16305.1		TTTGTGTAAATTCGTC ACCGGC	ATTGGCCATCGGATC TATCACG
SMESG0000 64592.1	MS3_03655	CGAACCGGATTGAAT TGGTGTC	AAATTGAATGGCAAC TGTCGGG
SMESG0000 08146.1	DANA\GF1 7998	TACTATGATGGGTCG GATTGCG	CCTTTGGGAAATTCC GTTGCAT
SMESG0000 29655.1	SHOC2	TTCCCGATTCCGTCC AGAAATT	GCCTATTTTCATCGGG CAAATC
SMESG0000 64833.1	MS3_06432	CCGCTTTGGGAAAGT TAAGTGG	TCTGGTTGCGGCATT GAAAATT
SMESG0000 50640.1		CGGAGTGTCGAATGA ATTGTCG	CGAAAAGCGGACAC CTCAAAAT

SMESG0000 34888.1	FRMD4BB	TCCGATTCCAAATGG AGACGTT	ATATTGGGAAGGGG GCAAATGT
SMESG0000 51245.1		GTCCAGTTGATCAGC AAGGAGA	TGTTCGTCCAACCAT GACTAGG
SMESG0000 52391.1		AAGGCAGATAAAACC GGTTTGC	AGATCGGGCTTGGCT GATAAAA
SMESG0000 55679.1	MS3_06966	ACAACAAAAGCCCGG TTTTTCA	GTTCTCCGGTGTGGG TTCTAAT
SMESG0000 79529.1		CTATCGTCATTGGTT GCGGTTT	CTTAGTCGTAGCTAG CGTTTTGC
SMESG0000 17127.1		G TTCCTCGTTATCTTG CGCAAA	AGGTCAAGCATGGTC AATGTCA
SMESG0000 27619.1	MS3_01614	GCTCATGAGGCGGAA AATGTTT	ATTCGGGTCGTGGTC GTATAAG
SMESG0000 72168.1	DRC1	TTTGGCTGATGAATG AGTCGGA	GACAGTTTCCTTGTT GTCGTCG
SMESG0000 52476.1		CGTCTCAATGCTGCA ATAGAGC	TTTAGGTGAATGCCG AGTGTGA
SMESG0000 19789.1		GCAAGAAAAGCAGA TGAAGGCA	TTGCTCATTGGCTTT GTGGAAG

SMESG0000 09072.1		TACGATGTCTGTGTT AACGGCA	AAGGCAGTGAAGTGT AAAACGC
SMESG0000 20792.1	TEKT3	ATGGCCGAATCTGAA GCCTTAT	GCGAGTTTGAGCAAC TTTCAGT
SMESG0000 49144.1	DNAH5	TGGTGGACATGAATC CGGAATT	AATGGCATCAACAG GTCCATCT
SMESG0000 10229.1		CATAGTCTGAGAGAT CCACCGC	TGCAACAGAGATCCT TGGTCTC
SMESG0000 09750.1	SLC39A3	ATCCGTATGCAGGTT TGTCACT	AAACTCTGGCACCAG CTATCAA
SMESG0000 35378.1	MS3_04354	AAGTGGTTGCAAATA AGGCGTC	TTTATGTGGAGGAGG ATGTGCC





## REFERENCES

- Abnave, P., and Ghigo, E. (2019). Role of the immune system in regeneration and its dynamic interplay with adult stem cells. *Semin Cell Dev Biol* 87, 160-168. 10.1016/j.semcdb.2018.04.002.
- Adiconis, X., Borges-Rivera, D., Satija, R., DeLuca, D.S., Busby, M.A., Berlin, A.M., Sivachenko, A., Thompson, D.A., Wysocker, A., Fennell, T., et al. (2013). Comparative analysis of RNA sequencing methods for degraded or low-input samples. *Nat Methods* 10, 623-629. 10.1038/nmeth.2483.
- Agata, K., Saito, Y., and Nakajima, E. (2007). Unifying principles of regeneration I: Epimorphosis versus morphallaxis. *Dev Growth Differ* 49, 73-78. 10.1111/j.1440-169X.2007.00919.x.
- Almendral, J.M., Sommer, D., Macdonald-Bravo, H., Burckhardt, J., Perera, J., and Bravo, R. (1988). Complexity of the early genetic response to growth factors in mouse fibroblasts. *Mol Cell Biol* 8, 2140-2148. 10.1128/mcb.8.5.2140-2148.1988.
- Alvarado, A.S. (2000). Regeneration in the metazoans: why does it happen? *Bioessays* 22, 578-590.
- Amamoto, R., Huerta, V.G.L., Takahashi, E., Dai, G., Grant, A.K., Fu, Z., and Arlotta, P. (2016). Adult axolotls can regenerate original neuronal diversity in response to brain injury. *Elife* 5, e13998.
- Arenas Gomez, C.M., Sabin, K.Z., and Echeverri, K. (2020). Wound healing across the animal kingdom: Crosstalk between the immune system and the extracellular matrix. *Dev Dyn* 249, 834-846. 10.1002/dvdy.178.
- Arthur, J.S., and Ley, S.C. (2013). Mitogen-activated protein kinases in innate immunity. *Nat Rev Immunol* 13, 679-692. 10.1038/nri3495.
- Badano, J.L., Mitsuma, N., Beales, P.L., and Katsanis, N. (2006). The ciliopathies: an emerging class of human genetic disorders. *Annu Rev Genomics Hum Genet* 7, 125-148. 10.1146/annurev.genom.7.080505.115610.
- Baguña, J. (1988). Cellular, molecular and genetic approaches to regeneration and pattern formation in planarians. *Fortschr Zool* 36, 65-78.
- Baldwin, A., Morris, A.R., and Mukherjee, N. (2021). An Easy, Cost-Effective, and Scalable Method to Deplete Human Ribosomal RNA for RNA-seq. *Curr Protoc* 1, e176. 10.1002/cpz1.176.
- Barberan, S., and Cebria, F. (2019). The role of the EGFR signaling pathway in stem cell differentiation during planarian regeneration and homeostasis. *Semin Cell Dev Biol* 87, 45-57. 10.1016/j.semcdb.2018.05.011.
- Baroni, A., Buommino, E., De Gregorio, V., Ruocco, E., Ruocco, V., and Wolf, R. (2012). Structure and function of the epidermis related to barrier properties. *Clin Dermatol* 30, 257-262. 10.1016/j.clindermatol.2011.08.007.
- Baylis, H.A., Furuichi, T., Yoshikawa, F., Mikoshiba, K., and Sattelle, D.B. (1999). Inositol 1,4,5-trisphosphate receptors are strongly expressed in the nervous system, pharynx, intestine, gonad and excretory cell of *Caenorhabditis elegans* and are encoded by a single gene (*itr-1*). *J Mol Biol* 294, 467-476. 10.1006/jmbi.1999.3229.
- Beane, W.S., Morokuma, J., Adams, D.S., and Levin, M. (2011). A chemical genetics approach reveals H,K-ATPase-mediated membrane voltage is required for planarian head regeneration. *Chem Biol* 18, 77-89. 10.1016/j.chembiol.2010.11.012.

Beck, C.W., Christen, B., Barker, D., and Slack, J.M.W. (2006). Temporal requirement for bone morphogenetic proteins in regeneration of the tail and limb of *Xenopus* tadpoles. *Mechanisms of Development* 123, 674-688. 10.1016/j.mod.2006.07.001.

Becker, T., Wullimann, M.F., Becker, C.G., Bernhardt, R.R., and Schachner, M. (1997). Axonal regrowth after spinal cord transection in adult zebrafish. *Journal of Comparative Neurology* 377, 577-595.

Beltrami, A.P., Endo, Y., Zhang, M., Yamaji, S., and Cang, Y. (2012). Genetic Abolishment of Hepatocyte Proliferation Activates Hepatic Stem Cells. *PLoS ONE* 7. 10.1371/journal.pone.0031846.

Bely, A.E., and Nyberg, K.G. (2010). Evolution of animal regeneration: re-emergence of a field. *Trends in Ecology & Evolution* 25, 161-170. 10.1016/j.tree.2009.08.005.

Benham-Pyle, B.W., Brewster, C.E., Kent, A.M., Mann, F.G., Jr., Chen, S., Scott, A.R., Box, A.C., and Sanchez Alvarado, A. (2021). Identification of rare, transient post-mitotic cell states that are induced by injury and required for whole-body regeneration in *Schmidtea mediterranea*. *Nat Cell Biol* 23, 939-952. 10.1038/s41556-021-00734-6.

Bereiter-Hahn, J., Matoltsy, A.G., and Richards, K.S. (2012). *Biology of the Integument: invertebrates* (Springer Science & Business Media).

Bereiter-Hahn, J., and Zylberberg, L. (1993). Regeneration of teleost fish scale. *Comparative Biochemistry and Physiology Part A: Physiology* 105, 625-641. 10.1016/0300-9629(93)90262-3.

Bernhardt, R.R., Tongiorgi, E., Anzini, P., and Schachner, M. (1996). Increased expression of specific recognition molecules by retinal ganglion cells and by optic pathway glia accompanies the successful regeneration of retinal axons in adult zebrafish. *The Journal of Comparative Neurology* 376, 253-264. 10.1002/(sici)1096-9861(19961209)376:2<253::Aid-cne7>3.0.Co;2-2.

Bibb, C., and Campbell, R.D. (1973). Tissue healing and septate desmosome formation in hydra. *Tissue and cell* 5, 23-35.

Blanpain, C., and Fuchs, E. (2009). Epidermal homeostasis: a balancing act of stem cells in the skin. *Nat Rev Mol Cell Biol* 10, 207-217. 10.1038/nrm2636.

Bridge, D., Cunningham, C.W., DeSalle, R., and Buss, L.W. (1995). Class-level relationships in the phylum Cnidaria: molecular and morphological evidence. *Molecular Biology and Evolution* 12, 679-689.

Brockes, J.P., and Kumar, A. (2008). Comparative aspects of animal regeneration. *Annu Rev Cell Dev Biol* 24, 525-549. 10.1146/annurev.cellbio.24.110707.175336.

Brown, M.D., and Sacks, D.B. (2009). Protein scaffolds in MAP kinase signalling. *Cellular Signalling* 21, 462-469. 10.1016/j.cellsig.2008.11.013.

Caira, J.N., and Littlewood, D.T.J. (2013). Worms, Platyhelminthes. In *Encyclopedia of Biodiversity*, pp. 437-469. 10.1016/b978-0-12-384719-5.00166-0.

Candia Carnevali, M.D., and Bonasoro, F. (2001). Microscopic overview of crinoid regeneration. *Microsc Res Tech* 55, 403-426. 10.1002/jemt.1187.

Carlson, B.M. (2005). Some principles of regeneration in mammalian systems. *Anat Rec B New Anat* 287, 4-13. 10.1002/ar.b.20079.

Carnevali, M.C. (2006). Regeneration in Echinoderms: repair, regrowth, cloning. *Invertebrate Survival Journal* 3, 64-76.

Cebria, F., and Newmark, P.A. (2005). Planarian homologs of netrin and netrin receptor are required for proper regeneration of the central nervous system and the maintenance of nervous system architecture. *Development* 132, 3691-3703. 10.1242/dev.01941.

Chandebois, R. (1979). The Dynamics of Wound Closure and Its Role in the Programming of Planarian Regeneration I-Blastema Emergence. *Development, Growth and Differentiation* 21, 195-204. 10.1111/j.1440-169X.1979.00195.x.

Chang, L., and Karin, M. (2001). Mammalian MAP kinase signalling cascades. *Nature* 410, 37-40. 10.1038/35065000.

Charg , S.B.P., and Rudnicki, M.A. (2004). Cellular and Molecular Regulation of Muscle Regeneration. *Physiological Reviews* 84, 209-238. 10.1152/physrev.00019.2003.

Chen, C.S., Tan, J., and Tien, J. (2004). Mechanotransduction at cell-matrix and cell-cell contacts. *Annu Rev Biomed Eng* 6, 275-302. 10.1146/annurev.bioeng.6.040803.140040.

Chen, E.Y., Tan, C.M., Kou, Y., Duan, Q., Wang, Z., Meirelles, G.V., Clark, N.R., and Ma'ayan, A. (2013). Enrichr: interactive and collaborative HTML5 gene list enrichment analysis tool. *BMC Bioinformatics* 14. 10.1186/1471-2105-14-128.

Cheng, L.C., Tu, K.C., Seidel, C.W., Robb, S.M.C., Guo, F., and Sanchez Alvarado, A. (2018). Cellular, ultrastructural and molecular analyses of epidermal cell development in the planarian *Schmidtea mediterranea*. *Dev Biol* 433, 357-373. 10.1016/j.ydbio.2017.08.030.

Chera, S., Ghila, L., Dobretz, K., Wenger, Y., Bauer, C., Buzgariu, W., Martinou, J.-C., and Galliot, B. (2009). Apoptotic Cells Provide an Unexpected Source of Wnt3 Signaling to Drive Hydra Head Regeneration. *Developmental Cell* 17, 279-289. 10.1016/j.devcel.2009.07.014.

Chisholm, A.D., and Hsiao, T.I. (2012). The *Caenorhabditis elegans* epidermis as a model skin. I: development, patterning, and growth. *Wiley Interdiscip Rev Dev Biol* 1, 861-878. 10.1002/wdev.79.

Cordeiro, J.V., and Jacinto, A. (2013). The role of transcription-independent damage signals in the initiation of epithelial wound healing. *Nat Rev Mol Cell Biol* 14, 249-262. 10.1038/nrm3541.

Culviner, P.H., Guegler, C.K., and Laub, M.T. (2020). A Simple, Cost-Effective, and Robust Method for rRNA Depletion in RNA-Sequencing Studies. *mBio* 11. 10.1128/mBio.00010-20.

Cummings, S.G., and Bode, H.R. (1984). Head regeneration and polarity reversal in *Hydra attenuata* can occur in the absence of DNA synthesis. *Wilhelm Roux's Archives of Developmental Biology* 194, 79-86. 10.1007/bf00848347.

Dahl, K.N., Ribeiro, A.J., and Lammerding, J. (2008). Nuclear shape, mechanics, and mechanotransduction. *Circ Res* 102, 1307-1318. 10.1161/CIRCRESAHA.108.173989.

David, C.N. (2012). Interstitial stem cells in *Hydra*: multipotency and decision-making. *The International Journal of Developmental Biology* 56, 489-497. 10.1387/ijdb.113476cd.

David, C.N., and Murphy, S. (1977). Characterization of interstitial stem cells in *hydra* by cloning. *Developmental Biology* 58, 372-383. 10.1016/0012-1606(77)90098-7.

Dickinson, D.J., Nelson, W.J., and Weis, W.I. (2011). A polarized epithelium organized by beta- and alpha-catenin predates cadherin and metazoan origins. *Science* 331, 1336-1339. 10.1126/science.1199633.

Dinsmore, C.E. (1991). *A history of regeneration research: milestones in the evolution of a science* (Cambridge University Press).

Dubois, F. (1949). Contribution à l'étude de la migration des cellules de régénération chez les Planaires dulcicoles. (Bulletin Biologique de la France et de la Belgique).

DuBuc, T.Q., Traylor-Knowles, N., and Martindale, M.Q. (2014). Initiating a regenerative response; cellular and molecular features of wound healing in the cnidarian *Nematostella vectensis*. *BMC Biol* 12, 24. 10.1186/1741-7007-12-24.

Duncan, E.M., and Sánchez Alvarado, A. (2019). Regulation of genomic output and (Pluri) potency in regeneration. *Annual Review of Genetics* 53, 327-346.

Dunn, S. (2009). Immunorecognition and immunoreceptors in the Cnidaria [For this article an Erratum has been published]. *Invertebrate Survival Journal* 6, 7-14.

Echeverri, K., Clarke, J.D.W., and Tanaka, E.M. (2001). In Vivo Imaging Indicates Muscle Fiber Dedifferentiation Is a Major Contributor to the Regenerating Tail Blastema. *Developmental Biology* 236, 151-164. 10.1006/dbio.2001.0312.

Echeverri, K., and Tanaka, E.M. (2002). Ectoderm to Mesoderm Lineage Switching During Axolotl Tail Regeneration. *Science* 298, 1993-1996. 10.1126/science.1077804.

Eisenhoffer, G.T., Kang, H., and Alvarado, A.S. (2008). Molecular Analysis of Stem Cells and Their Descendants during Cell Turnover and Regeneration in the Planarian *Schmidtea mediterranea*. *Cell Stem Cell* 3, 327-339. 10.1016/j.stem.2008.07.002.

Eley, L., Yates, L.M., and Goodship, J.A. (2005). Cilia and disease. *Current Opinion in Genetics & Development* 15, 308-314. 10.1016/j.gde.2005.04.008.

Engler, A.J., Sen, S., Sweeney, H.L., and Discher, D.E. (2006). Matrix elasticity directs stem cell lineage specification. *Cell* 126, 677-689. 10.1016/j.cell.2006.06.044.

Erickson, J.R., and Echeverri, K. (2018). Learning from regeneration research organisms: The circuitous road to scar free wound healing. *Dev Biol* 433, 144-154. 10.1016/j.ydbio.2017.09.025.

Forsthoefel, D.J., Cejda, N.I., Khan, U.W., and Newmark, P.A. (2020). Cell-type diversity and regionalized gene expression in the planarian intestine. *Elife* 9. 10.7554/eLife.52613.

Fraguas, S., Barberán, S., and Cebrià, F. (2011). EGFR signaling regulates cell proliferation, differentiation and morphogenesis during planarian regeneration and homeostasis. *Developmental Biology* 354, 87-101. 10.1016/j.ydbio.2011.03.023.

Galko, M.J., and Krasnow, M.A. (2004). Cellular and genetic analysis of wound healing in *Drosophila* larvae. *PLoS Biol* 2, E239. 10.1371/journal.pbio.0020239.

Galliot, B. (2013). Regeneration in hydra. eLS. Wiley, Chichester.

Gawriluk, T.R., Simkin, J., Thompson, K.L., Biswas, S.K., Clare-Salzler, Z., Kimani, J.M., Kiama, S.G., Smith, J.J., Ezenwa, V.O., and Seifert, A.W. (2016). Comparative analysis of ear-hole closure identifies epimorphic regeneration as a discrete trait in mammals. *Nat Commun* 7, 11164. 10.1038/ncomms11164.

Gierer, A., Berking, S., Bode, H., David, C.N., Flick, K., Hansmann, G., Schaller, H., and Trenkner, E. (1972). Regeneration of hydra from reaggregated cells. *Nat New Biol* 239, 98-101. 10.1038/newbio239098a0.

Gilbert, P.M., Havenstrite, K.L., Magnusson, K.E., Sacco, A., Leonardi, N.A., Kraft, P., Nguyen, N.K., Thrun, S., Lutolf, M.P., and Blau, H.M. (2010). Substrate elasticity regulates skeletal muscle stem cell self-renewal in culture. *Science* 329, 1078-1081. 10.1126/science.1191035.

Glazer, A.M., Wilkinson, A.W., Backer, C.B., Lapan, S.W., Gutzman, J.H., Cheeseman, I.M., and Reddien, P.W. (2010). The Zn Finger protein Iguana impacts Hedgehog signaling

by promoting ciliogenesis. *Developmental Biology* 337, 148-156. 10.1016/j.ydbio.2009.10.025.

Godwin, J.W., Debuque, R., Salimova, E., and Rosenthal, N.A. (2017). Heart regeneration in the salamander relies on macrophage-mediated control of fibroblast activation and the extracellular landscape. *npj Regenerative Medicine* 2. 10.1038/s41536-017-0027-y.

Goss, R.J. (1956). The regenerative responses of amputated limbs to delayed insertion into the body cavity. *The Anatomical Record* 126, 283-297. 10.1002/ar.1091260303.

Greenberg, M.E., Hermanowski, A.L., and Ziff, E.B. (1986). Effect of protein synthesis inhibitors on growth factor activation of c-fos, c-myc, and actin gene transcription. *Mol Cell Biol* 6, 1050-1057. 10.1128/mcb.6.4.1050-1057.1986.

Grohme, M.A., Schloissnig, S., Rozanski, A., Pippel, M., Young, G.R., Winkler, S., Brandl, H., Henry, I., Dahl, A., Powell, S., et al. (2018). The genome of *Schmidtea mediterranea* and the evolution of core cellular mechanisms. *Nature* 554, 56-61. 10.1038/nature25473.

Gudipaty, S.A., Lindblom, J., Loftus, P.D., Redd, M.J., Edes, K., Davey, C.F., Krishnegowda, V., and Rosenblatt, J. (2017). Mechanical stretch triggers rapid epithelial cell division through Piezo1. *Nature* 543, 118-121. 10.1038/nature21407.

Guerrero-Hernández, C., Doddihal, V., Mann, F.G., and Alvarado, A.S. (2021). A powerful and versatile new fixation protocol for immunohistology and *in situ* hybridization that preserves delicate tissues in planaria. *bioRxiv*, 2021.2011.2001.466817. 10.1101/2021.11.01.466817.

Gui, L., Song, K., Tritschler, D., Bower, R., Yan, S., Dai, A., Augspurger, K., Sakizadeh, J., Grzemska, M., Ni, T., et al. (2019). Scaffold subunits support associated subunit assembly in the *Chlamydomonas* ciliary nexin–dynein regulatory complex. *Proceedings of the National Academy of Sciences* 116, 23152-23162. 10.1073/pnas.1910960116.

Guillot, C., and Lecuit, T. (2013). Mechanics of epithelial tissue homeostasis and morphogenesis. *Science* 340, 1185-1189. 10.1126/science.1235249.

Gumbrys, A. (2017). Epidermis and Re-epithelialization in *Schmidtea mediterranea* (Open University (United Kingdom)).

Gurley, K.A., Rink, J.C., and Sanchez Alvarado, A. (2008). Beta-catenin defines head versus tail identity during planarian regeneration and homeostasis. *Science* 319, 323-327. 10.1126/science.1150029.

Harrison, F.W. (1991). *Microscopic anatomy of invertebrates* (Wiley-Liss).

Haruki, M., Nogawa, T., Hirano, N., Chon, H., Tsunaka, Y., Morikawa, M., and Kanaya, S. (2000). Efficient cleavage of RNA at high temperatures by a thermostable DNA-linked ribonuclease H. *Protein Eng* 13, 881-886. 10.1093/protein/13.12.881.

Hejnol, A., Obst, M., Stamatakis, A., Ott, M., Rouse, G.W., Edgecombe, G.D., Martinez, P., Baguña, J., Bailly, X., and Jondelius, U. (2009). Assessing the root of bilaterian animals with scalable phylogenomic methods. *Proceedings of the Royal Society B: Biological Sciences* 276, 4261-4270.

Hindley, C.J., McDowell, G.S., Wise, H., and Philpott, A. (2011). Regulation of cell fate determination by Skp1-Cullin1-F-box (SCF) E3 ubiquitin ligases. *The International Journal of Developmental Biology* 55, 249-260. 10.1387/ijdb.103171ch.

Hjeij, R., Onoufriadis, A., Watson, Christopher M., Slagle, Christopher E., Klena, Nikolai T., Dougherty, Gerard W., Kurkowiak, M., Loges, Niki T., Diggle, Christine P., Morante, Nicholas F.C., et al. (2014). CCDC151 Mutations Cause Primary Ciliary

Dyskinesia by Disruption of the Outer Dynein Arm Docking Complex Formation. *The American Journal of Human Genetics* 95, 257-274. 10.1016/j.ajhg.2014.08.005.

HORI, I. (1978). Possible Role of Rhabdite-forming Cells in Cellular Succession of the Planarian Epidermis. *Journal of Electron Microscopy* 27, 89-102. 10.1093/oxfordjournals.jmicro.a050112.

Hori, I. (1979). Regeneration of the Epidermis and Basement Membrane of the Planarian *Dugesia japonica* after Total-Body X Irradiation. *Radiation Research* 77. 10.2307/3575163.

Hori, I. (1989). Observations on planarian epithelization after wounding. *Journal of submicroscopic cytology and pathology* 21, 307-315.

Huls, M., Russel, F.G., and Masereeuw, R. (2009). The role of ATP binding cassette transporters in tissue defense and organ regeneration. *J Pharmacol Exp Ther* 328, 3-9. 10.1124/jpet.107.132225.

Illingworth, C.M. (1974). Trapped fingers and amputated finger tips in children. *Journal of Pediatric Surgery* 9, 853-858. 10.1016/s0022-3468(74)80220-4.

Jaenen, V., Fraguas, S., Bijnens, K., Heleven, M., Artois, T., Romero, R., Smeets, K., and Cebrià, F. (2021). Reactive oxygen species rescue regeneration after silencing the MAPK–ERK signaling pathway in *Schmidtea mediterranea*. *Scientific Reports* 11. 10.1038/s41598-020-79588-1.

Jang, E.R., and Galperin, E. (2016). The function of Shoc2: A scaffold and beyond. *Communicative & Integrative Biology* 9. 10.1080/19420889.2016.1188241.

Jang, H., Oakley, E., Forbes-Osborne, M., Kesler, M.V., Norcross, R., Morris, A.C., and Galperin, E. (2019). Hematopoietic and neural crest defects in zebrafishshoc2mutants: a novel vertebrate model for Noonan-like syndrome. *Human Molecular Genetics* 28, 501-514. 10.1093/hmg/ddy366.

Jazwińska, A., Badakov, R., and Keating, M.T. (2007). Activin- $\beta$ A Signaling Is Required for Zebrafish Fin Regeneration. *Current Biology* 17, 1390-1395. 10.1016/j.cub.2007.07.019.

Jopling, C., Sleep, E., Raya, M., Martí, M., Raya, A., and Belmonte, J.C.I. (2010). Zebrafish heart regeneration occurs by cardiomyocyte dedifferentiation and proliferation. *Nature* 464, 606-609. 10.1038/nature08899.

Kikuchi, K., Holdway, J.E., Werdich, A.A., Anderson, R.M., Fang, Y., Egnaczyk, G.F., Evans, T., MacRae, C.A., Stainier, D.Y.R., and Poss, K.D. (2010). Primary contribution to zebrafish heart regeneration by gata4<sup>+</sup> cardiomyocytes. *Nature* 464, 601-605. 10.1038/nature08804.

Kim, I.V., Ross, E.J., Dietrich, S., Doring, K., Sanchez Alvarado, A., and Kuhn, C.D. (2019). Efficient depletion of ribosomal RNA for RNA sequencing in planarians. *BMC Genomics* 20, 909. 10.1186/s12864-019-6292-y.

King, R.S., and Newmark, P.A. (2013). In situ hybridization protocol for enhanced detection of gene expression in the planarian *Schmidtea mediterranea*. *BMC Dev Biol* 13, 8. 10.1186/1471-213X-13-8.

Knopf, F., Hammond, C., Chekuru, A., Kurth, T., Hans, S., Weber, Christopher W., Mahatma, G., Fisher, S., Brand, M., Schulte-Merker, S., and Weidinger, G. (2011). Bone Regenerates via Dedifferentiation of Osteoblasts in the Zebrafish Fin. *Developmental Cell* 20, 713-724. 10.1016/j.devcel.2011.04.014.

Knust, E., and Bossinger, O. (2002). Composition and formation of intercellular junctions in epithelial cells. *Science* 298, 1955-1959. 10.1126/science.1072161.

Koopmans, T., van Beijnum, H., Roovers, E.F., Tomasso, A., Malhotra, D., Boeter, J., Psathaki, O.E., Versteeg, D., van Rooij, E., and Bartscherer, K. (2021). Ischemic tolerance and cardiac repair in the spiny mouse (*Acomys*). *NPJ Regen Med* 6, 78. 10.1038/s41536-021-00188-2.

Kragl, M., Knapp, D., Nacu, E., Khattak, S., Maden, M., Epperlein, H.H., and Tanaka, E.M. (2009). Cells keep a memory of their tissue origin during axolotl limb regeneration. *Nature* 460, 60-65.

Kramer, H. (2000). The ups and downs of life in an epithelium. *J Cell Biol* 151, F15-18. 10.1083/jcb.151.4.f15.

Kumar, A., Godwin, J.W., Gates, P.B., Garza-Garcia, A.A., and Brockes, J.P. (2007). Molecular Basis for the Nerve Dependence of Limb Regeneration in an Adult Vertebrate. *Science* 318, 772-777. 10.1126/science.1147710.

Kunnen, S.J., Malas, T.B., Semeins, C.M., Bakker, A.D., and Peters, D.J.M. (2018). Comprehensive transcriptome analysis of fluid shear stress altered gene expression in renal epithelial cells. *Journal of Cellular Physiology* 233, 3615-3628. 10.1002/jcp.26222.

Kwon, Y.C., Baek, S.H., Lee, H., and Choe, K.M. (2010). Nonmuscle myosin II localization is regulated by JNK during *Drosophila* larval wound healing. *Biochem Biophys Res Commun* 393, 656-661. 10.1016/j.bbrc.2010.02.047.

Kyuji, A., Patel-King, R.S., Hisabori, T., King, S.M., and Wakabayashi, K.-I. (2020). Cilia Loss and Dynein Assembly Defects in *Planaria* Lacking an Outer Dynein Arm-Docking Complex Subunit. *Zoological Science* 37. 10.2108/zs190082.

Lakshmanan, V., Bansal, D., Kulkarni, J., Poduval, D., Krishna, S., Sasidharan, V., Anand, P., Seshasayee, A., and Palakodeti, D. (2016). Genome-Wide Analysis of Polyadenylation Events in *Schmidtea mediterranea*. *G3 (Bethesda)* 6, 3035-3048. 10.1534/g3.116.031120.

Lalani, A.I., Moore, C.R., Luo, C., Kreider, B.Z., Liu, Y., Morse, H.C., and Xie, P. (2015). Myeloid Cell TRAF3 Regulates Immune Responses and Inhibits Inflammation and Tumor Development in Mice. *The Journal of Immunology* 194, 334-348. 10.4049/jimmunol.1401548.

Ledwon, J.K., Kelsey, L.J., Vaca, E.E., and Gosain, A.K. (2020). Transcriptomic analysis reveals dynamic molecular changes in skin induced by mechanical forces secondary to tissue expansion. *Scientific Reports* 10. 10.1038/s41598-020-71823-z.

Lenhoff, S.G., Lenhoff, H.M., and Trembley, A. (1986). *Hydra and the birth of experimental biology, 1744: Abraham Trembley's Mémoires concerning the polyps* (Boxwood Press).

Levin, M. (2007). Large-scale biophysics: ion flows and regeneration. *Trends in Cell Biology* 17, 261-270. 10.1016/j.tcb.2007.04.007.

Leys, S.P., and Riesgo, A. (2012). Epithelia, an evolutionary novelty of metazoans. *J Exp Zool B Mol Dev Evol* 318, 438-447. 10.1002/jez.b.21442.

Li, Q., Yang, H., and Zhong, T.P. (2015). Regeneration across Metazoan Phylogeny: Lessons from Model Organisms. *Journal of Genetics and Genomics* 42, 57-70. 10.1016/j.jgg.2014.12.002.

Li, Z., and Langhans, S.A. (2015). Transcriptional regulators of Na,K-ATPase subunits. *Frontiers in Cell and Developmental Biology* 3. 10.3389/fcell.2015.00066.

Lillywhite, H.B., and Maderson, P.F. (1988). The structure and permeability of integument. *American Zoologist* 28, 945-962.

Lin, Y.C., Grigoriev, N.G., and Spencer, A.N. (2000). Wound healing in jellyfish striated muscle involves rapid switching between two modes of cell motility and a change in the source of regulatory calcium. *Dev Biol* 225, 87-100. 10.1006/dbio.2000.9807.

Lo, D.C., Allen, F., and Brockes, J.P. (1993). Reversal of muscle differentiation during urodele limb regeneration. *Proceedings of the National Academy of Sciences* 90, 7230-7234.

Logan, C.Y., Miller, J.R., Ferkowicz, M.J., and McClay, D.R. (1999). Nuclear beta-catenin is required to specify vegetal cell fates in the sea urchin embryo. *Development* 126, 345-357. 10.1242/dev.126.2.345.

Losick, V.P., Fox, D.T., and Spradling, A.C. (2013). Polyploidization and cell fusion contribute to wound healing in the adult *Drosophila* epithelium. *Curr Biol* 23, 2224-2232. 10.1016/j.cub.2013.09.029.

Love, M.I., Huber, W., and Anders, S. (2014). Moderated estimation of fold change and dispersion for RNA-seq data with DESeq2. *Genome Biol* 15, 550. 10.1186/s13059-014-0550-8.

Mescher, A.L. (1976). Effects on adult newt limb regeneration of partial and complete skin flaps over the amputation surface. *Journal of Experimental Zoology* 195, 117-127. 10.1002/jez.1401950111.

Millard, T.H., and Martin, P. (2008). Dynamic analysis of filopodial interactions during the zipper phase of *Drosophila* dorsal closure. *Development* 135, 621-626. 10.1242/dev.014001.

Miller, D.J., and Fort, P.E. (2018). Heat Shock Proteins Regulatory Role in Neurodevelopment. *Front Neurosci* 12, 821. 10.3389/fnins.2018.00821.

Mizuno, N., Narita, A., Kon, T., Sutoh, K., and Kikkawa, M. (2007). Three-dimensional structure of cytoplasmic dynein bound to microtubules. *Proceedings of the National Academy of Sciences* 104, 20832-20837. 10.1073/pnas.0710406105.

Moon, B.-S., Kim, H.-Y., Kim, M.-Y., Yang, D.-H., Lee, J.-M., Cho, K.-W., Jung, H.-S., and Choi, K.-Y. (2011). Sur8/Shoc2 Involves Both Inhibition of Differentiation and Maintenance of Self-Renewal of Neural Progenitor Cells via Modulation of Extracellular Signal-Regulated Kinase Signaling. *Stem Cells* 29, 320-331. 10.1002/stem.586.

Morgan, T.H. (1901). *Regeneration* (Macmillan).

Morita, M., and Best, J.B. (1974). Electron microscopic studies of planarian regeneration. II. Changes in epidermis during regeneration. *Journal of Experimental Zoology* 187, 345-373. 10.1002/jez.1401870305.

Morlan, J.D., Qu, K., and Sinicropi, D.V. (2012). Selective depletion of rRNA enables whole transcriptome profiling of archival fixed tissue. *PLoS One* 7, e42882. 10.1371/journal.pone.0042882.

Morrison, J.I., Löff, S., He, P., and Simon, A.s. (2006). Salamander limb regeneration involves the activation of a multipotent skeletal muscle satellite cell population. *Journal of Cell Biology* 172, 433-440. 10.1083/jcb.200509011.

Newmark, P.A., and Sánchez Alvarado, A. (2000). Bromodeoxyuridine Specifically Labels the Regenerative Stem Cells of Planarians. *Developmental Biology* 220, 142-153. 10.1006/dbio.2000.9645.



Nishida, E., and Gotoh, Y. (1993). The MAP kinase cascade is essential for diverse signal transduction pathways. *Trends in Biochemical Sciences* 18, 128-131. 10.1016/0968-0004(93)90019-j.

Nye, H.L.D., Cameron, J.A., Chernoff, E.A.G., and Stocum, D.L. (2003). Regeneration of the urodele limb: A review. *Developmental Dynamics* 226, 280-294. 10.1002/dvdy.10236.

Ogawa, K., Ishihara, S., Saito, Y., Mineta, K., Nakazawa, M., Ikeo, K., Gojobori, T., Watanabe, K., and Agata, K. (2002). Induction of a noggin-like gene by ectopic DV interaction during planarian regeneration. *Developmental biology* 250, 59-70.

Omelchenko, T., Vasiliev, J.M., Gelfand, I.M., Feder, H.H., and Bonder, E.M. (2003). Rho-dependent formation of epithelial "leader" cells during wound healing. *Proc Natl Acad Sci U S A* 100, 10788-10793. 10.1073/pnas.1834401100.

Owlarn, S., Klenner, F., Schmidt, D., Rabert, F., Tomasso, A., Reuter, H., Mulaw, M.A., Moritz, S., Gentile, L., Weidinger, G., and Bartscherer, K. (2017). Generic wound signals initiate regeneration in missing-tissue contexts. *Nature Communications* 8. 10.1038/s41467-017-02338-x.

Pascolini, R., Tei, S., Vagnetti, D., and Bondi, C. (1984). Epidermal cell migration during wound healing in *Dugesia lugubris*. *Cell and Tissue Research* 236. 10.1007/bf00214237.

Peiris, T.H., Hoyer, K.K., and Oviedo, N.J. (2014). Innate immune system and tissue regeneration in planarians: an area ripe for exploration. In 4. (Elsevier), pp. 295-302.

Petersen, C.P., and Reddien, P.W. (2011). Polarized notum activation at wounds inhibits Wnt function to promote planarian head regeneration. *Science* 332, 852-855. 10.1126/science.1202143.

Petersen, H.O., Hoyer, S.K., Looso, M., Lengfeld, T., Kuhn, A., Warnken, U., Nishimiya-Fujisawa, C., Schnolzer, M., Kruger, M., Ozbek, S., et al. (2015). A Comprehensive Transcriptomic and Proteomic Analysis of Hydra Head Regeneration. *Mol Biol Evol* 32, 1928-1947. 10.1093/molbev/msv079.

Pierce, G.F., Mustoe, T.A., Altmann, B.W., Deuel, T.F., and Thomason, A. (1991). Role of platelet-derived growth factor in wound healing. *J Cell Biochem* 45, 319-326. 10.1002/jcb.240450403.

Plass, M., Solana, J., Wolf, F.A., Ayoub, S., Misios, A., Glazar, P., Obermayer, B., Theis, F.J., Kocks, C., and Rajewsky, N. (2018). Cell type atlas and lineage tree of a whole complex animal by single-cell transcriptomics. *Science* 360. 10.1126/science.aaq1723.

Porrello, E.R., Mahmoud, A.I., Simpson, E., Hill, J.A., Richardson, J.A., Olson, E.N., and Sadek, H.A. (2011). Transient Regenerative Potential of the Neonatal Mouse Heart. *Science* 331, 1078-1080. 10.1126/science.1200708.

Poss, K.D., Wilson, L.G., and Keating, M.T. (2002). Heart regeneration in zebrafish. *Science* 298, 2188-2190. 10.1126/science.1077857.

Potemkin, N., Cawood, S.M.F., Treece, J., Guevremont, D., Rand, C.J., McLean, C., Stanton, J.L., and Williams, J.M. (2022). A method for simultaneous detection of small and long RNA biotypes by ribodepleted RNA-Seq. *Sci Rep* 12, 621. 10.1038/s41598-021-04209-4.

Prassas, I., Eissa, A., Poda, G., and Diamandis, E.P. (2015). Unleashing the therapeutic potential of human kallikrein-related serine proteases. *Nat Rev Drug Discov* 14, 183-202. 10.1038/nrd4534.

Quint, E., Smith, A., Avaron, F., Laforest, L., Miles, J., Gaffield, W., and Akimenko, M.A. (2002). Bone patterning is altered in the regenerating zebrafish caudal fin after ectopic

expression of sonic hedgehog and bmp2b or exposure to cyclopamine. *Proceedings of the National Academy of Sciences* 99, 8713-8718. 10.1073/pnas.122571799.

Rajasekaran, A.K., and Rajasekaran, S.A. (2003). Role of Na-K-ATPase in the assembly of tight junctions. *American Journal of Physiology-Renal Physiology* 285, F388-F396. 10.1152/ajprenal.00439.2002.

Rapisarda, V., Malashchuk, I., Asamaowei, I.E., Poterlowicz, K., Fessing, M.Y., Sharov, A.A., Karakesisoglou, I., Botchkarev, V.A., and Mardaryev, A. (2017). p63 Transcription Factor Regulates Nuclear Shape and Expression of Nuclear Envelope-Associated Genes in Epidermal Keratinocytes. *J Invest Dermatol* 137, 2157-2167. 10.1016/j.jid.2017.05.013.

Razzell, W., Evans, I.R., Martin, P., and Wood, W. (2013). Calcium flashes orchestrate the wound inflammatory response through DUOX activation and hydrogen peroxide release. *Curr Biol* 23, 424-429. 10.1016/j.cub.2013.01.058.

Reddien, P.W., and Alvarado, A.S. (2004). Fundamentals of Planarian Regeneration. *Annual Review of Cell and Developmental Biology* 20, 725-757. 10.1146/annurev.cellbio.20.010403.095114.

Reddien, P.W., Bermange, A.L., Kicza, A.M., and Sanchez Alvarado, A. (2007). BMP signaling regulates the dorsal planarian midline and is needed for asymmetric regeneration. *Development* 134, 4043-4051. 10.1242/dev.007138.

Rink, J.C., Gurley, K.A., Elliott, S.A., and Sánchez Alvarado, A. (2009). Planarian Hh Signaling Regulates Regeneration Polarity and Links Hh Pathway Evolution to Cilia. *Science* 326, 1406-1410. 10.1126/science.1178712.

Rompolas, P., Azimzadeh, J., Marshall, W.F., and King, S.M. (2013). Analysis of Ciliary Assembly and Function in Planaria. In *Cilia, Part B*, pp. 245-264. 10.1016/b978-0-12-397944-5.00012-2.

Rompolas, P., Patel-King, R.S., and King, S.M. (2010). An outer arm Dynein conformational switch is required for metachronal synchrony of motile cilia in planaria. *Mol Biol Cell* 21, 3669-3679. 10.1091/mbc.E10-04-0373.

Rouhana, L., Weiss, J.A., Forsthoefel, D.J., Lee, H., King, R.S., Inoue, T., Shibata, N., Agata, K., and Newmark, P.A. (2013). RNA interference by feeding in vitro-synthesized double-stranded RNA to planarians: methodology and dynamics. *Dev Dyn* 242, 718-730. 10.1002/dvdy.23950.

Rysa, J., Tokola, H., and Ruskoaho, H. (2018). Mechanical stretch induced transcriptomic profiles in cardiac myocytes. *Sci Rep* 8, 4733. 10.1038/s41598-018-23042-w.

Saló, E., and Baguña, J. (1986). Stimulation of cellular proliferation and differentiation in the intact and regenerating planarian *Dugesia* (G) *tigrina* by the neuropeptide substance P. *Journal of Experimental Zoology* 237, 129-135.

Sanchez Alvarado, A., Newmark, P.A., Robb, S.M., and Juste, R. (2002). The Schmidtea mediterranea database as a molecular resource for studying platyhelminthes, stem cells and regeneration. *Development* 129, 5659-5665. 10.1242/dev.00167.

Satoh, A., Graham, G.M.C., Bryant, S.V., and Gardiner, D.M. (2008). Neurotrophic regulation of epidermal dedifferentiation during wound healing and limb regeneration in the axolotl (*Ambystoma mexicanum*). *Developmental Biology* 319, 321-335. 10.1016/j.ydbio.2008.04.030.

Schneider, S., Steinbeisser, H., Warga, R.M., and Hausen, P. (1996).  $\beta$ -catenin translocation into nuclei demarcates the dorsalizing centers in frog and fish embryos. *Mechanisms of Development* 57, 191-198. 10.1016/0925-4773(96)00546-1.

Scimone, M.L., Cote, L.E., and Reddien, P.W. (2017). Orthogonal muscle fibres have different instructive roles in planarian regeneration. *Nature* 551, 623-628. 10.1038/nature24660.

Seifert, A.W., Kiama, S.G., Seifert, M.G., Goheen, J.R., Palmer, T.M., and Maden, M. (2012). Skin shedding and tissue regeneration in African spiny mice (*Acomys*). *Nature* 489, 561-565. 10.1038/nature11499.

Seifert, A.W., and Muneoka, K. (2018). The blastema and epimorphic regeneration in mammals. *Dev Biol* 433, 190-199. 10.1016/j.ydbio.2017.08.007.

Sherratt, J.A., and Murray, J.D. (1990). Models of epidermal wound healing. *Proc Biol Sci* 241, 29-36. 10.1098/rspb.1990.0061.

Shimizu, H., Zhang, X., Zhang, J., Leontovich, A., Fei, K., Yan, L., and Sarras, M.P., Jr. (2002). Epithelial morphogenesis in hydra requires de novo expression of extracellular matrix components and matrix metalloproteinases. *Development* 129, 1521-1532. 10.1242/dev.129.6.1521.

Singh, B.N., Doyle, M.J., Weaver, C.V., Koyano-Nakagawa, N., and Garry, D.J. (2012). Hedgehog and Wnt coordinate signaling in myogenic progenitors and regulate limb regeneration. *Developmental Biology* 371, 23-34. 10.1016/j.ydbio.2012.07.033.

Sonnemann, K.J., and Bement, W.M. (2011). Wound repair: toward understanding and integration of single-cell and multicellular wound responses. *Annu Rev Cell Dev Biol* 27, 237-263. 10.1146/annurev-cellbio-092910-154251.

Stocum, D.L. (2011). The role of peripheral nerves in urodele limb regeneration. *European Journal of Neuroscience* 34, 908-916.

Sundelacruz, S., Levin, M., and Kaplan, D.L. (2009). Role of Membrane Potential in the Regulation of Cell Proliferation and Differentiation. *Stem Cell Reviews and Reports* 5, 231-246. 10.1007/s12015-009-9080-2.

Tasaki, J., Shibata, N., Nishimura, O., Itomi, K., Tabata, Y., Son, F., Suzuki, N., Araki, R., Abe, M., Agata, K., and Umesono, Y. (2011). ERK signaling controls blastema cell differentiation during planarian regeneration. *Development* 138, 2417-2427. 10.1242/dev.060764.

Technau, U., and Steele, R.E. (2011). Evolutionary crossroads in developmental biology: Cnidaria. *Development* 138, 1447-1458. 10.1242/dev.048959.

Tewari, A.G., Stern, S.R., Oderberg, I.M., and Reddien, P.W. (2018). Cellular and Molecular Responses Unique to Major Injury Are Dispensable for Planarian Regeneration. *Cell Rep* 25, 2577-2590 e2573. 10.1016/j.celrep.2018.11.004.

Tiozzo, S., and Copley, R.R. (2015). Reconsidering regeneration in metazoans: an evo-devo approach. *Frontiers in Ecology and Evolution* 3, 67.

Tu, K.C., Cheng, L.C., H, T.K.V., Lange, J.J., McKinney, S.A., Seidel, C.W., and Sanchez Alvarado, A. (2015). Egr-5 is a post-mitotic regulator of planarian epidermal differentiation. *Elife* 4, e10501. 10.7554/eLife.10501.

Tyler, S. (1984). Turbellarian platyhelminths. In *Biology of the integument*, (Springer), pp. 112-131.

Tyler, S. (2003). Epithelium--the primary building block for metazoan complexity. *Integr Comp Biol* 43, 55-63. 10.1093/icb/43.1.55.

Van Huizen, A.V. (2021). Regulation of Injury and Stress Responses in Planarians.

Van Lommel, A.T. (2003). From cells to organs: a histology textbook and atlas (Springer Science & Business Media).

van Wolfswinkel, J.C., Wagner, D.E., and Reddien, P.W. (2014). Single-cell analysis reveals functionally distinct classes within the planarian stem cell compartment. *Cell Stem Cell* 15, 326-339. 10.1016/j.stem.2014.06.007.

Vij, S., Rink, J.C., Ho, H.K., Babu, D., Eitel, M., Narasimhan, V., Tiku, V., Westbrook, J., Schierwater, B., and Roy, S. (2012). Evolutionarily ancient association of the FoxJ1 transcription factor with the motile ciliogenic program. *PLoS Genet* 8, e1003019. 10.1371/journal.pgen.1003019.

Wagner, Daniel E., Ho, Jaclyn J., and Reddien, Peter W. (2012). Genetic Regulators of a Pluripotent Adult Stem Cell System in Planarians Identified by RNAi and Clonal Analysis. *Cell Stem Cell* 10, 299-311. 10.1016/j.stem.2012.01.016.

Wagner, D.E., Wang, I.E., and Reddien, P.W. (2011). Clonogenic neoblasts are pluripotent adult stem cells that underlie planarian regeneration. *Science* 332, 811-816. 10.1126/science.1203983.

Wang, S., Tsarouhas, V., Xylourgidis, N., Sabri, N., Tiklova, K., Nautiyal, N., Gallio, M., and Samakovlis, C. (2009). The tyrosine kinase Stitcher activates Grainy head and epidermal wound healing in *Drosophila*. *Nat Cell Biol* 11, 890-895. 10.1038/ncb1898.

Wen, X., Jiao, L., and Tan, H. (2022). MAPK/ERK Pathway as a Central Regulator in Vertebrate Organ Regeneration. *International Journal of Molecular Sciences* 23. 10.3390/ijms23031464.

Wenemoser, D., Lapan, S.W., Wilkinson, A.W., Bell, G.W., and Reddien, P.W. (2012). A molecular wound response program associated with regeneration initiation in planarians. *Genes Dev* 26, 988-1002. 10.1101/gad.187377.112.

Wenemoser, D., and Reddien, P.W. (2010). Planarian regeneration involves distinct stem cell responses to wounds and tissue absence. *Developmental Biology* 344, 979-991. 10.1016/j.ydbio.2010.06.017.

Whited, J.L., and Tabin, C.J. (2009). Limb regeneration revisited. *Journal of Biology* 8. 10.1186/jbiol105.

Wirschell, M., Olbrich, H., Werner, C., Tritschler, D., Bower, R., Sale, W.S., Loges, N.T., Pennekamp, P., Lindberg, S., Stenram, U., et al. (2013). The nexin-dynein regulatory complex subunit DRC1 is essential for motile cilia function in algae and humans. *Nat Genet* 45, 262-268. 10.1038/ng.2533.

Wood, W., Jacinto, A., Grose, R., Woolner, S., Gale, J., Wilson, C., and Martin, P. (2002). Wound healing recapitulates morphogenesis in *Drosophila* embryos. *Nat Cell Biol* 4, 907-912. 10.1038/ncb875.

Wurtzel, O., Cote, L.E., Poirier, A., Satija, R., Regev, A., and Reddien, P.W. (2015). A Generic and Cell-Type-Specific Wound Response Precedes Regeneration in Planarians. *Dev Cell* 35, 632-645. 10.1016/j.devcel.2015.11.004.

Wurtzel, O., Oderberg, I.M., and Reddien, P.W. (2017). Planarian Epidermal Stem Cells Respond to Positional Cues to Promote Cell-Type Diversity. *Developmental Cell* 40, 491-504.e495. 10.1016/j.devcel.2017.02.008.

Xu, S., and Chisholm, A.D. (2011). A Galphag-Ca(2)(+) signaling pathway promotes actin-mediated epidermal wound closure in *C. elegans*. *Curr Biol* 21, 1960-1967. 10.1016/j.cub.2011.10.050.

Yokoyama, H., Ide, H., and Tamura, K. (2001). FGF-10 Stimulates Limb Regeneration Ability in *Xenopus laevis*. *Developmental Biology* 233, 72-79. 10.1006/dbio.2001.0180.

Zeng, A., Li, H., Guo, L., Gao, X., McKinney, S., Wang, Y., Yu, Z., Park, J., Semerad, C., Ross, E., et al. (2018). Prospectively Isolated Tetraspanin(+) Neoblasts Are Adult Pluripotent Stem Cells Underlying Planaria Regeneration. *Cell* 173, 1593-1608 e1520. 10.1016/j.cell.2018.05.006.

Zhao, S., Zhang, Y., Gamini, R., Zhang, B., and von Schack, D. (2018). Evaluation of two main RNA-seq approaches for gene quantification in clinical RNA sequencing: polyA+ selection versus rRNA depletion. *Sci Rep* 8, 4781. 10.1038/s41598-018-23226-4.

Zhao, W., He, X., Hoadley, K.A., Parker, J.S., Hayes, D.N., and Perou, C.M. (2014). Comparison of RNA-Seq by poly (A) capture, ribosomal RNA depletion, and DNA microarray for expression profiling. *BMC Genomics* 15, 419. 10.1186/1471-2164-15-419.

Zhu, S.J., and Pearson, B.J. (2018). Smed-myb-1 Specifies Early Temporal Identity during Planarian Epidermal Differentiation. *Cell Reports* 25, 38-46.e33. 10.1016/j.celrep.2018.09.011.

## VITA

1. Place of Birth
  - Khulna, Bangladesh
2. Educational institutions attended and degrees already awarded
  - Khulna University, Khulna, Bangladesh (BSc. in Biotechnology and Genetic Engineering)
3. Scholastic and professional honors
  - Ribble Pilot Grant, Department of Biology (Awardee)
  - Society for Developmental Biology (Member)
  - American Association for the Advancement of Science (Member)
4. Professional publications
  - Barai, P; Biswas, S; Duncan, EM "A novel method in identifying epidermal enriched genes required for planarian regeneration." (Manuscript in preparation).
  - Barai P; Hossain KM; Rahman SMM; Mazid MF Al; Gazi MS "Antidiarrheal Efficacy of Probiotic Bacteria in Castor Oil Induced Diarrheal Mice." Preventive nutrition and food science 23, 4 (2018): 294-300.
  - Azad Al; Hossain KM; Rahman SMM; Mazid MF Al; Barai P; Gazi MS "In ovo inoculation of duck embryos with different strains of Bacillus cereus to analyse their synergistic post-hatch anti-allergic potentialities." Veterinary medicine and science 6, 4 (2020): 992-999.
5. Pallob Barai